UNIVERSITY OF CALIFORNIA, SAN DIEGO

Anatomy of the cell extrinsic effects of endoplasmic reticulum stress in tumor facilitation

A dissertation submitted in partial satisfaction of the requirements for the degree of

Doctor of Philosophy

in

Biomedical Sciences

by

Jeffrey James Rodvold

Committee in charge:

Professor Maurizio Zanetti, Chair
Professor Webster Cavenee
Professor Jonathan Lin
Professor Cornelis Murre
Professor Victor Nizet

2017

The dissertation of Jeffrey James Rodvold is approved, and it is acceptable in quality and form for the publication on microfilm and electronically:

_____

_____

_____

_____

_____

Chair

University of California, San Diego

2017

DEDICATION

This work is the summation of innumerable people who have pushed me to arrive where we are today.
To Bethany. Undoubtedly without you this work would not exist. It is your patience that supported me through the finish line. It is your compassion that gave me comfort when things did not go as hoped. This is a credit to you. You're the constant.

To my parents. Mom, for teaching me to be passionate about what you do and realize the greater potential to help those around us. Dad, for teaching me to never half-ass a task no matter the size; whether mowing the lawn or completing a doctorate.

To the Buck Foundation, who took a chance on 17-year-old kid who when asked to described what kitchen utensil he would be best identified with a mop. Bob and Gloria, your unwavering support meant more than you will ever know.

To Clare and Damian. You two were the first to give me a taste of the beauty of science. It was a rare gift to give a 15-year-old but one that will stay with me for the rest of my life.

To Raffi. To this day, I don't know why you took me under your wing but I know my present and future would not be the where they are without your mentorship and friendship.

To Navin, while you left one hell of shadow to emerge from, you have been a steadfast supporter and believer of me this work. These accomplishments are yours as much as they are mine and I cherish being a part of the TERS journey with you.

To my friends. The Davis folk (Byron, Kevin) and those who followed me to UCSD (Collin, Greg, Rog). The ones I met once here as an undergrad (Jon, Ryan) and the ones I met as a grad (Jason, Julia). The beers always tasted better with you; thank you for keeping me sane and realize there's life beyond lab.

And finally, to Maurizio, thank you for taking a chance on that undergraduate student several years ago who uninspiringly sat across from you. The scientist I am today is because of your mentorship. I will never forget the late-night submissions or the calls to talk about data that may arrive at 7 in the morning or 11 at night. Your passion for science is the reason I have mine. I could not have asked for a more dedicated mentor who has coaxed out a true scientist, even when all signs pointed otherwise.

EPIGRAPH

There are none so blind as those who will not see.

Jonas Salk

TABLE OF CONTENTS

LIST OF FIGURES

LIST OF TABLES

ACKNOWLEDGEMENTS

Foremost, I would like to extend my appreciation and acknowledgement to Dr. Maurizio Zanetti. Thank you for navigating this uncharted journey with me.

The involvement of my committee members has been incredibly valuable from the outset of this dissertation. Dr. Jonathan Lin, for his unhesitant collaboration from the first to final day of this dissertation. Dr. Webster Cavenee for his vision of this project ahead of my own. Dr. Victor Nizet for his remarkable awareness of bridging my findings to the greater body of immunology. And Dr. Cornelius Murre for his genuine enthusiasm support for this project.

Chapter 1 of this dissertation is primarily composed from three presses: one from an invited book chapter that will be submitted to *Current Topics in Microbiology and Immunology* as: Rodvold, JJ, Hiramatsu N, Zanetti M, and Lin JH titled “The UPR and tumor immunity”. The other two source materials are: “Immune modulation by ER stress and inflammation in the tumor microenvironment,” published in *Cancer Letters* and written by J.J. Rodvold, N.R. Mahadevan, and M. Zanetti. The other text is in press is written by J.J. Rodvold and M. Zanetti as “Insidious communication among cancer cells,” in the journal *Molecular & Cellular Oncology*. The dissertation author is the primary author for all sources.

Chapter 2 is in full, a manuscript published in Science Signaling as: Rodvold, J.J, K. T. Chiu, N. Hiramatsu, J. K. Nussbacher, V. Galimberti, N. R. Mahadevan, K. Willert, J. H. Lin, M. Zanetti, Intercellular transmission of the unfolded protein response promotes survival and drug resistance in cancer cells. Sci. Signal. 10, eaah7177 (2017). The dissertation author is the primary author of this paper.

Chapter 3, in part, is a manuscript in preparation: Rodvold, J.J., Hiramatsu, N., Chiu, K.T., Iwawaki, T., Lin, J., Zanetti, M. The dissertation author is the primary investigator and author of this work.

Chapter 4 is full a manuscript in preparation Rodvold, J.J., Yang, I., Hiramatsu, N., Chiu, K.T., Quehenberger, O., Iwawaki, T., Lin, J.H., Fenical, W., Zanetti, M. The dissertation author is the primary investigator and author of this work.

CURRICULUM VITAE

Education:

PhD	UC San Diego	Biomedical Sciences (GPA: 3.98)	2011- 2017
BS	UC San Diego	Bioengineering: Biotechnology	2010

Research Experience:

Dr. Maurizio Zanetti (Thesis advisor)	UC San Diego, Dept. of Medicine	Jan 2009 - Sept 2011, Jul 2012 - present	Tumor immunology
Dr. Kevin Healy	UC Berkeley, Dept. of Bioengineering,	Jun 2007 - Sept 2008 (discontinuous)	Biomaterials
Dr. Clare Yellowley	UC Davis, Dept. of Vet. Medicine	Jan 2004 - Sept 2006 (discontinuous)	Bone biomechanics

Publications:

1. **Rodvold, J.J.**, Yang, I., Fenical, W., Zanetti, M. "The identification of tumor borne extrinsic ER stress and its role in immune dysregulation" In preparation.

2. **Rodvold, J.J.**, Tsui, B., Nussbacher, J., Nomura, N., Jiang, P., Carter, H., Zanetti, M., Kesari, S. "Cytotoxicity of mipsigargin in patient derived glioblastoma cells is heterogeneous and can be predicted by unique genetic signatures" In preparation.

3. **Rodvold, J.J**., Hiramatsu, N., Chiu, K.T., Lin., JH., Zanetti, M. "The IRE1α axis mediates tumor cell extrinsic polarization of tumor infiltrating myeloid cells to promote immune" In preparation.

4. **Rodvold, J.J.,** Zanetti, M. "Insidious communication among cancer cells." *Molecular and Cellular Oncology.* In press. (2017).

5. **Rodvold, J.J**, K. T. Chiu, N. Hiramatsu, J. K. Nussbacher, V. Galimberti, N. R. Mahadevan, K. Willert, J. H. Lin, M. Zanetti, "Intercellular transmission of the unfolded protein response promotes survival and drug resistance in cancer cells." *Sci. Signal*. 10, eaah7177 (2017).

6. **Rodvold, J.J.**, Zanetti, M. "Tumor microenvironment on the move and the Aselli connection." *Sci Signal.* 2016 Jun 28;9(434):fs13. doi: 10.1126/scisignal.aag2279. Review.

7. **Rodvold, J.J.**, Mahadevan N.R., Zanetti, M. "Immune modulation by ER stress and inflammation in the tumor microenvironment." *Cancer Lett.* 2016 Sep 28;380(1):227-36. doi: 10.1016/j.canlet.2015.09.009. Epub 2015 Oct 22.

8. Zanetti, M., **Rodvold, J.J.**, Mahadevan, M., "The evolving paradigm of cell-nonautonomous UPR-based regulation of immunity by cancer cells." *Oncogene.* 2016 Jan 21;35(3):269-78. doi: 10.1038/onc.2015.108. Epub 2015 Apr 20.

9. Almanza, G.*, Anufreichik, V.*, **Rodvold, J. J.***, Chiu, K. T., DeLaney, A., Akers, J. C., Chen, C.C., Zanetti, M. "Synthesis and delivery of short, noncoding RNA by B lymphocytes." *Proc Natl Acad Sci U S A.* 2013 Dec 10;110(50):20182-7. doi: 10.1073/pnas.1311145110. Epub 2013 Nov 25. * *Co-first author*

10. Mahadevan, N.R., **Rodvold, J.J.**, Zanetti, M. "A Janus-faced role of the unfolded protein response in antitumor immunity." *Oncoimmunology*. 2013 May 1;2(5):e23901.

11. Mahadevan, N.R., Anufreichik, V., **Rodvold, J.J.**, Sepulveda, H., Zanetti, M. "Cell Extrinsic effects of tumor ER stress imprint myeloid dendritic cells and impair CD8 T cell priming." *PLoS One.* 2012;7(12):e51845. doi: 10.1371/journal.pone.0051845. Epub 2012 Dec 18.

12. **Rodvold, J.J.**, Mahadevan N.R., Zanetti, M. "Lipocalin 2 in Cancer: When Good Immunity Goes Bad." *Cancer Lett. 2012* Mar 28;316(2):132-8. doi: 10.1016/j.canlet.2011.11.002. Epub 2011 Nov 7. Review.

13. Mahadevan N.R., **Rodvold, J.J.**, Almanza, G., Fernandez Perez, A., Wheeler, M.C., Zanetti, M. "ER stress drives Lipocalin 2 upregulation in prostate cancer cells in an NF-κB-dependent manner." *BMC Cancer.* 2011 Jun 7;11:229. doi: 10.1186/1471-2407-11-229.

14. Mahadevan N., **Rodvold, J.**, Sepulveda, H., Rossi, S., Drew, A., Zanetti, M. "Transmission of endoplasmic reticulum stress and pro-inflammation from tumor cells to myeloid cells." *Proc Natl Acad Sci U S A.* 2011 Apr 19;108(16):6561-6. doi: 10.1073/pnas.1008942108. Epub 2011 Apr 4.

15. Mahadevan N.R., Fernandez A., **Rodvold, J.J**., Almanza, G., Zanetti, M. "Tumor cells undergoing ER stress in vitro and in vivo activate transcription of pro-inflammatory cytokines" *J Inflamm Res.* 2010;3:99-103. doi: 10.2147/JIR.S11190. Epub 2010 Aug 20.

Posters and relevant conferences:

1. Participant, AACR, Translational Cancer Research for Basic Scientists Workshop. Boston, MA. 2015
2. **Rodvold, J.J.**, Hiramatsu, N., Chiu, K., Mahadevan, N., Lin, J., Zanetti, M. "Tumor ER stress transmission to infiltrating myeloid cells *in vivo* require IRE1α and TLR4." Abstract from 2013 AACR "Frontiers in Basic Cancer Research". Poster B53. 2013
3. **Rodvold, J.J.**, Woolery, M., Hiramatsu, N., Chiu, K.T., Lin, J.H., Fenical, W., Zanetti, M. "The role of tumor transmissible ER stress on cancer cells and identifying its dual identity" Abstract from 2015 FASEB "From Unfolded Proteins in the ER to Disease". Poster 38. 2015.
4. Forquar, L., **Rodvold, J**. Genetos, D., Yellowley, C. "Conditioned Media From Osteocytic Cells Exposed to Hypoxic Conditions Induces Migration of Human Mesenchymal Stem Cells" Abstract from 52nd Meeting of the Orthopedic Research Society. Paper No: 0988 (2006).

Book chapters:

1. **Rodvold, J.J.**, Hiramatsu, N., Zanetti, M., Lin, J. "The UPR and tumor immunity." Current Topics in Microbiology and Immunology. 2016. In preparation.
2. **Rodvold, J.J.**, Mahadevan, N.R., Zanetti, M., "Cell non-autonomous ER stress mediated dysregulation of immunity by cancer cells." Chapter 18. Stress Response Pathways in Cancer. 2015.

Honors and Awards:

- March of Dimes: Greater Capital Division Award for Volunteer Excellence, 2005.
- Certificate of Special Congressional Recognition from Congresswoman Susan Davis,

2006.
- California State Assembly Certificate of Appreciation from Assembly Member Laurie Saldana, 2006.
- California Legislature Assembly Certificate of Recognition from Assembly Member George Plescia, 2006.

Scholarships and Fellowships
- The Frank H. Buck Scholarship (2005-2016)
- UCSD Initiative for Maximizing Student Diversity (2011-2013)

ABSTRACT OF THE DISSERTATION

Anatomy of the cell extrinsic effects of endoplasmic reticulum stress in tumor facilitation

by

Jeffrey James Rodvold

Doctor of Philosophy in Biomedical Sciences

University of California, San Diego, 2017

Professor Maurizio Zanetti, Chair

The tumor microenvironment is harbor to a variety of insults that privilege tumor cells to co-opt host immunity. Many of these insults, including nutrient deprivation and hypoxia, create endoplasmic reticulum (ER) stress for resident tumor cells. Emerging reports also suggest that ER stress in infiltrating myeloid cells leads to the immune dysfunction, rendering these inept in the eliminating the tumor and instead facilitative of tumor growth. We previously reported that this polarization may be mediated by factors derived from tumor cells undergoing ER stress that target immune infiltrating cells to then similarly undergo ER stress, termed transmissible ER stress (TERS).

This dissertation advances the findings of TERS through three central aims. In Chapter 2, I probe the role of TERS on cancer cells using a prostate cancer cell model. My findings reveal that TERS experienced cancer cells gain cytoprotection over tumor microenvironmental challenges as well as chemotherapies, which was centrally mediated by the PERK arm of the UPR. Chapter 3 reports that myeloid cells infiltrating the tumor microenvironment undergo a polarization consistent with those affected by TERS. Chemical inhibition of IRE1α during TERS led to dramatic reduction in TERS driven inflammation, immune-suppression, and angiogenesis. Finally, Chapter 4 elucidates the identity of the molecules responsible for TERS. I found TERS activity is assignable to lipid soluble molecules. Lipidomic analysis identified TERS contained enriched eicosanoids, which could not cause ER stress but drive immune suppressive features. The ER stress inducing factor behind TERS is a novel mono-unsaturated fatty acid that caused increases in ER stress, pro-inflammation, and angiogenesis in myeloid cells as well as drove the surface expression of CD86 and PD-L1.

These lines provide the elucidation of the novel factors tumor cells undergoing ER stress secrete to promote immune evasion. These results identify potential novel biomarkers of the tumor microenvironment as well as emphasize that targeting the UPR, and specifically the IRE1α axis, may serve an important target to bolster anti-tumor immunity.

Chapter 1

INTRODUCTION

Since Rudolph Virchow's pioneering observations that solid malignancy contains hematopoietic and nontransformed cells, immunologists and oncologists alike have attempted to explain the role immune cells have in determining tumor destruction and tumor development. What followed is a century long quest to understand the role of the immune system in cancer and more recently, the birth of immunotherapy to treat cancer. While immunotherapy has the potential to fundamentally change how cancer is treated, the current state of the art has shortcomings. In fact, responsiveness in susceptible cancer types is around 20-40%. Therefore, there exists a wide gap between the promised potential and current reality of immunotherapy. This difference may be explained through a better understanding of the role of tumor microenvironment and its effects on immune function.

In the 1960s, Australian virologist Macfarlane Burnet championed the theory of immune surveillance, though German physician Paul Ehrlich nearly half a century prior had already suggested the role of immunity in the control of cancer, noting that without immunity, cancer would arise with "enormous frequency" (1). The immune surveillance theory posits that T lymphocytes are not just the sentinels against foreign pathogens (non-self) but are equally critical to fight malignant/transformed cells (self), which become antigenically distinct from the cell of origin through DNA mutations. Burnet went on to theorize that immune suppressive molecules of unknown origin can also restrain effector anti-tumor immunity. Thus, our immune system is a guardian against malignancy yet can be, and ultimately is, undermined by its target.

When first proposed, the immune surveillance hypothesis was criticized but in more recent times, it has garnered wide acceptance and undergone substantial revision.

Robert Schreiber, Lloyd Old, and Mark Smyth proposed the cancer immunoediting model, which represents the most significant amendment to Burnet's immune surveillance theory (2). Cancer immunoediting posits that immune cells and tumor cells interact in a sequential way and can be staged into three phases: elimination, equilibrium, and escape. Central to the immunoediting theory is that the tumor not only progressively renders immunity unable to kill malignant cells, but coerces it to facilitate tumor growth.

In this introductory section, I will present new views on immune surveillance and posit that the tumor microenvironment disables anti-tumor immunity through the activation of the unfolded protein response (UPR). My work allows me to conclude that the UPR can be transmitted from tumor cells to neighboring cells, both cancer and immune cells, co-opting them toward greater survival and the facilitation of immune escape and tumor growth, respectively.

Immune surveillance and immunoediting

Understanding cancer still remains a formidable challenge, even in today's genomic era. Yet a connection with immunity is deeply rooted in the historical observations of cancer. In the mid 19th century, German physician/pathologist Rudolph Virchow proposed the theory of "chronic irritation" as an important determinant in the genesis of cancer (3). Virchow based his theory on the microscopic observation that carcinomas often contained infiltrating white blood cells. In modern terms, Virchow's "chronic irritation" is inflammation, whose role as a key factor in tumorigenesis has been recently rediscovered. Whereas a causative link between inflammation and cancer is now widely accepted, oddly some forms of chronic inflammation (e.g., arthritis and psoriasis) do not lead to greater risk of cancer (4). However, infection by bacteria (*H. pylori*), viruses (HPV, HBV, HCV, EBV, HHV-8, HTLV-1), and parasites (*Schistosoma hematobium,*

Opisthorchis viverrini) leads to tumor-promoting chronic inflammation. The WHO estimates that 18% of all cancers are caused by microbial pathogens, a percentage that rises to 25% in developing countries.

At the turn of the 20th century, German pathologist Georg Schone, working on transplantable tumors in rodents, concluded that the immune system plays a significant role in controlling tumor growth. His work led him to postulate that tumors are rejected according to rules later recognized as those of the adaptive immune response, in which degree of foreignness and the effect of prior sensitization of the host to the same tumor cells (e.g., immunological memory) play a key role (In (5)).

In the aftermath of WWII, physician virologist/immunologist MacFarlane Burnet proposed the immune surveillance theory, which postulates that T cells patrol the body to identify transformed cells where significant amounts of new antigen is expressed, eliminating these cells in essentially the same way as an allograft is destroyed (1). Malignancy progresses, Burnet went on to theorize, because of a cancer cell's low antigenicity, which could be the consequence of changes in the genome but also if "intrinsic malignancy is such that it can establish immune paralysis at an early stage" (6). The early iterations of immune surveillance viewed the immune system capable of destroying altered somatic cells in an antigen-dependent manner. Malignant cells, invariably, avoid this elimination by becoming non-antigenic and impeding the immune response.

In the years to follow, new observations implicated immune cells not only as bystanders that are incapable of destroying a tumor, but actually as actors of tumor promotion. In a classical experiment, Richmond Prehn showed that splenocytes from (immune) tumor-bearing mice stimulate, rather than prevent, tumor growth *in vivo* (7). More recently, we have come to realize that the anti-tumor immune response can be

hampered, and tumor growth promoted, by soluble mediators such as the pro-inflammatory cytokines IL-6 and IL-23 (8, 9), and by different types of immune cells. These facilitators include CD4 and CD8 regulatory T cells (Tregs) (10, 11), B cells (12-14), and myeloid cells (monocyte/macrophages and dendritic cells) (15, 16). Studies in mice that develop sporadic cancer through the rare spontaneous activation of a dormant oncogene show that these tumors are immunogenic and do not evade recognition by T cells but rather actively induce tolerance associated with the expansion of non-functional T cells (17). Thus, it appears as if adaptive anti-tumor T cell responses depend on a delicate balance between activation of T cells specific for tumor antigens and mechanisms controlling their state of activation and function, which may involve complex mechanisms and diverse cell types.

These observations are consistent with the more recent proposal that immune surveillance can be temporally staged, the core concept of “cancer immunoediting”. Cancer immunoediting views immune surveillance as a three-step process in which there is a sequence of dynamic interactions between tumor cells and the host immune system: a phase of elimination of tumor cells by immune cells, a phase of equilibrium through which a Darwinian selection-process tumor cell escape variants are generated, and an escape phase, in which tumor cell variants selected in the equilibrium phase now can grow unchecked in an immunologically incompetent environment (18). The evidence for an elimination phase of cancer immunoediting has yet to be clinically demonstrated but a variety of experimental models provide evidence for its existence. This phase is where immune cells recognize and destroy transformed cells. Immunoediting posits this destruction of potential malignancy requires coordination between the innate and adaptive immune systems. For instance, $Rag1^{-/-}$ and $Rag2^{-/-}$ mice, who are deficient in B and T lymphocytes, are more susceptible to chemically induced sarcomas than mice with an

intact immune system. Even more striking, the tumors that emerge for Rag-deficient mice are more immunogenic such that when transplanted into immune competent mice, the tumors are invariably rejected 40% of the time (19). This finding suggests lymphocytes provide a selective pressure to eliminate transformed cells that when otherwise removed, allow for more immunogenic clones to emerge. Eosinophil depleted mice also have increased susceptibility to chemically induced sarcomas than immune competent mice (20), suggesting a similar phenomenon occurs for innate immune cells as well.

During the equilibrium phase, there exists an impermanent draw between tumor cell and immune cell whereby anti-tumor immunity is equally matched by immune suppressive forces generated by tumor cells. This phase, which may be the longest of the three, posits that a Darwinian selection occurs where heterogeneous tumor cells are either destroyed or evade immune surveillance (21).

Finally, in the escape phase, the dual selective pressures of the tumor microenvironment and host immunity generate tumor cell variants that are fit enough to not only avoid immune destruction but are also effective in co-opting immunity to become tumor promoting. This third phase of cancer immunoediting results in action taken by the tumor cell to not only avoid existing immune detection but also subvert any future attempt by infiltrating lymphocytes. Intrinsic cellular drivers for immune escape include the decrease in antigen presentation through changes in the expression of a variety of genes including tapasin (TAP1), a necessary cofactor for proper MHC I presentation to occur (22). Similarly, the upregulation of the protein programmed death ligand 1 (PD-L1) is known to inhibit T cell activation, which is partly why it has become a darling in the field of immunotherapy (23). However, tumor cells go well beyond cell-intrinsic mechanisms to secure their survival by establishing a tumor microenvironment that disables anti-tumor immunity.

Tumors establish an immune suppressive environment through the production of a variety of suppressive cytokines, sourced both by tumor cells and infiltrating immune cells. Myeloid derived suppressor cells (MDSCs), which can be defined based on their surface expression ($CD11b^+$, Granzyme 1 $(Gr1)^+$, $F480^-$), are known for their secretion of various immune suppressive cytokines (15). However, MDSCs are not the only suppressive immune cell within the tumor microenvironment. Evidence suggests that $Gr1^-$ macrophages may in fact be more suppressive than their $Gr1^+$ counterparts in some contexts (24). Patients with lung, breast, and head and neck cancers have reduced peripheral blood dendritic cells (DCs) and those that infiltrate the tumor draining lymph node are immature (25). Importantly, these immature myeloid cells inhibit the activation of anti-tumor T cells, undermining a competent adaptive response (26). Innate immune cells secrete a variety of immune suppressive soluble factors including IL-10, indoleamine-2,3-dioxygenase (IDO), and transforming growth factor β (TGFβ) (Reviewed in (27, 28)). These cytokines favor a Th2 response. The cytokine vascular endothelial growth factor (VEGF) is well recognized for its role in coordinating angiogenesis within the tumor microenvironment but also impedes DC anti-tumor immunity (29). The production of Arginase 1 by myeloid cells impedes T cell expansion to evade antigen-specific elimination (30, 31). Antigen presenting cells, like dendritic cells, that infiltrate the tumor microenvironment have aberrant lipid metabolism that yields poor antigen presentation (32). Thus, various soluble mediators restrain $CD8^+$ T cells from exacting their toll on transformed cells. Importantly, peripheral tolerance can promote T cell differentiation into Tregs, allowing for further inhibition of anti-tumor immunity (33).

The coordination of the tumor microenvironment may not by exclusively immune suppressive. The production of a host of pro-inflammatory cytokines like IL-23 also promote tumor growth (34, 35). Mice deficient in IL-23 respond better to IL-2

immunotherapy as it suppresses natural killer (NK) cell mediated clearance of tumor cells and metastases (36). Concordantly, a body of literature supports that various inflammatory cytokines promote immune escape (37). IL-6 facilitates defective Th1 differentiation of $CD4^+$ T cells, increasing tumor incidence and burden, while its chemical blockade or genetic deletion improves $CD8^+$ T cell mediated tumor elimination (38). Tumor necrosis factor-α (TNF-α) signaling reportedly has a role in both facilitating immune elimination (39) while other studies found TNF-$\alpha^{-/-}$ mice also appeared insensitive to chemically induced skin melanoma approaches (40). These contradictory studies may be reconciled in a recent report where in a mouse Ras model, tumor cells hijack TNF-α signaling to co-opt immunity in a cell nonautonomous manner hence promoting immune escape (41). Collectively, this new evidence shows that the tumor microenvironment creates an environment that is both inflammatory and immune suppressive to coordinate its successful immune escape.

These momentous ideas continue to influence our work while trying to understand cancer development and, more importantly, generate rational strategies that can ameliorate the prognosis and survival of cancer patients. They also reveal that the immune system has in all likelihood antithetic effects on tumorigenesis, with inflammation playing a tumorigenic role and adaptive T cell immunity a tumor-protecting role.

After decades of poor acceptance, if not outright refute, the concept of immune surveillance has been rehabilitated and is no longer questioned thanks also to the clinical success of adoptive T cell therapies (42) and immune checkpoint inhibitors (43).

The tumor microenvironment & endoplasmic reticulum (ER) stress

The escape phase of cancer immunoediting posits that tumor cells establish a local environment that prevents effector immune cell activity while also recruiting regulatory and innate immune cells to help evade surveillance by sustaining an immune suppressive, pro-inflammatory environment. While no one doubts the contribution of genetic instability in clonal selection of highly proliferative, non-antigenic cancer cells (tumor escape), the distinct environment these cells establish appears to be of equal importance. The tumor microenvironment (TME) harbors rapidly proliferating cells that are insensitive to cell death signals and contact inhibition.

Cancer cells are consistently exposed to tumor microenvironmental endoplasmic reticulum (ER) stress-inducing *noxae*; these include nutrient deprivation, due in part to a chaotic vasculature and highly active nutrient (i.e. glucose) consumption, known as the Warburg effect (44), as well as an imbalance between demand and supply of oxygen (hypoxia), and the cell's inability to readily detoxify reactive oxygen species (ROS), contributing to oxidative stress. There also exist cancer cell-intrinsic conditions that induce an ER stress such as malformed/misfolded proteins, undue demand of protein synthesis due to aberrant growth, and defects in glycosylation (45). Collectively, the conditions of the TME and the residents themselves are rife to experience aberrant protein folding.

The unfolded protein response (UPR)

Mammalian cells cope with ER stress by initiating the phylogenetically-conserved signaling event called the unfolded protein response (UPR) (Fig. 1.1). The UPR is mediated in eukaryotes by three initiator/sensor ER transmembrane molecules: inositol-requiring enzyme 1 (IRE1), PKR-like ER kinase (PERK), and activating transcription factor 6 (ATF6). For cells not undergoing ER stress, these proteins are maintained in an inactive state through association with 78 kDa glucose-regulated protein (GRP78) (46). When a

cell experiences a burden of mis/unfolded protein, GRP78 disassociates from each of the three sensor molecules to preferentially bind to excess misfolded protein, derepressing the three arms and allowing each to activate downstream signaling cascades, which broadly serve to normalize protein folding and secretion. PERK phosphorylates eukaryotic initiation factor 2α (eIF2α), resulting in the selective inhibition of translation to effectively reduce ER client protein load. During protracted ER stress, PERK activation leads to the expression of activating transcription factor 4 (ATF4), which promotes the expression of CCAAT-enhancer binding protein homologous protein (CHOP), which coordinates apoptosis (47). There are two isomers of IRE1, IRE1α, which is ubiquitously expressed in all tissue, and IRE1β, whose expression appears to be exclusive to the gut lining (48). IRE1α oligomerizes and autophosphorylates, activating its endonuclease domain, resulting in the cleavage of X-box binding protein 1 (*XBP-1)* mRNA to generate a spliced isoform (XBP-1s). Spliced XBP-1 serves as a transcription factor for the production of various ER chaperones to restore ER homeostasis. IRE1α oligomerization also leads to kinase activation to target various proteins including JNK (c-JUN N-terminal kinase) through TRAF2-ASK1 signaling (49). In addition, under prolonged ER stress or forced autophosphorylation, IRE1α's RNase domain can cause endonucleolytic decay of many ER-localized mRNAs through a phenomenon termed regulated IRE1α-dependent decay (RIDD) (50). ATF6 translocates to the Golgi, where it is cleaved into its functional form and acts in parallel with XBP-1s to restore ER homeostasis, amongst other cellular targets (51).

In the past decade, it has become increasingly apparent that the ER exerts quality control on the proteins it makes, so that properly folded proteins are packaged into vesicles destined to secretion, whereas those that are misfolded do not pass the quality control checkpoints and instead are delivered to the proteasome for degradation. Because this

mechanism is present in cells of all tissue types, a dysregulation of ER homeostatic function has consequence in a variety of diseases. These include metabolic diseases (type 2 diabetes and non-alcoholic fatty liver disease), neurodegeneration, retinal dystrophies, and cystic fibrosis (52-55). Because the UPR determines cellular adaptation as well as cell fate (survival or death), it is decidedly involved in tumorigenesis in a variety of neoplasias.

The UPR in cancer cells

Primary human tumor cells of several origins, including breast (56), lung (57), liver (58), colon (59), prostate (60), and brain (61), have increased expression of the UPR. Additionally, the abundant expression of the master regulator of the UPR, GRP78, within and at the surface of cancer cells, predicts chemoresistance (62, 63) (64) (61).

A role for the ER stress response/UPR in tumorigenesis and cancer growth has been reviewed recently (65, 66). In the mouse, the conditional deletion of *Pten* and *Grp78* ($cPten^{fl/fl}Grp78^{fl/fl}$) in the prostate or endometrial epithelium prevents the development of prostate adenocarcinoma and endometrioid adenocarcinoma, respectively, while those carrying just the *Pten* deletion develop tumors (67, 68). Likewise, the inactivation of a *Grp78* allele in the *MMTV-PyT* murine model of breast cancer yields decreased tumor survival and diminished tumor growth (69). The inhibition of *XBP-1* in human fibrosarcoma cells using siRNA decreases tumor growth and angiogenesis in a xenograft model, whereas overexpression of XBP-1s in human fibrosarcoma cells expressing a dominant-negative IRE1α mutant rescues growth and angiogenesis in xenografts (69, 70). Additionally, human glioma cells expressing a dominant-negative IRE1α mutant have decreased growth and impaired angiogenesis when orthotopically transplanted into immunodeficient mice (71). Recently, it was shown that XBP-1 is activated in triple

negative breast cancer (TNBC) and plays a pivotal role in tumorigenicity and cancer progression (72). Depletion of *XBP-1* inhibits tumor growth and tumor relapse, and reduces $CD44^{high}CD24^{low}$ cells, which reportedly identify circulating cancer stem/progenitor cells (73, 74) and are associated with poor outcome in TNBC (75). A meta-analysis of independent cohorts of TNBC patients defined 96 genes directly bound and upregulated by XBP-1, which correlated highly with HIF1α and hypoxia-driven signatures as well as with poor prognosis (72).

The inactivation of PERK results in less aggressive tumors, and transformed cells in hypoxic areas of tumors in which PERK or IRE1α are inactive yield poor tumor growth *in vivo* (70, 76). Thus, the tumor UPR is a central mechanism to initiate a cell-intrinsic signaling program that promotes tumor cell adaptation to the tumor microenvironment with enhanced tumor cell survival and proliferation.

The complexity of UPR signaling lends itself to some paradoxical considerations. Earlier work concluded that IRE1α enhances cell viability during times of ER stress (77), suggesting that it sustains tumor growth. Recently, however, it was found that IRE1α, through XBP-1 independent signaling, can also serve as a cell death signal, which appears to be mediated by RIDD (78). These findings are consistent with the notion that prolonged RIDD activation increases apoptosis (79). RIDD activation and apoptosis may involve the recruitment of TNF receptor-associated factor 2 (TRAF2) and JNK (reviewed in (80)). However, tumor cells can also exploit the UPR to survive and avoid apoptosis through microRNA regulation. For instance, PERK can induce miR-211, which in turn attenuates stress-dependent expression of CHOP, facilitating cell survival by diminishing apoptotic signaling (81). The apparent paradox that cancer cells survive in spite of CHOP accumulation could be explained by a UPR-initiated feed-back regulation involving microRNAs. Collectively, this suggests that not only is the UPR present in a variety of solid

malignancies, but also that it enables successful tumor survival.

The UPR and immune surveillance

While there are numerous lines evidence that the UPR in cancer cells is tumor promoting, does there exist a link between the UPR and immune surveillance? A series of reports from the laboratory of Guido Kroemer suggested that such a relationship might exist. The authors found that artificially-induced hyperploid cells undergo constitutive ER stress, which was confirmed through detecting the phosphorylation of PERK and eIF2α. The protracted ER stress driven by hyperploidy led to the surface relocalization of the ER-resident protein calreticulin (CRT) on polyploid cells. CRT relocalization serves as an "eat me" signal to promote phagocytosis by infiltrating macrophages and DCs of polyploid cells, leading to *de novo* activation/restimulation of tumor antigen in CRT^+ specific T cells. Importantly, this response only selectively eliminated hyperploid tumor cells (82, 83). Concordantly, CRT expression was found to be directly correlated with eIF2α phosphorylation in non-small cell lung carcinoma patients and predicted a more favorable clinical outcome (84). These observations point to the tumor UPR as a mediator for immune elimination.

This axis of ploidy based UPR to mediate immune elimination, however, is at odds with several key clinical features. Most notably, 90% of solid malignancy have some level of aneuploidy (85) and increased aneuploidy correlates with poor prognosis (86). Since Kroemer's proposed model posits that the T cell response set in motion by hyperploidy eliminates only CRT^+ hyperploid cells, sparing CRT^- semi-diploid tumor cells, one could argue that if aneuploidy-driven UPR favors immune surveillance, it must do so in a very limited way. The proposal that aneuploidy driven ER stress promotes immune elimination is also at odds with recent evidence that aneuploidy corresponds with poor T cell infiltration

and increased immune suppression in a variety of solid malignancies (87). This study found that decreased aneuploidy correlates with favorable response to checkpoint inhibitors in melanoma patients.

To reconcile this apparent conundrum, one needs to imagine that the UPR is similar to Virchow's smoldering inflammation (88), which is to say that the UPR may play roles both in immune elimination and immune escape. Specifically, the immune stimulatory functions of the UPR that are operative early in elimination transition to favor escape due to immune- and tumor- selective pressures. Should this hypothesis be true, it therefore would be important to demonstrate that the UPR in immune cells facilitates tumor growth.

The UPR in tumor infiltrating immune cells

Based on the foregoing, it is possible that the UPR in immune infiltrate plays a contributing role towards successful tumor growth. The most prominent feature linking the UPR and immunity is in the production of pro-inflammatory mediators. Importantly, tumor promoting inflammation is an emerging hallmark of cancer (89). However, there is considerable evidence that the UPR in tumor associated immune cells extends beyond just tumor promoting inflammation to enable immune escape. Hereunder, I discuss the role of the UPR in immune associated pro-inflammation, antigen presentation, and other generalizable tumor promoting functions in a variety of immune cells.

a. UPR regulation of inflammatory mediators in myeloid cells

Besides promoting cellular adaptation to increased mis/unfolded protein burden, the UPR activates a pro-inflammatory cascade of soluble regulators and mediators with tumor-promoting and cell survival effects. The UPR is directly linked to the production of

the tumorigenic cytokines IL-6, IL-23, and TNF-α, which hamper anti-tumor immunity. A microarray analysis of mouse lymphoma cells treated with thapsigargin, a sesquiterpene lactone canonical ER stress inducer that inhibits SERCA (sarco/endoplasmic reticulum calcium transport ATPase), results in the transcriptional upregulation of *Il-6*, *Il-23p19* and *Tnf-α* (90). Furthermore, *Grp78* expression in murine prostate cancer cells grown in a heterotopic transplant correlates with the levels of *Il-6*, *Il-23p19*, and *Tnf-α* transcription (91). Others have shown that CHOP is necessary for IL-23 production by dendritic cells (92), and macrophage produced IL-6 and TNF-α (93).

Multiple lines of evidence indicate that the UPR activates NF-κB (94) through apparently distinct mechanisms. PERK-mediated translational inhibition reduces the ratio of the IκB to NF-κB, thus permitting the nuclear migration of NF-κB and transcription of downstream inflammatory genes (95, 96). Upon auto-phosphorylation, IRE1α forms a complex with TRAF2 at its cytosolic domain, and the subsequent complex mediates direct IκB phosphorylation via IκB kinase (IKK), leading to NF-κB activation (97). ATF6 participates in NF-κB activation in an AKT-dependent manner (98).

IRE1α and PERK signaling may play redundant roles in IL-6 and TNF-α production in macrophages (93, 99). Upon nuclear translocation, XBP-1s binds to the *IL-6* and *TNF-α* promoters, and in fact *Xbp-1*-deficient macrophages display impaired Il-6 and Tnf-α production in response to pharmacological ER stress and infectious TLR agonism (99). The UPR also synergizes with TLR4 agonism in macrophages to increase IL-23 production (100).

Another component of the UPR, the ER resident chaperone molecule glucose-regulated protein 94 (GRP94), also affects myeloid cell polarization. GRP94 is a paralog of HSP90, and much like GRP78, is transcriptionally co-regulated with other chaperones to increase the efficiency of protein folding in the ER (101). GRP94 distinguishes itself by

preferentially targeting immunological client proteins including MHC II, immunoglobulin heavy and light chain, and integrins (reviewed in (102)). Importantly, the ablation of GRP94 in macrophages, while not affecting their differentiation, has a significant impact on their pro-inflammatory cytokine response (inclusive of TNF-α, IL-6, IL-1β and IL-23) to canonical agonists of TLR2, TLR4, TLR5, TLR7, and TLR9 (103). GRP94 serves as a chaperone for multiple TLRs in a manner that is dependent on another ER luminal protein, CNPY3. In fact, genetic disruption of gp96–CNPY3 interaction completely abolishes the TLR chaperone function, suggesting that CNPY3 serves as a TLR-specific co-chaperone for GRP94 (104). Thus, within the tumor microenvironment GRP94 may play a role in fine-tuning the inflammatory response. Indeed, tumor-infiltrating macrophages lacking GRP94 produce significantly less inflammatory cytokines as their wild type counterparts in a colon cancer model (105), and this phenotype is associated with reduced tumor incidence and burden. GRP94 may also contribute to immune suppression. In fact, mice whose $Fox3^{+}$ compartment was depleted of GRP94 die within 100 days of birth of severe inflammatory syndrome due a lack of Tregs, in part through impaired production of TGFβ (106).

b. The UPR dysregulates antigen presentation

Successful T cell mediated anti-tumor immunity requires the presentation of tumor antigens by professional antigen presenting cells, DCs and macrophages. This event is restricted by Major Histocompatibility Complex (MHC) molecules, which collectively form a highly polymorphic system that is species-specific. Similar to other membrane proteins, antigens that undergo antigen processing depend on the functionality of the ER. Briefly, 8-9 amino acid-long peptides from enzymatically degraded endogenous protein assemble with the MHC I molecule in the ER lumen, with other subunits including the proteins tapasin and ERp57. During this assembly, the peptide is properly loaded onto MHC I to

form a complex that is then trafficked through the Golgi and ultimately expressed at the cell surface (Reviewed in (107)). Evidence suggests that the UPR can negatively affect antigen presentation. For instance, B cells with enforced accumulation of protein in the ER mount a UPR and upregulate MHC Class II and costimulatory molecules but display fewer high affinity peptide/MHC Class II complexes (90). The overexpression of misfolded proteins or the constitutive expression of active ATF6 or XBP-1s is associated with decreased levels of MHC Class I in 293T cells (108). Similarly, ER stress induced by palmitate or glucose deprivation decreases MHC Class I antigen presentation in mouse thymoma cells (109). Interestingly, when the UPR is induced with thapsigargin or by trichostatin A, a histone deacetylase inhibitor, tapasin, which is involved in quality control of MHC I/peptide complexes in the ER (110), is transcriptionally downregulated. This downregulation results in a decreased presentation of high affinity antigen peptides (90, 110). Furthermore, IRE1α signaling upregulates miR-346, which, in turn, downregulates the protein transporter associated with antigen processing 1 (TAP1), decreasing MHC Class I-associated antigen presentation (111). Most recently, it was shown that in $CD8\alpha^+$ dendritic cells, RIDD activity affects mRNAs coding for components of the MHC Class I presentation pathway, including tapasin, leading to dysfunctional cross presentation and poor cross-priming of naïve antigen-specific $CD8^+$ T cells (112). Collectively, antigen presenting cells undergoing ER stress experience remodeling of the processing machinery yielding decreased presentation of high affinity, immunodominant peptides.

Is the UPR operative in tumor infiltrating immune cells?

Tumor promoting inflammation and defective antigen presentation may be UPR-dependent. These findings, though suggestive that the UPR enables immune escape, do not adequately address whether tumor infiltrating immune cells themselves undergo ER

stress. Hereunder, I discuss evidence in support that the pro-tumor activity of immune cells associates with UPR expression.

a) Macrophage/Monocytes

Tumor infiltrating macrophages (TAMs) and their lineage precursors, monocytes, are well-recognized tumor infiltrates. TAMs strongly predict increased vascularization of breast tumors and are associated with reduced relapse-free survival and poor overall survival (113). Many of the cytokines recognized to be produced by TAMs are reported to be the product of ER stress. Aside from IL-6, IL-23, and TNF-α, another product secreted by TAMs is VEGF, which improves angiogenesis within the tumor microenvironment. While there is scant evidence to directly implicate a causal link between ER stress and TAM produced VEGF, various reports do find that the UPR stimulates VEGF production in a variety of other cell types. Treatment of oxidized lipids led to robust VEGF secretion in HUVECs in a ATF4 dependent manner (114). Concordantly, hypoxic stress leads to the activation of ATF4, driving broad translational inhibition of protein production while uniquely protecting *VEGF* transcription (115). UPR mediated production of VEGF may also operate independently of ER stress (116). Using endothelial cells, Karali et al. reported that the deletion of *ATF6* or *eIF2α* led to markedly reduced VEGF mediated vascularization via the mTOR pathway during ER stress independent conditions (117). There also exists a potential role for IRE1α mediated control of VEGF. Glioma cells with dominant negative expression of IRE1α have markedly reduced vascularization and decreased production of IL-6 and VEGF-A (118). Moreover, HIF1α activation may be mediated by XBP-1s as it co-occupies several known HIF1α targets and the two co-immunoprecipitate during hypoxic stress (72). Collectively, unique arms of the UPR all seem to have a role in hypoxic signaling and the production of VEGF. Human

macrophages treated with the supernatant of tumor ER stressed cancer cells undergo their own ER stress and secrete large amounts of VEGF (119), while macrophages under hypoxic conditions produce VEGF through SERCA 2 activation (120).

IL-1β produced by macrophages is reported to play a variety of tumorigenic functions (121). Interestingly, ER stressed macrophages secrete IL-1β during TLR4 agonism (122) and *Il-1*β transcription is mediated by IRE1α-dependent GSK-3β activation during times of ER stress (123). However, the inhibition of IRE1α endonuclease activity has no effect in *Il-1β* transcription, while it did for *Tnf-α*. This finding suggests that macrophage IRE1α mediated production of IL-1β may operate independently of XBP-1 signaling.

The first and only observation that TAMs undergo a UPR is from a 2004 study in mice transgenic for the Grp78 promoter. Here, the authors demonstrated that macrophages infiltrating tumor allografts had robust *Grp78* promoter activity compared to those in the peritoneum (124). A recent report probed the molecular phenotype of blood monocytes of renal cell carcinoma (RCC) patients and healthy donors (125). The authors found RCC patient derived monocytes were inflammatory and angiogenic, with increased transcription for *IL-1*β and *VEGF* relative to healthy donor monocytes. Interestingly, the expression of several UPR genes, including *ERN1,* which codes for IRE1α, were increased in RCC monocytes relative to healthy donor monocytes. The implication of such findings is that tumor infiltrating macrophages undergo ER stress and contribute to remodeling the TME.

b) Myeloid derived suppressor cells (MDSCs)

MDSCs are a unique class of tumor infiltrating monocytes that are best defined for their co-expression of the myeloid marker CD11b and the granulocyte marker Gr1 (16).

This subset of myeloid cells inhibits effector function of anti-tumor cytotoxic T cells through the secretion of T cell inhibiting factors, which interfere with a competent anti-tumor response. Gabrilovich and colleagues reported that patient derived tumor infiltrating MDSCs have increased expression of UPR genes, including *GRP78*, *ATF4*, *CHOP*, and *XBP-1*, relative to splenic derived control neutrophils. MDSC survival, which was shorter than other myeloid infiltrate including neutrophils, was linked to TRAIL-R expression, a target of ER stress (126). Interestingly, the authors found that naïve primary derived MDSCs treated with tumor conditioned media undergo ER stress and upregulate TRAIL-R expression, suggesting that yet-unidentified tumor-borne factors may drive TRAIL-R expression in MDSCs. Perhaps more relevant, MDSC function may be dependent on CHOP expression. Thevenot et al. found the deletion of Chop in MDSCs reduced Il-6 production and led to increased T cell anti-tumor response (127). These findings provide new insight into the role of Chop in MDSC mediated anti-tumor immune response. Since these results could not be reproduced in independent studies (128), the role of UPR signaling in MDSC function remains to be precisely determined.

c) *Dendritic cells*

The role of dendritic cells (DCs) in tumor development include their production of tumor promoting cytokines and antigen presentation enabling anti-tumor T cell responses. Monitoring spliced XBP-1 through the fluorescent protein, Venus, Osorio et al. found that IRE1α plays a role in the development and maintenance of DCs. Loss of XBP-1 in $CD11c^+$ DCs led to defects in phenotype, ER homeostasis, and antigen presentation by $CD8\alpha^+$ DCs, but not in $CD11b^+$ DCs (112). Specific to tumor infiltrating DCs, a recent study by the Glimcher group reported that ovarian cancer infiltrating DCs had increased UPR gene expression relative to their splenic counterparts, including increased *XBP-1s*, *GRP78*, and

CHOP (129). Mice with an aggressive form of ovarian cancer survived better when reconstituted with bone marrow DCs in which XBP-1 was deleted, suggesting that DCs are tumor promoting in a XBP-1-dependent manner. These tumor infiltrating DCs had dysregulated lipid metabolism and poor antigen presentation function. The conditional silencing of *Xbp-1* within DCs improved host survival in vivo and anti-tumor T cell immunity in vitro. The source of ER stress in DCs appeared to have been induced by lipid peroxidation. Two similar reports corroborate the fact that lipid peroxidation can lead to DC dysfunction. An initial report showed that tumor derived oxidized lipids blocked cross-presentation, leading to poor anti-tumor T cell immunity, though a UPR role was not explicitly implicated (130). A follow-up study showed that the accumulation of lipids in tumor infiltrating DCs prevented correct antigen processing, again leading to reduced anti-tumor immunity (32). Together, it appears that tumor derived factors, likely lipid in nature, co-opt tumor infiltrating DCs by triggering an *IRE1α* dependent phenotype to oppose immune surveillance.

d) *T lymphocytes*

There has yet to be any definitive reports that tumor infiltrating lymphocytes (TILs) undergo a UPR and if UPR activation in TILs contributes to tumor facilitation or rejection. Consequently, any possible role of the UPR in T cells can only be inferred from studies in unrelated experimental settings outside of tumor immunology. $CD4^+$ Th2 helper cells are often found in tumor infiltrates where they can suppress anti-tumor immunity (131). In vitro, $CD4^+$ T cells activated through TCR ligation undergo eIF2α phosphorylation and increased mRNA expression of the *IL-4* and *IFN-γ* genes. eIF2α is dephosphorylated upon lymphocyte restimulation, promoting the secretion of IL-4 and IFN-γ. This suggests that Th2 effector function utilizes UPR signaling (132). Using an acute infection model,

Kamimura and colleagues found $CD8^+$ T cells undergo increased expression in unspliced XBP-1 during IL-2 potentiation, followed by XBP-1 splicing during TCR ligation. Interestingly, the deletion of XBP-1 led to the reduction of $KLRG1^{hi}$ effector cells (133), suggesting that IRE1α signaling is necessary for the differentiation of effector $CD8^+$ T cells. The depletion of L-arginine, which can be mediated by myeloid cell produced Arginase I, hampers T cell function and proliferation, and drives ER stress in peripheral mitogen activated T-cells that ultimately lead to autophagy and apoptosis (134). Finally, Franco et al. (135) studied the relationship between ER stress and *IL-10* transcription in human $CD4^+$ (134) and $CD8^+$ Treg clones. The induction of ER stress by thapsigargin enhanced *IL-10* transcription while salubrinal, a small molecule inhibitor of eIF2α dephosphporylation, dramatically inhibited it. *IL-10* transcription is also enhanced by exogenous TNF-α. This study uncovered a possible role for ER stress in driving T cell plasticity.

The cell extrinsic effects of the tumor UPR

Collectively, the UPR in tumor infiltrating immune cells, including macrophages and DCs, play a relevant, and possibly necessary, role in tumor outgrowth. These phenotypes are consistent with those necessary for successful tumor escape (21). Absent from this discussion thus far, however, is the source of the UPR in tumor infiltrating immune cells responsible for this polarization. We hypothesized that stimuli native to the tumor microenvironment may be responsible for initiating a UPR in myeloid cells.

Naïve primary derived macrophages treated with the conditioned media of cancer cells undergoing ER stress were shown to undergo a *de novo* UPR, which includes transcriptional activation of *Grp78*, *Chop*, and *Xbp-1s* (136). We termed this phenomenon transmissible ER stress, or TERS. TERS conditioned medium from unique cancer cell lines also led macrophages to produce the pro-tumorigenic cytokines Il-6, Tnf-α, and Il-

23, and the inflammatory chemokines Mip-1α and Mip-1β. Their production was synergized by TLR4 agonism but independent of TLR2 or IL-6R. Others demonstrate that TERS treated macrophages also produce Vegf (119). Dendritic cells treated with TERS also undergo ER stress with increased production of pro-inflammatory cytokines (137). Strikingly, TERS treated DCs also have increased expression of the immune suppressive gene *Arg1* and PD-L1 surface expression. Because of the role of Arginase 1 and PD-L1 in restraining T cell clonal activation, these findings suggest a new angle in the genesis of local immune suppression.

The effects of TERS treated DCs in T cell activation are also quite dramatic. First, we found that TERS treated DCs display an activated and mature phenotype with upregulation of the costimulatory molecules CD80 and CD86, but are less efficient at presenting antigen, i.e., fewer peptide/MHC complexes at their surface. Using an in vitro model of $CD8^+$ T cell cross-priming, we found that naïve $CD8^+$ T cells can be activated (CD69 expression) but do not clonally expand, suggesting a state of anergy. Anergic $CD8^+$ T cells induced by TERS treated DCs could not be resolved by supplementation with exogenous IL-2, unlike classically anergic T cells. The defect could be overcome, however, by adding the Arginase 1 inhibitor L-norvaline. T cells cross-primed by TERS treated DCs had increased gene transcription of *Il-2*, *Il-10*, upregulated FoxP3, and decreased CD28 expression, suggesting a plastic differentiation into a regulatory T cell fate. Because of these findings, tumor derived ER stress not only can co-opt infiltrating innate immune cells, but may also have broad consequences on adaptive immunity that disable immune surveillance and endue tumor escape.

Conclusions

Unraveling the mechanisms behind poor immune surveillance is of paramount importance to design rational ways to intervene against cancer. A wealth of reports suggests that the UPR is facilitative in tumor development by affecting both resident tumor cells and infiltrating immune cells. Reports from our lab demonstrate that transmissible ER stress is a novel mechanism of immune hijacking mediated by tumor cells in a cell extrinsic manner. However, the current understanding of the TERS phenomenon remains poorly characterized.

Overlooked within this paradigm is what role TERS may have on cancer cells. There are numerous reports that find that the UPR is tumor promoting due to cancer cell intrinsic processes. What remains unaccounted is whether TERS-associated cell extrinsic consequences, which alter host immunity, also effect receiver cancer cells.

When I began my PhD work, I identified three key questions that remained unanswered: 1) Is there a role for transmissible ER stress amongst cancer cells? I reasoned that if TERS exerts its pro-tumor effects on immune cells, it was highly probable it could similarly exert effects on unstressed cancer cells that occupy the same space within the TME; 2) Do myeloid cells resident in the tumor microenvironment – i.e. in the natural setting of tumor growth – express TERS responsive genes, and if so, what is the mechanism behind their polarization?; 3) Can the factor or factors responsible for ER stress transmission and the mixed pro-inflammatory/immune suppressive phenotype of myeloid cells be identified? This dissertation will present the work of five years that at times was difficult but always rewarding, through which I was able to provide an answer to all three questions.

ACKNOWLEDGEMENTS

Chapter 1 of this dissertation is primarily composed from three presses: one from an invited book chapter that will be submitted to *Current Topics in Microbiology and Immunology* as: Rodvold, JJ, Hiramatsu N, Zanetti M, and Lin JH titled “The UPR and tumor immunity”. The other two source materials are: “Immune modulation by ER stress and inflammation in the tumor microenvironment,” published in *Cancer Letters* and written by J.J. Rodvold, N.R. Mahadevan, and M. Zanetti. The other text is in press is written by J.J. Rodvold and M. Zanetti as “Insidious communication among cancer cells,” in the journal *Molecular & Cellular Oncology*. The dissertation author is the primary author for all sources.

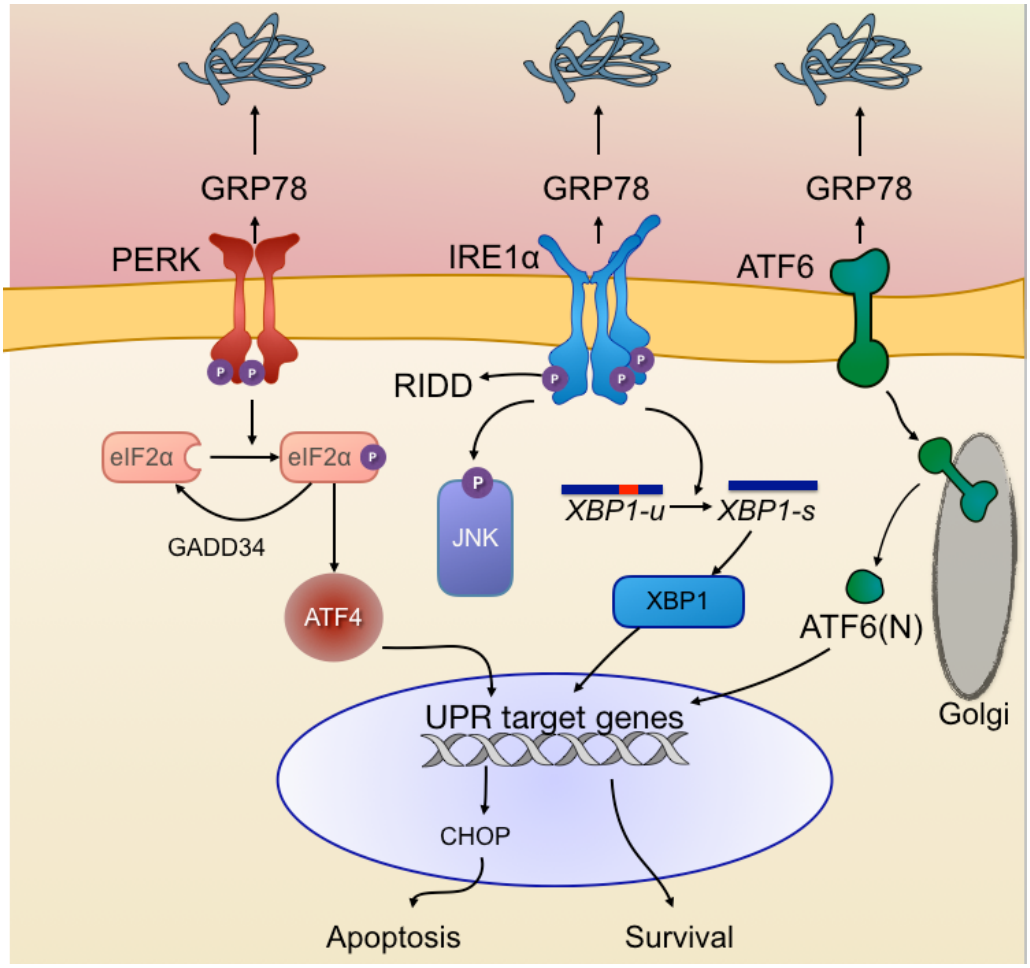

Figure 1.1: The unfolded protein response. Signaling pathways of the ER stress response/UPR. The UPR is mediated by three initiator/sensor ER transmembrane molecules: inositol-requiring enzyme 1 (IRE1α), PKR like ER kinase (PERK), and activating transcription factor 6 (ATF6), which in the unstressed state are associated with 78 kDa glucose-regulated protein (GRP78). Upon ER stress, GRP78 dissociates from each of the three sensor molecules to bind un/misfolded proteins, allowing each sensor to activate downstream signaling cascades and ER stress responsive genes to normalize protein folding and secretion. PERK phosphorylates eIF2α, resulting in the selective inhibition of translation, effectively reducing ER client protein load. eIF2α also targets the activating transcription factor 4 (ATF4), which is a transcription factor. IRE1α autophosphorylates, activating its endonuclease domain, cleaving XBP-1 mRNA to generate a spliced XBP-1 isoform (XBP-1s), which drives the production of various ER chaperones to restore ER homeostasis. Under prolonged ER stress or forced autophosphorylation, IRE1α RNase domain degrades many ER-localized mRNAs (IRE1α -dependent decay or RIDD). ATF6 translocates to the Golgi where its active domain is cleaved (ATF6n) serving as a transcription factor. If ER stress persists, compensatory mechanisms fail and downstream signaling through the PERK ATF4 axis activates the transcription factor CHOP (CCAAT/-enhancer binding protein homologous protein), which initiates apoptosis.

SPECIFIC AIMS

The focus of this dissertation is to better characterize the phenomenon first described as transmissible ER stress (TERS). I hypothesize that there exist unique molecules within tumor cell ER stressed conditioned medium that facilitate tumor outgrowth by affecting UPR signaling in receiver myeloid cells and cancer cells. I will examine this hypothesis through the following aims:

Aim 1: Describe the consequences of transmissible ER stress as it relates to cancer cells.

a. Investigate the existence of TERS between cancer cells.
b. Characterize the biologic effects TERS endows upon receiver cancer cells as compared to unexperienced cells.
c. Determine the mechanism behind any differential phenotypes.

Aim 2: Demonstrate the existence of the TERS responsive genes in myeloid cells in vivo and determine the UPR mechanism behind this polarization in vitro and in vivo.

a. Probe for the presence of TERS affected genes in tumor infiltrating myeloid cells in vivo.
b. Demonstrate TLR4 dependence in vivo.
c. Elucidate the mechanism of TERS polarization in receiver myeloid cells in vitro and in vivo.

Aim 3: Identify the molecule or molecules behind TERS signaling.

a. Elucidate the biomolecular features of the moieties involved in TERS.
b. Provide a partial, if not complete, identification of the molecules involved in TERS.
c. Demonstrate the bioactivity of these molecules to reproduce TERS effects.

CHAPTER 2

Intercellular transmission of the unfolded protein response promotes survival and drug resistance in cancer cells.

Jeffrey J. Rodvold[1], Kevin T. Chiu[1], Nobuhiko Hiramatsu[2], Julia K. Nussbacher[3], Valentina Galimberti[1], Navin R. Mahadevan[1], Karl Willert[3], Jonathan H. Lin[2], and Maurizio Zanetti[1]

[1] The Laboratory of Immunology, Department of Medicine and Moores Cancer Center, University of California at San Diego, La Jolla, 92093 CA, USA;

[2]Department of Pathology and Ophthalmology, University of California at San Diego, La Jolla, 92093 CA, USA

[3]Department of Cellular and Molecular Medicine
University of California at San Diego, La Jolla, 92093 CA, USA

PREFACE TO CHAPTER 2

Chapter 2 is a full manuscript that has been published in *Science Signaling* (138). This work directly addresses Specific Aim 1 of my dissertation: the effects of TERS on cancer cells. This work demonstrates that transmissible ER stress occurs between cancer cells and provides cellular fitness over their inexperienced counterparts when challenge in vitro or in vivo. This cytoprotection was PERK dependent. In addition, TERS promoted Wnt signaling in receiver cells and the cytoplasmic relocalization of TERT. Together, these results demonstrate that the effects of TERS are not constrained to affect the myeloid compartment and have equally repercussive results on unstressed cancer cells.

ABSTRACT

In the tumor microenvironment, various *noxae* induce endoplasmic reticulum (ER) stress, which initiates the cellular response termed the unfolded protein response (UPR). Previously, we reported that cancer cells mounting a UPR release factors that induce a de novo UPR in bone marrow derived myeloid cells, macrophages and dendritic cells, that facilitate pro-tumorigenic characteristics in vitro and tumor growth in vivo. Here, we sought to determine whether this new type of inter-cellular signaling, which we have termed transmissible ER stress (TERS), might also be operative between cancer cells and what its functional consequences might be within the tumor. We found that TERS signaling induced a UPR in recipient human prostate cancer cells that included the cell surface expression of the chaperone GRP78. TERS also activated Wnt signaling in recipient cancer cells and enhanced resistance to nutrient starvation and common chemotherapies, namely the proteasome inhibitor bortezomib and the microtubule inhibitor paclitaxel. Using chemical inhibitors, we found that TERS-induced activation of Wnt signaling required the UPR protein IRE1. However, using KO MEFs and 293T cells, we determined that TERS-enhanced cell survival was predominantly mediated by PERK signaling and reduction in ATF4 protein, which prevented the activation of the transcription factor CHOP and consequently the induction of apoptosis, resulting in increased cell survival. When implanted in mice, TERS treated cancer cells gave rise to faster growing tumors than vehicle treated cancer cells. Collectively, our data demonstrate that transmissible ER stress is a mechanism of intercellular communication through which tumor cells can adapt to stressful environments.

INTRODUCTION

Endoplasmic reticulum (ER) stress in solid tumors results from a dysregulation of protein synthesis, folding, secretion, and aberrant glycosylation, which are heightened by microenvironmental stimuli such as nutrient deprivation, hypoxia, oxidative stress, and chronic viral infection (139, 140). To cope with ER stress, tumor cells initiate an evolutionarily conserved signaling process known as the unfolded protein response (UPR), which is coordinated by three ER transmembrane-bound sensors, inositol-requiring transmembrane kinase/endoribonuclease 1 α (IRE1α), activating transcription factor 6 (ATF6), and protein kinase R (PKR)-like ER kinase (PERK), which are maintained inactive in unstressed cells through luminal association with the ER chaperone glucose-regulated protein 78 [GRP78; also known as binding immunoglobulin protein (BiP)] (47). Upon excessive client protein burden, GRP78 disassociates from these three sensor proteins to preferentially bind unfolded or misfolded proteins, enabling each sensor to activate downstream signaling cascades that attempt to normalize protein folding and secretion. PERK phosphorylates eukaryotic initiation factor (eIF2α), resulting in selective inhibition of translation to reduce ER client protein load. IRE1α autophosphorylates, oligomerizes, and activates its endoribonuclease function that generates a spliced isoform of X-box binding protein 1 (XBP-1s), which drives the production of various ER chaperones. ATF6 translocates to the Golgi where it is cleaved into its functional form and acts in tandem with XBP-1s to restore ER homeostasis (141). Persistent ER stress activates the transcription factor CCAAT-enhancer-binding protein homologous protein (CHOP), which can initiate apoptosis (142).

The role of the UPR in tumorigenesis and cancer progression is typically distinguished by cell-intrinsic functions that enhance cell fitness and survival, and cell-extrinsic functions, which are mediated by soluble messenger molecules released by

cancer cells undergoing a UPR that coopt recipient cells (119, 136, 143-145). In support of the former, conditional homozygous knockout of *Grp78* in the prostate of mice with *Pten* inactivation protects against cancer growth (146), whereas the inactivation of PERK or expression of a dominant-negative PERK mutant in cancer cells yields smaller and less aggressive tumors in mice (76). Human tumor cells have high amounts of GRP78 (64), which confers resistance to chemotherapy (147). In addition, the translocation of GRP78 to the cell surface is proposed to serve as a signaling molecule that activates phosphoinositide-3-kinase (PI3K) (148, 149), which promotes proliferation. As to cell-extrinsic effects, we previously found that cancer cells undergoing a UPR can transmit ER stress to bone marrow-derived myeloid cells, macrophages and dendritic cells (119, 136, 143-145), and impart these cells with a mixed pro-inflammatory/immune suppressive phenotype (145) that is associated with defective activation of naïve $CD8^+$ T cells (144). The existence of a similar UPR-based cell-nonautonomous communication in *C. elegans*, which promotes stress resistance and organismal longevity (150), suggests that this phenomenon may be evolutionarily conserved (151). We propose it may also be leveraged by the tumor to promote its survival and outgrowth.

The induction of the UPR in cancer cells triggers the release soluble factors *per se* that are able to transmit ER stress to recipient myeloid cells (119, 136, 144). We termed this phenomenon transmissible ER stress (TERS). Here, we investigated whether TERS is operative amongst cancer cells and what the consequence of this phenomenon might be in recipient cancer cells. Our findings reveal a hitherto unappreciated role for a UPR-based intercellular signaling mechanism within tumors through which tumor cells gain fitness and the capability to cope with metabolic, proteotoxic, or genotoxic stress. Additionally, because spatial heterogeneity in UPR activation within a tumor correlates

with tumor growth rates (152), the phenomenon may ultimately contribute to the clonal heterogeneity and fitness of tumor cells in vivo.

RESULTS

Prostate cancer cells transmit ER stress to homologous and heterologous cancer cells

We generated conditioned medium, herein called TERS-conditioned medium (TERS CM), using the human prostate cancer cell line PC3 cultured with the sarco/endoplasmic reticulum Ca^{2+}-ATPase (SERCA) inhibitor thapsigargin (Tg) as previously described (136). Unstressed homologous PC3 cells (Fig. 2.1, A and B) or heterologous DU145 cells (Fig. 2.1.C) were cultured in TERS CM or CM from vehicle-treated (control) cells (Veh CM) for five days. These "recipient" cells were harvested on days 1, 3 and 5, and analyzed by RT-qPCR for the expression of three key UPR genes: *GRP78*, spliced *XBP-1* (*XBP-1s*) and *CHOP (*Fig. 2.1, A and C). GRP78 protein abundance was also analyzed by Western blot (Fig. 2.1.B). TERS CM treatment engaged a global UPR in both cell lines throughout the five-day culture period as well as promoted inflammation, as determined by gene expression for *IL-6* (Fig. 2.1.D) in PC3 treated cells. ER stress transmission was not limited to human prostate cancer cells; the same phenomenon occurred in other human cancer cell lines, including breast and pancreatic cancer cells. This suggests that transmissible ER stress, as a phenomenon, is not restricted to only affect receiver myeloid cells and it is independent of the type of transmitting and receiver cancer cells.

The ER-resident chaperone GRP78 plays numerous roles in the tumorigenesis of various organs, including the prostate (20). GRP78 also translocates to the surface of prostate cancer cells (148, 149, 153), where it serves as a signaling molecule for cell

growth by activating phosphoinositide-3-kinase (PI3K) (148, 149). The two-day treatment with TERS CM markedly increased cytoplasmic expression of GRP78 (Fig. 2.1.E). By staining for the C-terminus of GRP78, which is surface exposed upon translocation to the cell membrane (154), we found that TERS CM provided a progressive translocation of surface GRP78 (sGRP78) that began on day 3 and persisted through day 5 (Fig. 2.1.F). This suggests that TERS may be a stimulus to induce the translocation of GRP78 to the cell surface.

TERS endows recipient tumor cells with a unique UPR

We reasoned that because TERS CM induced the progressive translocation of the ER-resident chaperone GRP78 to the cell surface, a short-term exposure to TERS CM could alter ER function and dynamics. Tumor cells in vivo may be subject to UPR-based cell-nonautonomous effects in a transient and possibly iterative manner as a result of cell-intrinsic or tumor microenvironment-borne perturbations (4, 143). To mimic the stochastic way ER stress transmission amongst cancer cells may occur in vivo*,* naive PC3 cells were treated with TERS CM or vehicle CM for two days followed by a two-day rest period in standard growth medium to enable the resolution of ER stress (Fig. 2.2.A). At the end of the rest period, we noted that PC3 cells had a substantial increase in sGRP78 expression (Fig. 2.2.B). In light of previous reports which found that this translocation corresponds with improved cytoprotection and chemoresistance (155-157), we provisionally conclude that sGRP78 abundance in TERS CM-cultured cells was reflective of a functionally unique population potentially better able to cope with a subsequent UPR. We termed these cells “TERS-primed”, because this ER stress adaptation is reminiscent of earlier observations that cells exposed to protracted mild ER stress undergo an adaptive UPR (158).

To study the consequences of TERS priming on the response to physiological tumor microenvironmental stressors, TERS-primed and vehicle-primed PC3 cells were challenged by nutrient deprivation through culture in glucose- and serum protein-free medium for 48 hours. TERS-primed cells had increased protein abundance of GRP78 compared with vehicle-primed cells both in normal as well as nutrient-deprived conditions despite the fact that nutrient starvation markedly increased GRP78 in vehicle-primed cells (Fig. 2.2.C). We, interestingly, also found reduced transcriptional activation of UPR genes in the TERS-primed cells. The differential expression of GRP78 led us to investigate whether PERK was also differentially affected between TERS- and vehicle-primed cells. In nutrient (glucose and serum)-deprived conditions, we found a distinct decrease in the amount of phosphorylated PERK and eIF2α in TERS-primed cells relative to vehicle-primed cells (Fig. 2.2.D). TERS-primed cells also displayed a marked reduction in the abundance of ATF4 and the downstream protein CHOP during nutrient deprivation (Fig. 2.2.D). Of note, the PERK pathway in TERS-primed cells was repressed in standard cell culture conditions as well relative to vehicle-primed cells. These findings suggested that TERS priming differentially affects PERK pathway activation, providing protection from CHOP-mediated apoptotic signaling due to diminished ATF4 activation. We quantified the viability of vehicle- or TERS-primed PC3 cells cultured in glucose/serum-depleted or glucose/serum-replete, by annexin V apoptosis staining and found that cell survival was greater in TERS-primed cultures than in vehicle-primed cultures (Fig. 2.2.E). This cytoprotection against nutrient starvation similarly occurred in TERS-primed DU145 and LNCaP cells. These findings demonstrate that TERS signaling improves recipient cancer cells' ability to survive amidst nutrient starvation that is common in the tumor microenvironment.

TERS-primed cells are protected against proteasome inhibition-mediated toxicity

Bortezomib (Velcade) is a proteasome inhibitor used in the treatment of multiple myeloma (159) and is also proposed for the treatment of solid tumors, including prostate cancer (160, 161). Its mechanism of action involves the induction of unresolvable ER stress, leading to apoptosis (162). We investigated whether TERS priming also impinges on bortezomib-mediated cytotoxicity. The treatment of bortezomib increased total GRP78 levels in both vehicle- primed and TERS-primed PC3 cells. However, TERS-primed cells maintained increased protein abundance throughout the titration of the drug (Fig. 2.3.A). These results confirm that bortezomib induces a UPR and that TERS-primed cells display a larger amount of GRP78 during bortezomib-induced stress. We found a similar trend in relation to surface abundance of GRP78: bortezomib treatment increased sGRP78 in vehicle-primed cells, albeit modestly, as well as in TERS-primed cells relative to unstimulated conditions (Fig. 2.3.B). However, bortezomib treated TERS-primed cells displayed a marked increase in sGRP78 over bortezomib treated vehicle primed cells (Fig. 2.3.B). The cytotoxicity of bortezomib is reportedly mediated through ATF4-dependent activation, whereas IRE1α signaling is dispensable for its effects (163). We therefore compared the relative PERK response between TERS-primed and vehicle-primed PC3 cells after bortezomib exposure. Whereas there appeared to be relatively comparable amounts of phosphorylated PERK and eIF2α in bortezomib-treated, TERS- or vehicle-CM cultured cells, TERS-primed cells had substantially reduced abundance of ATF4 and CHOP protein relative to vehicle-primed cells in response to bortezomib (Fig. 2.3.C). Because GRP78 and ATF4 can play cytoprotective roles, we probed the viability of TERS- or vehicle-primed PC3 cells in response to bortezomib. TERS-primed cells had improved survival over vehicle-primed cells across a 2-log titration of bortezomib (Fig. 2. 3.D). TERS-primed DU145 and LNCaP cells were similarly protected against bortezomib.

We next probed the durability of TERS-induced cytoprotection in bortezomib cytotoxicity. We reasoned that increased GRP78 abundance signaled the presence of an adaptive UPR pursuant to TERS priming, providing cells with a greater ability to cope with bortezomib cytotoxicity. Although GRP78 abundance decreased under both conditions in the 5 days after cells were rested (meaning, returned to normal medium), GRP78 was maintained at a greater abundance in TERS-primed cells than in vehicle-primed cells (Fig. 2.3.E). This correlated with persistent cytoprotection from bortezomib (Fig. 2.3.F).

TERS protects against non-UPR mediated cytotoxicity

Cytoprotection from UPR-inducing *noxae* prompted us to investigate if TERS-primed cells are also protected against genotoxicity. Paclitaxel, a microtubule stabilizer that is frequently used to treat patients with various types of solid tumors, including prostate cancer, did not induce transcriptional activation of the UPR in either vehicle- or TERS-primed PC3 cells, on the basis of UPR-related gene expression (Fig. 2.4.A) or protein abundance (Fig. 2.4, B and C). Although this is at odds a previous report that found paclitaxel initiates a UPR (164), cell- and tissue-specific differences may account for the discrepancy. We then determined the effect of TERS priming on paclitaxel-mediated cytotoxicity. Forty-eight hours after treatment, the percentage of apoptotic cells in vehicle-primed PC3 cells was markedly higher than that in TERS-primed PC3 cells (Fig. 2.4.D).

Paclitaxel promotes apoptosis in part by causing cell cycle arrest in the form of a mitotic block in early M phase or, for those cells progressing through aberrant mitosis, in G1 (165, 166). Because TERS-mediated resistance to paclitaxel appeared to be independent of ER stress induction, we explored the possibility that TERS priming affects the cell cycle. A BrdU analysis revealed that unstimulated TERS-primed cells were twice as enriched in the G2/M phase compared with vehicle-primed cells (Fig. 2.4.E), suggesting

that the cytoprotective effect of TERS derives from preventing progression through the M phase. Because the G2/M phase arrest enables DNA damage repair during the cell cycle before mitotic entry in response to genotoxic stress (167), we also explored whether TERS priming affects the DNA damage response caused by paclitaxel. Staining for γ-H2AX, a marker for double-stranded DNA breaks, was detected in response to paclitaxel in both vehicle- and TERS-primed PC3 cells, but TERS-primed cells had fewer γ-H2AX foci per cell than did vehicle-primed cells (Fig. 2.4.F). Collectively, we infer that these findings suggest that TERS protects cancer cells against DNA damage during chemotherapy-induced genotoxicity.

TERS promotes β-catenin-mediated Wnt signaling

One possible mechanism accounting for cytoprotection and an enrichment in the G2/M phase could be the activation of Wnt signaling, given that it has already been demonstrated that Wnt signaling is predominant during the G2/M phase (168). Specifically, we thought that TERS could stabilize β-catenin, a subunit of the cadherin protein complex and an intracellular signal transducer of the Wnt pathway (169, 170). We analyzed PC3 cells cultured in TERS CM over 5 days and monitored the transcriptional activation of *CTNNB1* and its negative regulator, *AXIN2* (171). We found that TERS CM modestly increased *CTNNB1* transcription on day 1 which continued to increase on days 3 and 5. TERS CM also increased the transcription of *AXIN2* the latter days (Fig. 2.5.A). As *AXIN2* activation occurred on day 3, the delayed kinetics suggested that TERS activation of the Wnt pathway is unlikely to involve a Wnt ligand. To better elucidate the kinetics of TERS-mediated Wnt signaling, we transduced PC3 cells with the T-cell factor (TCF) optimal promoter (TOP) reporter system, which expresses green fluorescent protein (GFP) when TCF is transcriptionally activated by the nuclear translocation of β-catenin

(172-174). We observed reporter activation in these cells within 24 hours of treatment with GSK-XV, a small molecule inhibitor of glycogen synthase kinase-3 (GSK-3), which stimulates Wnt signaling (175). Progressive activation of the TOP reporter was observed throughout TERS priming (Fig. 2.5.B). From these data thus far, we concluded that TERS activates Wnt signaling and likely does so independently of a canonical Wnt ligand (176). To elucidate whether Wnt signaling provides cytoprotection, we treated LNCaP cells with human recombinant, soluble WNT3a protein (rWNT3a) for two days and then challenged them with either nutrient deprivation, bortezomib, or paclitaxel. Wnt signaling provided cytoprotection from nutrient deprivation but not from bortezomib or paclitaxel (Fig. 2.5.C). Surprisingly, rWNT3a provided no protection against paclitaxel but only against nutrient starvation. This direct way to drive Wnt signaling perhaps provides adaptive responses in cells, which do not entirely mimic TERS-mediated cytoprotection.

The observation that TERS initiates Wnt signaling is, to our knowledge, the first to suggest a link between the UPR and Wnt signaling. To see whether UPR signaling is necessary *per se* for TERS-mediated Wnt stimulation, PC3.TOP cells were cultured in TERS CM for 48 hours in the absence or presence of either an IRE1α inhibitor [4μ8C (177)] or a PERK inhibitor [GSK2656157 (178)], and probed for Wnt signaling using the TOP reporter system by flow cytometry. IRE1α inhibition prevented TOP expression whereas PERK inhibition had no effect (Fig. 2.5, D and E). This finding suggested that TERS induces Wnt signaling through IRE1α activation. To determine if ER stress is per se sufficient to drive Wnt signaling we treated PC3.TOP cells with the canonical ER stress inducer tunicamycin (5 μg/ml) for 48 hours with or without 4μ8C or GSK2656157, and analyzed TOP reporter expression. Tunicamycin did not induce TOP reporter expression (Fig. 2.5.F), indicating that TERS-induced Wnt signaling may not occur through ER stress. That IRE1α activity was necessary for TERS-mediated Wnt signaling led us to hypothesize

that IRE1α's role in TERS-induced Wnt induction was independent of its function in ER stress signaling. To investigate this hypothesis, we incubated PC3.TOP cells with rWNT3a and either 4μ8C or GSK2656157 (Fig. 2.5.G). Unexpectedly, 4μ8C inhibited TOP expression whereas GSK2656157 had no apparent substantial effect. These findings suggest that TERS-induced Wnt signaling in recipient cancer cells is not simply attributable to pharmacologically induced ER stress, but is nevertheless dependent on IRE1α signaling. The precise mechanism(s) and their influence in TERS-mediated cytoprotection remains to be fully determined.

Because β-catenin can transcriptionally activate telomerase reverse transcriptase (TERT) (179) and TERT is reportedly cytoprotective independent of the catalytic activity of telomerase (180, 181), we hypothesized that the cytoprotective effects of TERS could be due to activation of TERT, potentially via β-catenin. To this end, we probed the effect of TERS on TERT. We found no change in *TERT* transcription in PC3 cells cultured in TERS CM for 48 hours (Fig. 2.5.H). To confirm this finding, we used a luciferase reporter gene assay for the *TERT* promoter (182). In repeat experiments, transiently transfected LNCaP cells cultured in TERS CM for 48 hours showed no evidence of *TERT* promoter activation (Fig. 2.5.I). However, in parallel treatment conditions, cells transfected with a luciferase reporter gene for the *ATF6* promoter had robust activation (Fig. 2.5.I), ruling out confounding effects associated with transfection or with the potency of TERS CM. In light of these results, we then explored the possibility that the transmission of ER stress could cause the redistribution of TERT inside the cells. Previous studies showed that during oxidative stress (183) or after treatment with thapsigargin (181), TERT gradually accumulates in the cytoplasm where it allegedly plays cytoprotective roles. Indeed, by confocal microscopy, TERS CM-cultured PC3 cells showed a marked accumulation of the TERT protein in the cytoplasm compared with vehicle CM-cultured cells (Fig. 2.5.J).

Collectively, these findings show a correlation between TERS and cytoplasmic TERT accumulation, which could not be established as a causal relationship between β-catenin and TERT relocalization to the cytosol. Nor could we establish whether the β-catenin/Wnt/TERT axis is the sole mechanism responsible for cytoprotection. Further exploration will need to address this issue.

The PERK pathway mediates TERS-induced cytoprotective effects

Next, we sought to better understand the mechanism behind TERS-mediated cytoprotection, which cannot be fully explained through the Wnt axis. In our initial experiments, we had noted that the PERK pathway was differentially affected in TERS-primed cells relative to control cells by there being a marked decrease in ATF4 and CHOP protein, particularly during nutrient starvation and bortezomib stress conditions. These findings may each explain cytoprotection by TERS, independent of Wnt signaling. Concordantly, the PERK pathway, and its downstream effector ATF4, have been implicated in pro-survival signaling during nutrient deprivation (184, 185), bortezomib (163) and paclitaxel (186) cytotoxicities. We, therefore, hypothesized that the PERK pathway is central to the facilitation of TERS induced cytoprotection. We leveraged mouse embryonic fibroblasts (MEF) to first confirm that the TERS-induced cytoprotective effects existed in non-transformed cells. Wild-type MEF cells were cultured in vehicle CM or TERS CM generated from murine prostate cancer TRAMP C1 (TC1) cells and then challenged for 48 hours by either nutrient starvation, bortezomib, or paclitaxel, and cell viability was determined by 7AAD exclusion. TERS-primed MEF cells survived better than their vehicle-primed counterpart in each stress condition (Fig. 2.6.A), confirming that TERS is not restricted to cancer cells. We next challenged *PERK* KO MEFs using the

same approach and found that the cytoprotection gains in wild-type cells was lost in each instance (Fig. 2.6.B). This demonstrates that the PERK pathway is key to the cellular adaptation induced by TERS, which leads to improved cell survival. On the other hand, we found that the role of IRE1α and ATF6 was not as unambiguous, in that *IRE1α* and *ATF6* KO MEFs did not have complete loss of cytoprotection across the three challenge conditions as it was in the case of *PERK* KO cells. We conclude that while IRE1α and ATF6 likely play contributory roles towards cytoprotection, perhaps through cross-communication amongst the arms of the UPR, PERK signaling is centrally involved in mediating the cytoprotective effects of TERS priming. Our findings recognize PERK as the central facilitator of TERS-mediated cytoprotection.

To further validate this finding, we leveraged CRISPR/Cas9 technology to target *ATF4*, which we found to be downregulated during TERS priming (Fig. 2.2.D, 2.3.C). We designed guides targeting exon 2 of the *ATF4* gene using the px458 Cas9 plasmid (Fig. 2.6.C). Transfected 293XT cells were positively sorted on the basis of GFP positivity. Selected clones were confirmed for deletion of the target exon by PCR blot analysis (Fig. 2.6.D). *ATF4* deletion appeared to inhibit TERS-induced cytoprotection in recipient 293XT cells versus their wild-type counterparts (Fig. 2.6, E and F). Together, these data demonstrate that the UPR, and particularly the PERK-ATF4 axis, are necessary for TERS-mediated cytoprotection.

TERS-primed cells are more tumorigenic in vivo

Because TERS enabled cells to better cope with various *noxae* in culture, we hypothesized that TERS could provide cancer cells with growth advantage over naive cancer cells in a co-culture system. To this end, we tagged murine TC1 cells through stable transduction with a red fluorescence protein (RFP) gene driven by the CMV

promoter. Tagged or untagged TC1 cells were then separately primed with TC1 vehicle or TERS CM, respectively (Fig. 2.7.A). The cell populations were then admixed and separately challenged with one of the following conditions: thapsigargin, 2 deoxy-D-glucose, bortezomib, or paclitaxel. After a 24 hour challenge, we measured the relative percentage of live cells among RFP positive *vs.* negative cell populations. TERS-primed TC1 cells emerged as the prevalent cell population in each challenge condition (Fig. 2.7.B). To control for any confounding factors due to ectopic RFP expression, priming conditions were reversed (meaning TC1.RFP were TERS-primed and TC1 were vehicle-primed) and co-cultured with identical challenges. Thus, we conclude that TERS-primed cancer cells have a survival advantage over control cells, a conclusion that could bear considerable relevance to cell dynamics in the tumor microenvironment.

To test this possibility in vivo, we injected TERS-primed or vehicle-primed murine TC1 cells subcutaneously into C57BL/6 mice. To eliminate host variability, TERS-primed and vehicle-primed cells were injected into opposite flanks of the same mouse. TERS-primed tumors became palpable on day 8 while control tumors emerged only after 14 days (Fig. 2.7.C). On day 19 post-injection, the average volume of TERS-primed tumors was substantially larger than vehicle-primed tumors. At sacrifice (day 30), tumors derived from TERS-primed cells were significantly greater in weight (Fig. 2.7.D) and size (Fig. 2.7.E) than those derived from vehicle-primed cells. As TERS-primed cells had no proliferative advantage over vehicle-primed cells, as reflected in lack of enrichment in G1 phase (Fig. 2.4.E), we conclude that the advantage of TERS-primed tumors over vehicle-primed tumors was the consequence of acquired adaptive fitness.

DISCUSSION

A UPR-based cell-nonautonomous regulation of tumorigenesis is an emerging concept in tumor biology and immunobiology (143, 151). This new idea stems from the observation that cancer cells experiencing a UPR release soluble factor(s) able to reproducibly transmit ER stress and elicit a UPR in $CD11b^{+}$ macrophages and dendritic cells (119, 136, 144, 187). Here, we demonstrate that a similar intercellular signaling event confers a pro-survival phenotype and clonal fitness to cancer cells upon challenge with microenvironmental and exogenous stressors.

One aspect of this TERS-induced phenotype was the initiation of Wnt signaling. β-catenin is a central effector of the Wnt pathway and is involved in diverse cellular processes, including growth, differentiation, and transcription of Wnt responsive genes (169, 170, 188), while driving the expression of several oncogenes, e.g., *c-Myc, Cyclin D1* and *Nos2* (189-191). TERS-mediated Wnt signaling activation required IRE1α. Since canonical ER stress conditions did not mimic this effect, we conclude that TERS-mediated Wnt signaling activation is unique. Although Wnt signaling driven by recombinant WNT provided cytoprotective effects during nutrient starvation, this phenomenon may be independent from, or unrelated to, TERS-mediated cytoprotection. The full interaction and dynamics of the TERS/Wnt pathways remain to be fully elucidated. Interestingly, Wnt signaling was recently shown to occur in circulating prostate cancer cells of patients with antiandrogen resistance (192).

A salient finding of our study is the marked decrease in PERK-ATF4 activation in TERS-primed cells. While unexpected this finding provided a possible clue into the mechanism of cytoprotection. The activation of the PERK pathway leads to the transcription and translation of ATF4, which itself coordinates the activation of the downstream target CHOP to drive apoptosis (47). Here we show that in TERS-primed cells, this classical cascade of events was substantially decreased since TERS-primed

cells subject to nutrient deprivation or bortezomib treatment showed a pattern of ATF4 and downstream CHOP reduction. While it has been reported that ATF4 can be regulated independently of the stress response (193), our data support a central role of the PERK-ATF4 axis in TERS induced cellular fitness. In this context, we found that the pro-survival adaptive response to TERS required the attenuation of PERK and ATF4 activation, an effect lost through the deletion of the *PERK* or *ATF4* genes. Arguably, TERS may fine tune ATF4 to promote cytoprotection. In support of our conclusion mild ER stress conditions were reported to promote the degradation of two downstream ATF4 targets, CHOP and GADD34, and lead to cellular adaptation and survival (158). More importantly, a slow translation of ATF4 was found to confer cytoprotection (194), presumably by preventing the activation of CHOP. Thus, because ATF4 can exert opposing roles in controlling cell fate (survival vs. apoptosis), depending on its state of activation and abundance, we view ATF4 as a cellular rheostat able to gauge the effects of TERS in receiver cancer cells.

Other effects may also contribute to cytoprotection in TERS-primed cells. One possibility is the progressive increase in surface expression of GRP78 induced by TERS priming. GRP78 is considered the master regulator of the UPR (65, 195) and has been directly implicated in tumor progression in murine models of cancer (146, 196, 197). High levels of GRP78 predict poor prognosis in a variety of carcinoma (198), the development of therapy resistance, and cancer recurrence (60). GRP78 surface expression, while a relatively less characterized phenomenon (155, 199), has been shown to mediate growth signals for cancer cells through PI3K/AKT signaling and promote chemoresistance (148, 149, 200). Since surface relocalization of GRP78 was not associated with increased transcription, it is possible that TERS signaling induces post-translational modifications of GRP78 to improve its overall function and stability, for instance through AMPylation of

threonine 518 (201). Interestingly, a mild adaptive UPR promotes GRP78 protein half-life stability while not affecting its gene transcription (158). This demonstrates that some UPR driven stimuli favor the stabilization of GRP78 as we observed in our durability experiments (Fig. 2.3, E and F). The abundance of the GRP78 chaperone would allow cells to better cope with subsequent pressures. Thus, a second possibility is that TERS-induced adaptive fitness reflects a stable level of chaperones. A final alternative mechanism to explain cytoprotection is TERT, which we found to accumulate in the cytoplasm. Through its noncanonical functions (202), TERT protects cells from apoptosis, enhances genomic stability and DNA repair (203), and attenuates ER stress induced cell death (180). The mechanisms of TERS on receiver cells discussed above are summarized in the model shown in Fig. 8.

The cell-extrinsic effects of the tumor UPR represent a novel mechanism through which cancer cells adapt to tumor microenvironmental *noxae* (hypoxia, nutrient starvation, biosynthetic errors, and viral infection) and apoptosis-inducing chemotherapeutic agents. An unresolved aspect of our work concerns the exact chemical nature and identity of TERS. Undergoing studies show that TERS is present at remarkably low abundance in cancer cell conditioned medium, making it particularly arduous to isolate to purity. Recent reports emphasized the role of byproducts of lipid oxidation (204, 205) as responsible actors in phenomena closely related to TERS. However, we have verified that by mass spectrometry and bioactivity assays TERS is not the products claimed in these reports, but is instead a unique factor yet to be conclusively isolated. While work on the final identification of TERS is continuing, the results of the present study show that a UPR-based cell-nonautonomous regulation amongst cancer cells endows receiver cells with cellular fitness by exerting a selective pressure. Because cytoprotection is relatively durable, one can also predict that daughter cells of the initial receiver cells may also be

protected, suggesting that transmissible ER stress may have epigenetic consequences on target cells. In light of the unique regulation of both UPR- and Wnt-related genes, it is likely that TERS affects other cellular processes, such as autophagy, which may also bolster cell survival. Of note, TERS-primed cells did not have a proliferative advantage over vehicle-primed cells but rather a fitness advantage. Therefore, the persistence of a TERS-primed population within the tumor microenvironment may lay dormant until a new selective pressure initiates the emergence of the fittest clones.

Our findings corroborate the conclusions of recent reports that showed that individual tumor cells within a uniform genetic lineage can acquire functionally different behaviors in vivo, implying that functional clonal diversity may in fact reflect the outgrowth of cells with greater fitness and extended survival generated by cell-nonautonomous signaling and processes (206, 207). Accordingly, future management of cancer should take into consideration these new aspects of cancer cell dynamics within the tumor microenvironment.

FIGURES

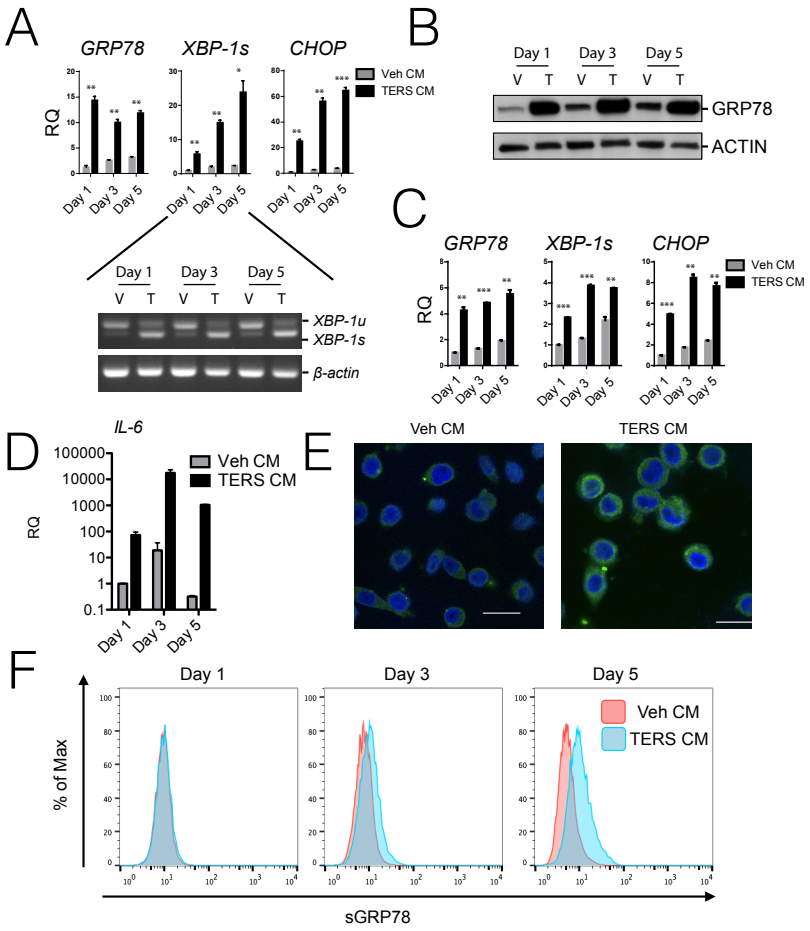

Figure 2.1. **Prostate cancer cells undergoing ER stress can transmit a ER stress response to recipient cells. (A)** Expression of the indicated mRNA (RT-qPCR) in PC3 cells cultured for 1, 3 or 5 days in vehicle- or TERS-conditioned medium (Veh CM; TERS CM) (n=2 per condition). Gene expression was normalized to Veh CM day 1 condition to determine relative quantification (RQ). * $P < 0.05$ ** $P < 0.01$ *** $P < 0.001$, paired two-tailed Student's t-test. Inset shows gel banding for unspliced *(XBP-1u*) and spliced *(XBP-1s*) *XBP-1.* **(B)** Western blot analysis for GRP78 abundance in whole cell lysates from PC3 cells cultured as described in (A). V, Veh CM; T, TERS CM. **(C)** RT-qPCR in DU145 cells as described in (A) treated with PC3 generated Veh or TERS CM (n=2 per condition). Gene expression was normalized to Veh CM day 1 condition to determine relative quantification (RQ). ** $P < 0.01$ *** $P < 0.001$, paired two-tailed Student's t-test. (**D**) RT-qPCR analysis for *IL-6* expression in PC3 cells cultured with Veh- or TERS-CM as described in A. Values are normalized to Veh-CM day 1 (n=2 per condition). (**E**) Confocal microscopy for GRP78 in PC3 Veh- or TERS-CM treated PC3 cells for 48 hours. Scale bar, 25 μm. (**F**) Flow cytometric analysis of surface abundance of GRP78 (sGRP78) in Veh- or TERS-CM-cultured, unpermeabilized PC3 cells. Error bars are representative of SEM. Panels C-E are representative of two, and panels A, B, and F of three independent experiments.

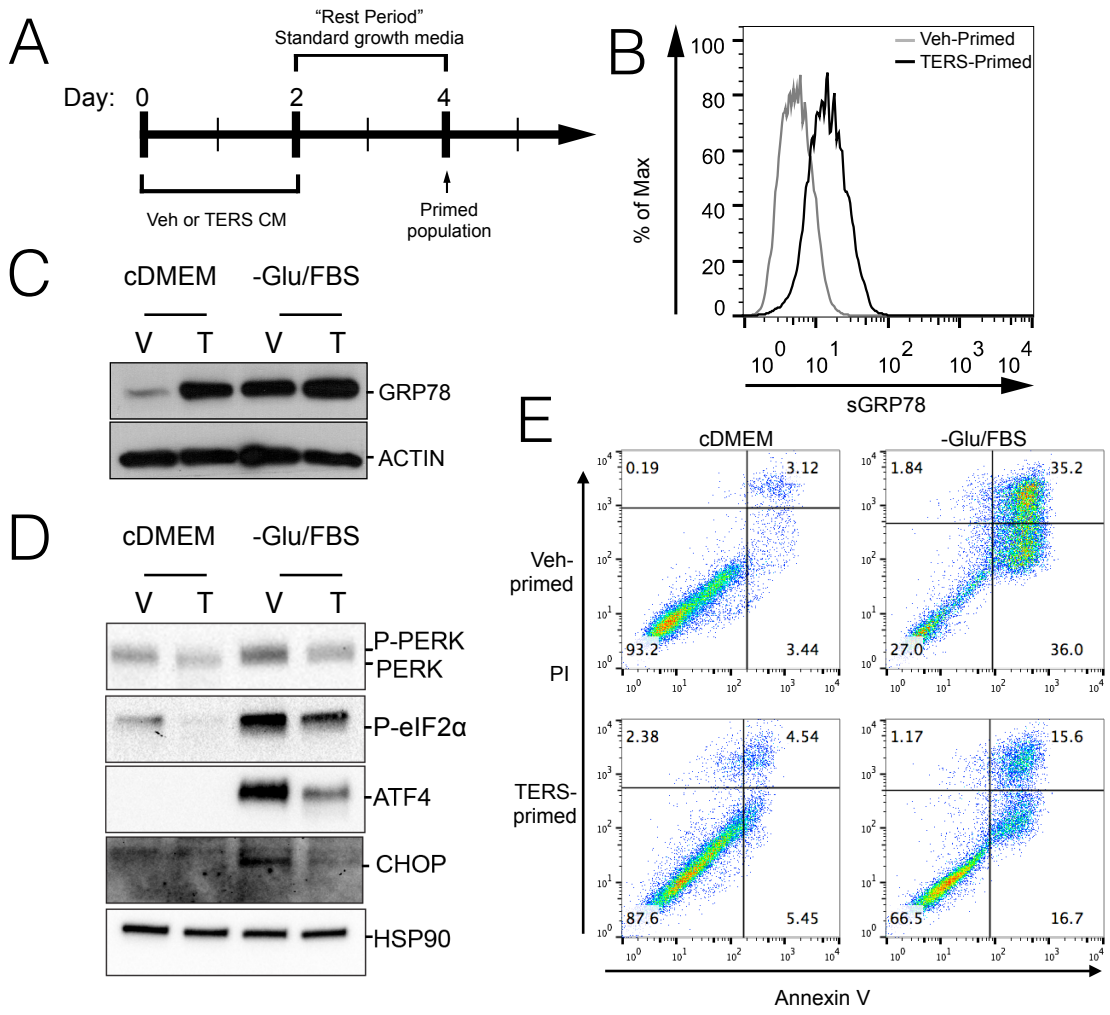

Figure 2.2. **TERS primed cancer cells display a unique UPR and are protected against nutrient deprivation.** (**A**) Treatment design of TERS priming: two-day culture in Veh- or TERS CM followed by two-day rest period. Cells were then challenged and analyzed as indicated. (**B**) Flow cytometric analysis for surface abundance of GRP78 in Veh- or TERS-primed PC3 cells grown in standard growth media. **(C)** Western blot analysis of GRP78 in Veh (V)- or TERS (T)-primed PC3 cells after 48 hours culture in standard growth medium (cDMEM) or in nutrient deprived condition (-Glu/FBS). **(D)** Western blot analysis of proteins of the PERK pathway in V or T primed PC3 cells after 48 hours culture in cDMEM or in -Glu/FBS. **(E)** Apoptosis analysis by flow cytometric detection of annexin V in Veh- or TERS-primed PC3 cells after 48 hours culture in cDMEM or in -Glu/FBS; (each plot represents at least 10,0000 events per condition). Panel D is representative of two, and panels B,C,E of three or more independent experiments.

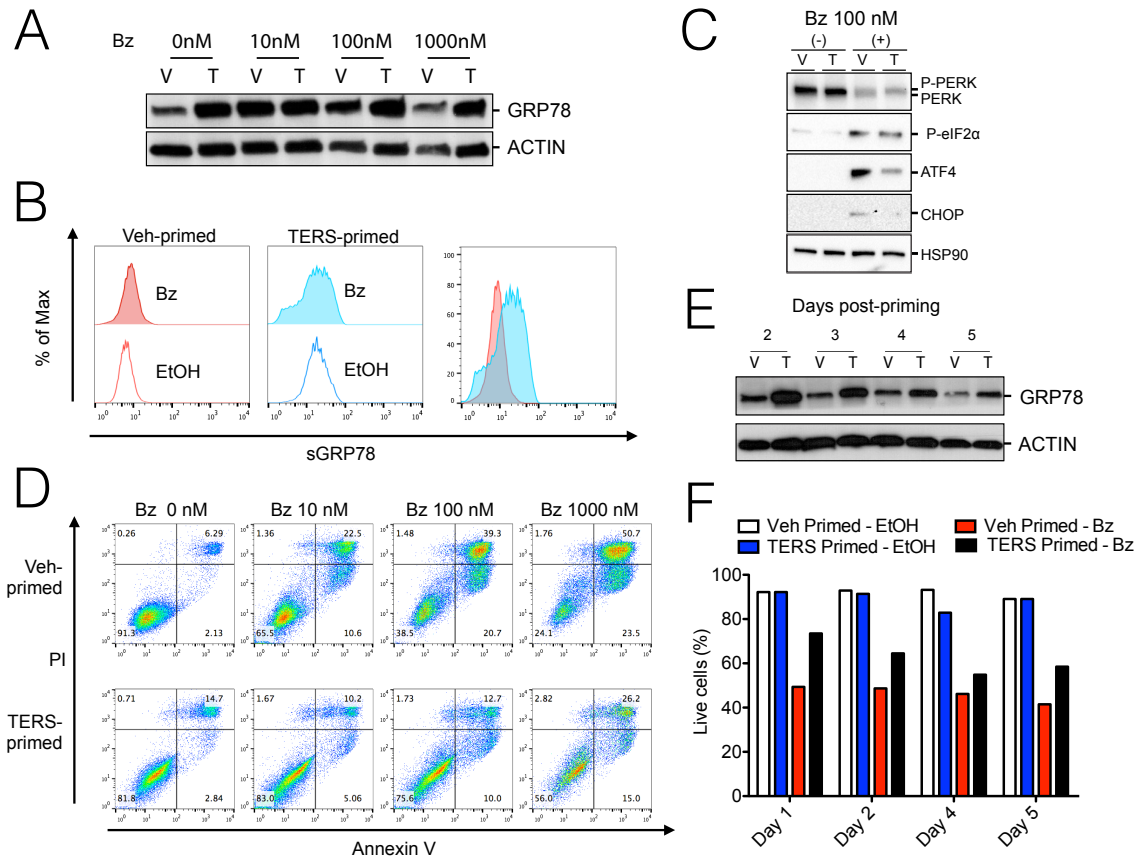

Figure 2.3. Proteasome inhibition mediated cytotoxicity is less effective in TERS primed cells. (**A**) Western blot analysis of GRP78 in Veh (V)- or TERS (T)-primed PC3 cells after 24 hours culture with various concentrations of bortezomib (Bz). (**B**) Flow cytometric analysis for the abundance of GRP78 (sGRP78) on the surface of Veh- or TERS-primed PC3 cells 24 hours after EtOH control solution or bortezomib (Bz; 100 nM) treatment. Data are shown individually and as an overlay for comparison. (**C**) Western blot analysis of PERK pathway proteins of V or T primed PC3 cells 24 hours after addition of Bz. (**D**) Apoptosis analysis by annexin V/PI staining in Veh- or TERS-primed PC3 cells 24 hours after addition of Bz (each plot represents at least 10,0000 events per condition). (**E**) Western blot of GRP78 expression in V or T-primed PC3 cells cultured in cDMEM and harvested at the specified post-priming day. (**F**) Percent live cells determined by flow cytometric analysis of annexin V/PI apoptosis staining in Veh- or TERS-primed PC3 cells treated with EtOH control solution or Bz (100 nM). Panels A, C,E are representative of two, panels B,F of three, and panel D of five independent experiments.

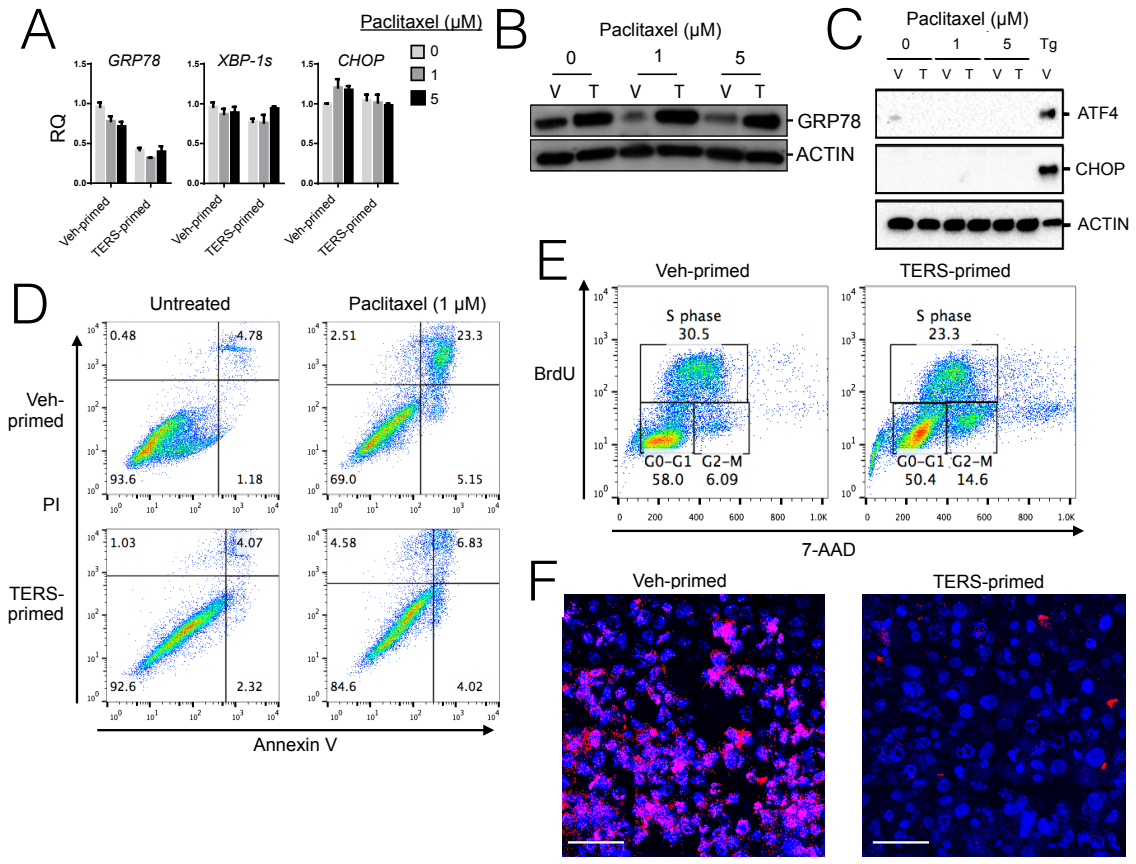

Figure 2.4. **TERS primed cells are protected against genotoxic insults in the absence of ER stress.** (**A**) Vehicle (V) or TERS (T) primed PC3 cells treated with increasing concentrations of paclitaxel and analyzed after 24 hours by RT-qPCR for relative gene expression of UPR genes. Samples were normalized to 0 μM Veh primed gene expression (n=2 per condition). (**B**) Western blot analysis of GRP78 in PC3 primed cells treated with paclitaxel for 24 hours. **(C)** Western blot analysis of PERK signaling in PC3 Veh or TERS primed cells treated with paclitaxel for 24 hours. PC3 cells treated with thapsigargin (Tg; 300 nM) serve as positive control. (**D**) Annexin V apoptosis assay of primed PC3 cells untreated or treated with paclitaxel for 48 hours (each plot represents at least 10,0000 events per condition). (**E**) Cell cycle analysis as determined by BrdU incorporation in Veh- or TERS-primed PC3 cells (each plot represents at least 10,0000 events per condition). (**F**) DNA double stranded breaks visualized through γ-H2AX staining (pink), and imaged by confocal microscopy in Veh- or TERS-primed PC3 cells after 24-hour treatment with Paclitaxel (1 μM). Scale bar, 100 μm. Panels B,C,F are representative of two, and panels A,D, E of three or more independent experiments.

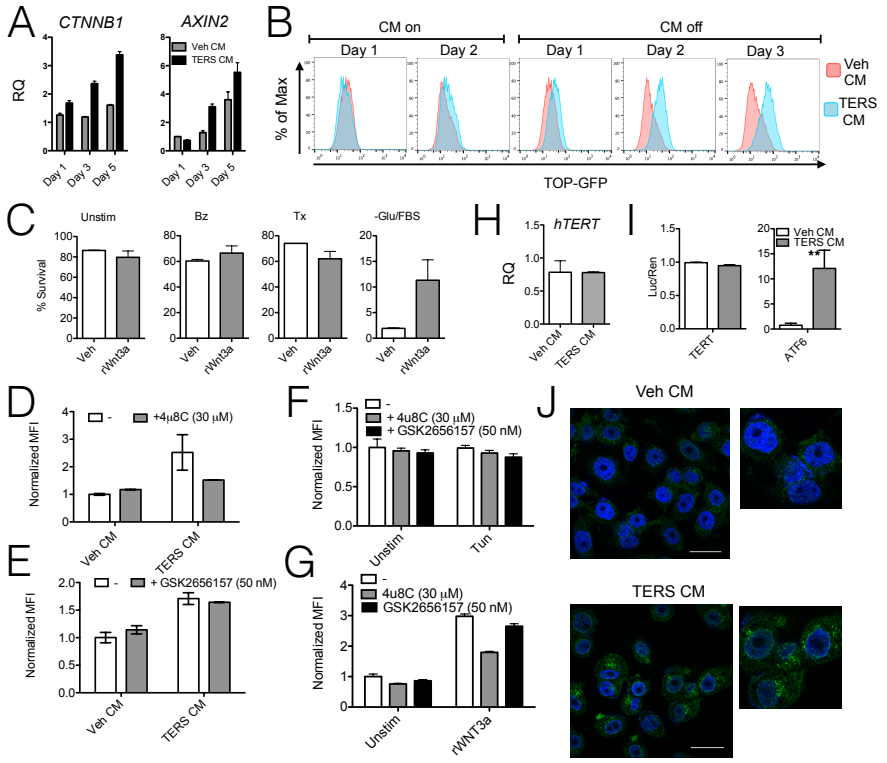

Figure 2.5. **TERS induces WNT signaling and cytoplasmic export of TERT. (A)** RT-qPCR analysis of the transcriptional activation of *CTNNB1* and *AXIN2* of Veh CM or TERS CM treated PC3 cells throughout 5 days of culture with CM resupplementation every other day. Relative quantification (RQ) of gene expression of samples is normalized to Veh CM day 1 condition (n=2 per group). **(B)** TOP-GFP expression of PC3 cells during TERS priming, determined by flow cytometry (at least 10,000 events were analyzed per condition). **(C)** 7AAD-based analysis of viability of LNCaP cells cultured with vehicle (Veh) or recombinant WNT3a (rWNT3a; 20 ng/ml for 2 days) and treated as indicated for an additional 48 hours. Bz, bortezomib (100 nM); Tx, paclitaxel (1 μM); -Glu/FBS, nutrient-deprived medium. PC3.TOP cells treated with Veh CM or TERS CM for 48 hours in the absence or presence of **(D)** the IRE1 inhibitor 4μ8C or **(E)** the PERK inhibitor GSK2656157, and measured for mean fluorescence intensity (MFI). MFI expression was then normalized to Veh CM uninhibited value (n= 2, at least 10,000 events were analyzed per condition). **(F)** Normalized MFI expression of PC3.TOP cells treated with tunicamycin (5μg/ml) for 48 hours during IRE1 or PERK inhibition (n= 2, at least 10,000 events were analyzed per condition). **(G)** Normalized MFI expression of PC3.TOP stimulated for 48 hours with recombinant WNT3a (rWNT3a) (20ng/ml) during IRE1 or PERK inhibition (n= 2, at least 10,000 events were analyzed per condition). **(H)** *hTERT* RT-qPCR analysis of 48 hour Veh- or TERS-CM treated PC3 cells (n=3 per condition). **(I)** Relative firefly TERT promoter-luciferase or ATF6 promoter-luciferase of dually transfected LNCaP cells. Cells were treated to LNCaP Veh or TERS CM for 48 hours and normalized for expression by Renilla-luciferase (n=3 per condition). ** $P < 0.01$ Student's t test (paired two-tailed). **(J)** Immunofluorescent staining for TERT in 48 hour treated PC3 cells. Scale bar, 25 μm. Error bars represent SEM. Panels C,D,H are representative of two, and panels A,B,F,G,I of at least three independent experiments.

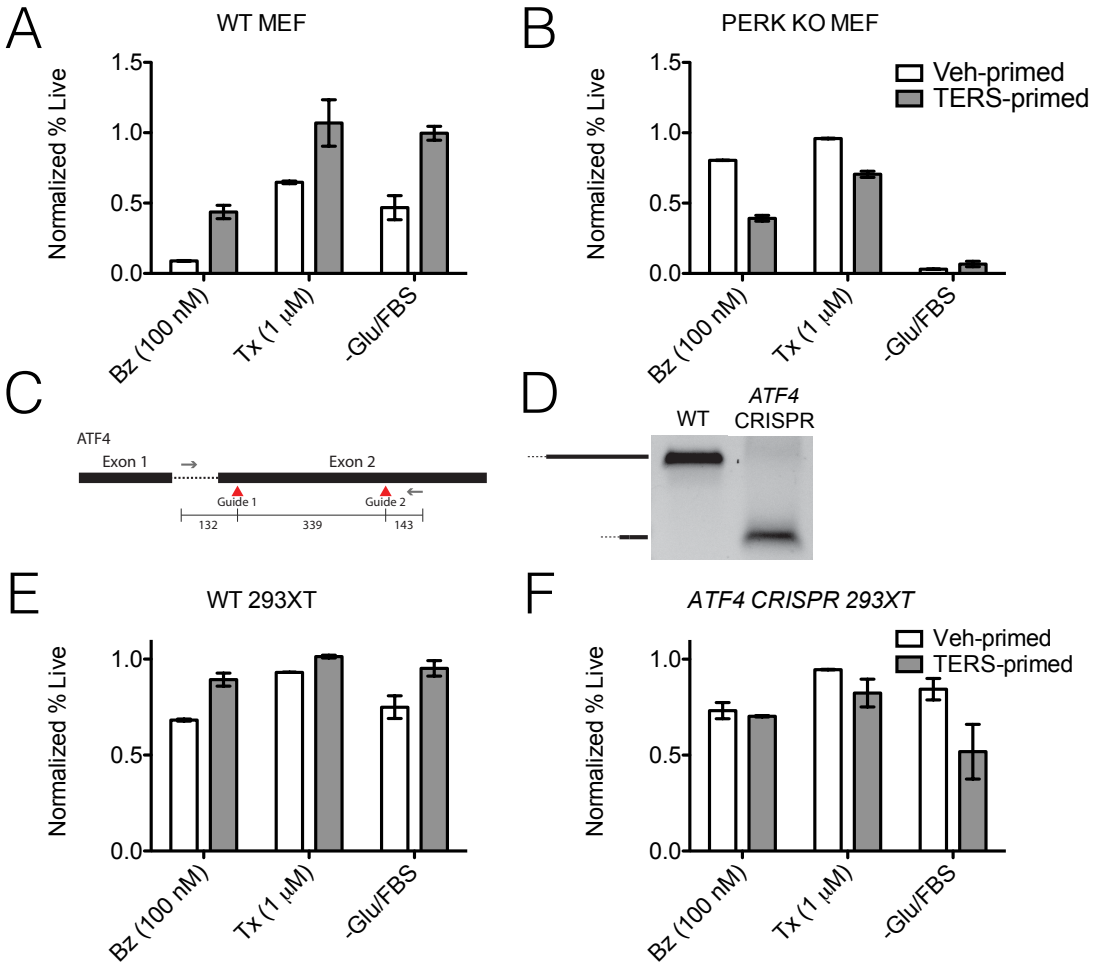

Figure 2.6. **PERK signaling is necessary for TERS-mediated cytoprotection. (A)** Survival of (**A**) wild type (WT) or **(B)** PERK KO MEFs primed by TC1 Veh or TERS CM and challenged for 48 hours as specified (Bz, bortezomib; Tx, Paclitaxel). Survival determined by flow cytometric analysis via 7AAD exclusion. Percent (%) survival calculated by normalizing the percent live ($7AAD^-$) population of the unstimulated condition for each line (n=2 per group, at least 10,000 events analyzed per condition). **(C)** CRISPR/Cas9 design of guide targets within the *ATF4* gene. **(D)** PCR detection of *ATF4* WT and *ATF4* CRISPR 293XT cells. **(E)** WT 293XT and **(F)** ATF4 CRISPR 293XT cells were primed with PC3 Veh or TERS CM, and survival measured by 7AAD exclusion after 48 hours of treatment as specified. (n=2 per condition, at least 10,000 events were analyzed per condition). Error bars represent SEM. Panels A,B,D are representative of two, and panels E,F of three independent experiments.

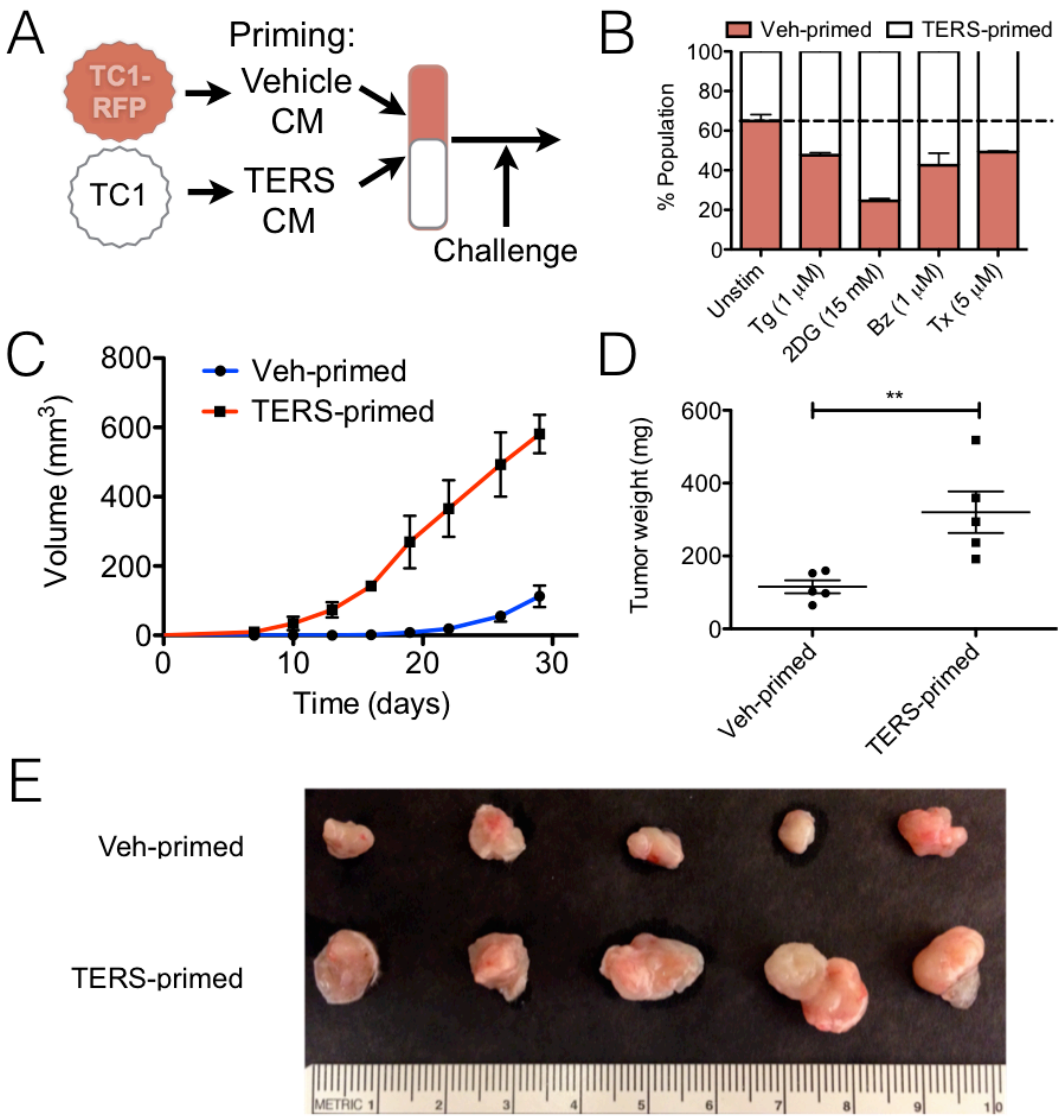

Figure 2.7. **TERS -primed murine prostate cancer cells have improved cellular fitness in vitro and in vivo. (A)** Cartoon of co-culture experimental design. Briefly, RFP-tagged TC1 cells (TC1-RFP) are primed with homologous Veh CM while untagged TC1 cells are primed with TERS CM. After priming, cell populations are co-cultured overnight and subsequently challenged. **(B)** Flow cytometric analysis to determine the percent RFP^+ (Veh primed) and RFP^- (TERS primed) TC1 cells 7AAD excluded after 24 hours treatment with thapsigargin (Tg), 2-deoxyglucose (2DG), bortezomib (Bz) or Paclitaxel (Tx) (n=2 per co-culture, at least 10,000 events were analyzed per condition). **(C)** Growth kinetics of Veh- or TERS-primed TC1 cells subcutaneously injected into immune competent C57BL/6 mice (n=5 per group). **(d)** Weight of Veh- or TERS-primed tumors after 30 days. **(E)** Gross visualization of excised tumors. ** $P < 0.01$ Student's t-test (paired two-tailed). Error bars are SEM. Data are representative of two independent experiments.

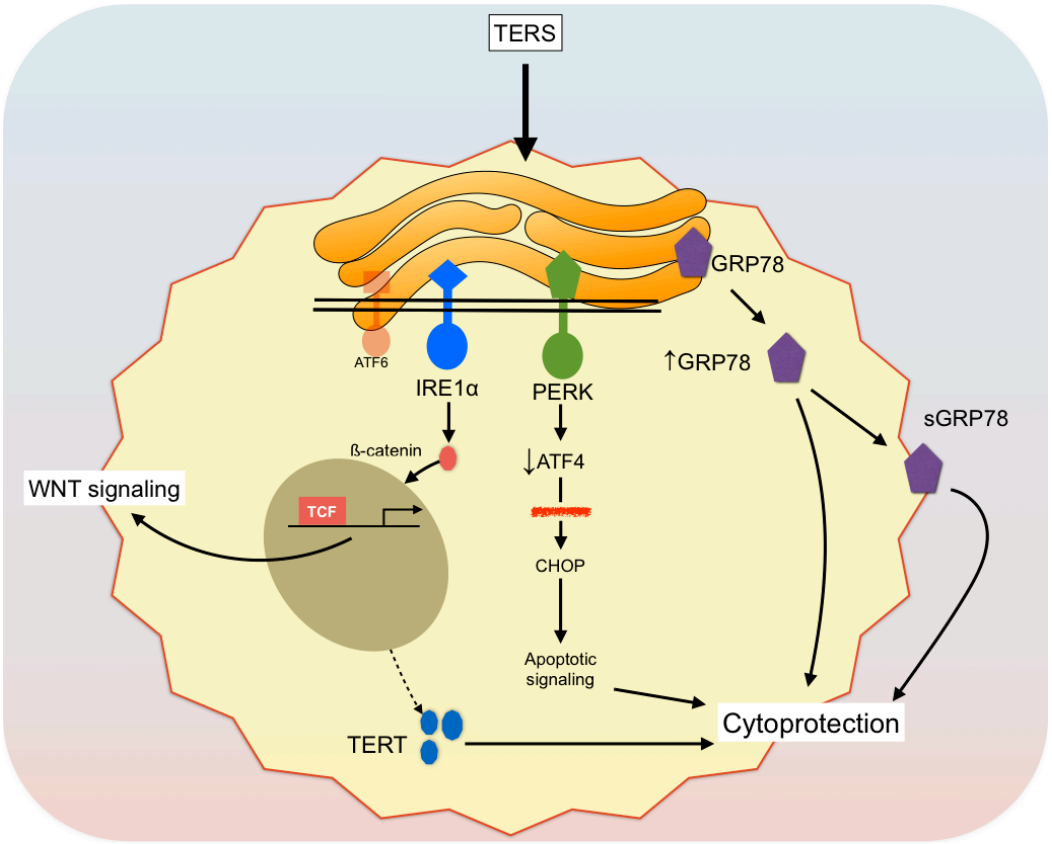

Figure 2.8. Model of TERS mediated signaling in cancer cells. We propose a model in which cancer cells exposed to TERS undergo an adaptive UPR that involves diverse signaling events. One effect is the activation of Wnt signaling. TERS drives Wnt signaling through the activation of the T-cell factor (TCF). This effect appears to be IRE1-dependent. The other relevant event is cytoprotection. In this case, TERS engages PERK but also leads to reduced ATF4 activation. Reduced levels of ATF4 are insufficient to drive a full activation of apoptosis through the downstream CHOP target (red strikethrough). In this respect ATF4 serves as a rheostat for cell survival. TERS also increases the amounts of GRP78, both intracellularly and at the cell surface. Finally, TERS induces the export of TERT to the cytoplasm. These effects, possibly in combination, promote cytoprotection and, ultimately, cell fitness to endogenous (nutrient) and exogenous (chemotherapeutic) stress.

MATERIALS AND METHODS

Cell Lines and cell culture

PC3, LNCaP, DU145, and TC1 prostate cancer cells and 293XT cells were grown in RPMI or DMEM (Corning) supplemented with 10% fetal bovine serum (FBS) (HyClone) and 1% penicillin/streptomycin/L-glutamine, non-essential amino acids, sodium pyruvate, HEPES (cDMEM). All cell lines were maintained at 37ºC incubation with 5% O_2. All cell lines were mycoplasma free as determined PCR assay (Southern Biotech). Mouse embryonic fibroblast (MEF) lines (the kind gift of Dr. Jonathan Lin) were previously derived and described: PERK KO (208), IRE1 KO (49), and ATF6 KO (209). They were cultured in standard cDMEM conditions.

TERS Conditioned Media (CM) Generation

Transmitting cells as specified in each experiment were induced to undergo ER stress through treatment with thapsigargin (300 nM) (Tg; Enzo Life Sciences) for 2 hours. Control cells were similarly treated with an equal volume of vehicle (0.02% ethanol). Cells were washed twice with Dulbecco's PBS (Corning), and then incubated in fresh, standard growth medium for 16 hours. Conditioned medium was then harvested, centrifuged for 10 min at 2,000 RPM, filtered through a 0.22-μm filter (Millipore), and used to treat cells. For TERS priming, conditioned medium was generated from homologous cells unless otherwise specified.

Nutrient starvation studies

To create nutrient starvation conditions, cells were washed x2 with PBS and cultured in Glucose-free DMEM (Gibco) supplemented only with 1% penicillin/streptomycin.

RT-qPCR

RNA was harvested from cells using Nucleospin II Kit (Machery-Nagel). The concentration and purity of RNA were quantified on a NanoDrop (ND-1000) spectrophotometer (Thermo Scientific), and analyzed with NanoDrop Software v3.8.0. RNA was normalized between conditions and cDNA generated using the High Capacity cDNA Synthesis kit (Life Technologies). RT-qPCR was performed on a ABI 7300 Real-Time PCR system using TaqMan reagents for 50 cycles under universal cycling conditions according to the manufacturer's specifications (KAPA Biosystems). Target gene expression was normalized to *β-actin*, and relative expression was determined using the –ΔΔCt relative quantification method. Validated FAM-labeled Human *HSPA5* (GRP78) (Life Technologies, Catalog # Hs00607129_gH), *XBP-1s* (F = 5'-CCGCAGCAGGTGCAGG-3'; R = 5'-GAGTCAATACCGCCAGAATCCA-3')"(Integrated DNA Technologies) *DDIT3* (CHOP) (Life Technologies, Catalog # Hs00358796_g1), *IL-6* (Life Technologies, Catalog #Hs00985639_m1), *CTNNB1* (β-catenin) (Life Technologies, Catalog # Hs00355049_m1), *AXIN2* (Integrated DNA Technologies) (F = 5'-GAC AGT GAG ATATCC AGT GAT GC-3'; R = 5'-GTT TCT TACTGC CCA CAC GAT A-3'), *hTERT* (F = 5'-CGGTTGAAGGTGAGACTGG-3'; R = 5'-GCACGGCTTTTGTTCAGATG -3')"(Integrated DNA Technologies) (Integrated DNA Technologies) and VIC-labeled Human *β-actin* TaqMan primer/probe sets (Life Technologies, Catalog # 4326315E) were used.

Flow Cytometry

Apoptosis assays were performed on single cell suspensions, stained with FITC-conjugated annexin V and propidium iodide using the annexin V FITC Apoptosis Detection

Kit (BD Biosciences). Data were acquired on a FACSCalibur flow cytometer (BD Biosciences) and analyzed using CellQuest Pro (BD Biosciences) and FlowJo software (Tree Star). For surface GRP78 detection, single cell suspensions were washed once with PBS and then stained with goat polyclonal antibody to surface-expressed human GRP78 (Santa Cruz Biotechnology, Catalog #SC-1051). Cells were then washed with PBS and counterstained with FITC-labeled donkey polyclonal antibody to goat immunoglobulin (Ig) (Santa Cruz Biotechnology). Stained cells were washed again with PBS and resuspended in 7AAD staining buffer and analyzed by flow cytometry with 7AAD exclusion. Cell cycle analysis was performed by BrdU per manufacturer's protocol (BD Biosciences).

TOP reporter system

Lentiviral TOP-GFP construct was previously described (174), and was the kind gift of Dr. Karl Willert. PC3 cells were transduced with lentivirus supplemented with polybrene (4 μg/ml; Sigma) for 48 hours. After incubation, cells were cultured in standard growth medium for 24 hours. Positively-transduced cells were selected under puromycin (1 μg/ml) for 2 weeks. PC3.TOP cells were then treated as described and analyzed for TOP activity using a FACSCalibur flow cytometer (Becton Dickinson) probing for GFP expression on 7AAD negative cells. Stimulation of PC3.TOP cells with rWNT3a (20 ng/ml) (Humanzyme) was performed for 48 hours. UPR inhibitors 4μ8C (Axon MedChem) and GSK2656157 (Selleckchem) were used at the dose indicated in Fig. 5.

Promoter Activity Assay

The TERT core promoter luciferase construct was previously designed (182) through the insertion of WT promoter sequence into the pGL4.10 (Promega) vector and was the kind gift of Dr. Joseph Costello (UCSF). The ATF6 luciferase reporter construct

was previously designed (82) and was provided by Dr. Jonathan Lin. Cells were transiently transfected for 18 hours with Lipofectamine 3000 (Thermo Fisher) with either the TERT or the ATF6 promoter construct. For normalization control, cells were concomitantly transfected with a Renilla plasmid driven by the TK promoter (Promega). Transiently transfected cells were washed, treated as specified in text, and subsequently analyzed for luciferase and Renilla expression using the Dual-Luciferase Reporter Assay (Promega) according to manufacturer's protocol.

Confocal microscopy

Cells were plated on glass slides in a tissue culture plate and treated as specified in Fig. 1, 4, and 5. After treatment, the medium was gently removed by aspiration. Cells were then washed with cold PBS and fixed using 4% formaldehyde (Fisher Scientific) for 15 min. The formaldehyde solution was gently removed by aspiration and the cells were washed 3x with PBS. The fixed cells were then blocked/permeabilized with 5% BSA (Fisher Scientific) and 0.3% TritonX-100 (Fisher Scientific) in PBS for 1 hour. Cells were washed 3x with PBS and then probed with antibodies to hTERT (Santa Cruz Biotechnology, Catalog #SC7215), β-catenin (Cell Signaling Technology, Catalog #8480P), or GRP78 (Santa Cruz Biotechnology, Catalog #SC-1050) by incubating at the manufacturer's recommended dilution in PBS-BSA at 4°C overnight. After incubation with the primary antibody, cells were washed 3x with PBS and counterstained with a FITC-conjugated antibody as follows: polyclonal donkey antibody to goat Ig (Santa Cruz Biotechnology) for hTERT, or polyclonal goat antibody to rabbit Ig (Biomeda) for β-catenin and GRP78, in the dark for 1 hour. Cells were then washed 3x with PBS and mounted onto microscope slides using the ProLong Gold Antifade Reagent with DAPI (Invitrogen). Once mounted, the slides were imaged using a BIOREVO BZ-9000 microscope or a Zeiss

LSM510 Laser Scanning Confocal microscope at the UCSD Microscopy Core. Staining for γ-H2AX was performed according to (210).

Western Blot Analysis

After treatment, PC3, DU145, or LNCaP cells were washed with ice cold PBS and suspended in RIPA Lysis Buffer: 1X RIPA buffer and cocktail of protease inhibitors (Santa Cruz Biotechnology). Cell lysates were centrifuged at 16,000xg for 15 min and the supernatants were collected. Protein concentration was determined using the Pierce BCA Protein Assay Kit (Thermo Scientific). Samples were heat-denatured and equal concentrations of protein were loaded onto a 4-20% Mini-PROTEAN TGX Precast Gels (Bio-Rad), electrophoresed and transferred onto 0.2 μm PVDF membrane in Tris-Glycine transfer buffer containing 20% methanol. The membranes were then blocked with 5% non-fat milk in TBS containing 0.1% Tween-20 (TBS-T) for 1 hour at room temperature. The membranes were then incubated with the specified primary antibodies overnight at 4ºC. Membranes were washed for 5 min at room temperature 3x by TBS-T, incubated with a horse radish peroxidase (HRP)-labeled secondary antibody in 5 % non-fat milk for 1 hour at room temperature, and washed for 5 min at room temperature 3x in TBS-T. Bound antibodies were detected by chemiluminescence reaction using Pierce ECL Blotting Substrate (Thermo Scientific). The following primary antibodies were used: mouse monoclonal antibody to human GRP78 (BD Biosciences), rabbit monoclonal antibody to human PERK (Cell Signaling Technology), rabbit monoclonal antibody to phospho-eIF2α (Ser^{51}) (Cell Signaling Technology), rabbit polyclonal antibodies to human ATF4 (CREB-2) (Santa Cruz Biotechnology), mouse monoclonal antibody to human CHOP (GADD153) (Santa Cruz Biotechnology), rabbit polyclonal antibodies to human HSP90 (GeneTex), and HRP-conjugated goat antibodies to β-actin (Santa Cruz Biotechnology). Secondary

antibodies were HRP-conjugated anti-mouse IgG or anti-rabbit IgG (Santa Cruz Biotechnology).

Cell tagging:

The tRFP cDNA was amplified from pTRIPZ plasmid (Open Biosystems) by PCR using specific primer (F: 5'-ttggtaccgagctcggatccGCCACCATGAGCGAGCTG-3' and R: 5'-ccctctagatgcatgctcgagTTATCTGTGCCCCAGTTTGC-3'). The amplified tRFP fragment was purified by agarose gel, and assembled with pLPC-puro retrovirus vector digested with HindIII and XhoI using Gibson Assembly master mix (New England Biotechnology). For retrovirus packaging, Phoenix ampho cells in 10 cm dish were transfected with 10 µg of plasmid using PEI-Max (1 µg/µl: Polyscience Inc.), and the supernatant containing retrovirus particles was collected at 48 and 72 hours after transfection. TC1 cells were retrovirally transduced with tRFP using 8 µg/ml polybrene. Puromycin selection was initiated 2 days after transduction, and cells were maintained in the presence of 5 µg/ml Puromycin until use.

In vivo studies

TC1 cells were primed with vehicle or TERS CM. Cells were enzymatically detached from plastic and resuspended in PBS at a final concentration of 5e6 cells/ml. C57BL/6 mice were injected with 100 µl of vehicle cell suspension into the left flank and 100 µl of TERS primed cells in the contralateral right flank. Mice were initially monitored for tumor take by palpation. When tumors became palpable, tumor size was determined through two-dimensional caliper measurements every three days. Mice were sacrificed when a tumor reached 20 mm in any one dimension, per UCSD animal welfare standards, or after 30 days post implantation. Tumor volume was calculated using the ellipsoid

formula: V = ½ (H x W^2). Upon mouse sacrifice, tumors were resected. For histological analysis, tumors were frozen in OCT compound and processed at the UCSD histology core, staining for Ki67 or H&E.

CRISPR/CAS9 studies

Two pairs of Cas9 guides were designed using the CHOPCHOP (211) software (available at http://chopchop.cbu.uib.no/). The sequence for Guide 1 was (F) caccgGCAACGTAAGCAGTGTAGTC and (R) aaacGACTACACTGCTTACGTTGCc; and the sequence for Guide 2 was (F): caccgGGATTTGAAGGAGTTCGACT and (R) aaacAGTCGAACTCCTTCAAATCCc (lower case indicates overhangs). Guides were cloned into the SpCas9-2A-GFP (px458) backbone modified to contain an EIF1α promoter (px458-ef1a) (212). Px458 was a gift of Dr. Feng Zhang (Addgene plasmid #48138). Briefly, Cas9 guides were then purchased as oligonucleotides from Integrated DNA Technologies. These oligonucleotide guide pairs were phosphorylated, annealed and ligated into *BbsI*-digested px458 backbone. The ligated plasmid was then transformed into DH5α bacteria and grown on carbenicillin plates overnight at 37ºC. Single colonies were picked and cultured overnight, and the plasmids isolated by mini or midi-prep (Invitrogen), and sequence validated. 293XT cells were grown in DMEM with 10% FBS. 24 hours before transfection with the guide-containing px458-ef1α plasmids (using Lipofectamine 3000), $8x10^4$ cells/cm^2 were seeded onto 6-well plates. Three days after transfection, cells were sorted by FACS on the basis of GFP positivity. Cells were then cultured in DMEM with 10% FBS for at least 1 week, validated, and used in TERS priming experiments. To demonstrate Cas9 efficiency, genomic DNA (gDNA) was isolated and PCR amplified using GoTaq (Promega) according to manufacturer instructions. The PCR product was then resolved on a 0.8% agarose gel and imaged under ultraviolet light.

Acknowledgments:

We thank Dr. Joseph Costello (UCSF) for providing the TERT core promoter luciferase construct; Dr. Jonathan Lin (UCSD) the ATF6 luciferase reporter, and Dr. Karl Willert (UCSD) for providing the lentiviral TOP-GFP construct.

Funding: This work was supported by DoD grant W81XWH-12-1-0156 to M.Z., and NIH R01NS088485, NIH U54OD020351 and VA BX002284 to JHL. J.J.R. acknowledges the support of the Frank H. and Eva B. Buck Foundation. N.H. was supported by a Japan Society for the Promotion of Science Postdoctoral Fellowship for Research Abroad.

Authors contributions: JJR designed and performed the experiments, analyzed the data, and wrote the manuscript. KTC designed and performed the experiments. NH created cell-tagging constructs, performed Western blot analysis, and aided in luciferase assays. JKN designed CRISPR system. VG performed TERT luciferase assay experiments. NRM analyzed the data and provided suggestions for the experimental design. KW provided TOP.GFP construct and provided guidance on Wnt signaling. JHL provided ATF6 reporter and provided constructive criticisms on ER-related studies. MZ helped design experiments and wrote the manuscript.

Chapter 2 is in full, a manuscript published in Science Signaling as: Rodvold, J.J, K. T. Chiu, N. Hiramatsu, J. K. Nussbacher, V. Galimberti, N. R. Mahadevan, K. Willert, J. H. Lin, M. Zanetti, Intercellular transmission of the unfolded protein response promotes survival and drug resistance in cancer cells. Sci. Signal. 10, eaah7177 (2017). The dissertation author is the primary author of this paper.

CHAPTER 3

Tumor mediated polarization of infiltrating myeloid cells is IRE1 dependent

Jeffrey J. Rodvold[1], Nobuhiko Hiramatsu[2], Kevin T. Chiu[1], Takao Iwawaki[3], Jonathan H. Lin[2], and Maurizio Zanetti[1]

[1] The Laboratory of Immunology

Department of Medicine and Moores Cancer Center

University of California, San Diego

9500 Gilman Drive

La Jolla, CA 92093-081

[2]Department of Pathology and Ophthalmology

University of California, San Diego

La Jolla, California, USA

[3]Division of Cell Medicine

Medical Research Institute, Kazanawa Medical University

Ishikawa, Japan

PREFACE TO CHAPTER 3

Chapter 3 is a manuscript in preparation for submission to the journal Science Immunology. The body of this chapter addresses Specific Aim 2 of this dissertation. Specifically, this chapter sets out to identify if TERS-associated effects on myeloid cells described in vitro exist in vivo and to further identify the mechanism behind this phenomenon. I analyzed tumor infiltrating myeloid cells in two unique mouse models and found that they are polarized in much the same way as those treated with TERS in vitro. This polarization was partially dependent on TLR4 signaling and its deletion curbed tumor development and prolonged host survival. Further investigation revealed that TERS polarization of myeloid cells appeared to be IRE1α dependent. Further, IRE1α was also partially responsible for TERS production while other arms of the UPR were dispensable. These studies validate previous in vitro observations and shed light on the possible in vivo mechanism behind the TERS phenomenon.

ABSTRACT

Tumor infiltrating myeloid cells play critical roles in the establishment and maintenance of a tumor microenvironment to favor occupant tumor cells and restrain anti-tumor immunity. These efforts can be coordinated through the production of pro-inflammatory and immune suppressive factors. We previously reported that primary derived myeloid cells treated in vitro with the conditioned medium of cancer cells undergoing endoplasmic reticulum (ER) stress undergo a polarization that is pro-inflammatory and immune suppressive, all the while undergoing ER stress themselves. Here, we report that tumor infiltrating myeloid cells display this same phenotype in unique tumor types. Further, using in vivo and in vitro models, we demonstrate this polarization of myeloid cells is mediated by TLR4 and IRE1α signaling. Stress induced expression of PD-L1 was similarly dependent on IRE1α activity. Finally, using mouse embryonic fibroblasts, we demonstrate the production of the transmissible factors behind this event are dependent on IRE1α. Collectively, our results provide novel insight into the mechanism behind the cell nonautonomous effects of tumor transmissible ER stress.

INTRODUCTION

Contained within the tumor microenvironment (TME) are a variety of immune cells that coordinate with resident tumor cells to create an environment that favors tumor survival and progression. Bone marrow derived cells, including myeloid cells, are the most common TME infiltrate. Tumor infiltrating stromal cells enhance tumorigenesis by affecting a variety of features necessary for successful tumor outgrowth (213). The cooperation of these nontransformed cells promotes tumor angiogenesis, immune suppression, inflammation, and metastasis.

Also present within the TME are a variety of stimuli that can promote endoplasmic reticulum (ER) stress. These insults include environmental ones, such as nutrient deprivation and hypoxia, and cell-intrinsic defects, such as aneuploidy and viral infection, all of which may lead to protein misfolding. Eukaryotic cells initiate the unfolded protein response (UPR) to cope with ER stress. The UPR is coordinated by three transmembrane proteins, IRE1α, PERK and ATF6, which are initiated upon excessive misfolded or unfolded protein burden. Immune cells of various origin are potentiated by the UPR to carry out their diverse function and have been implicated in a variety of processes including infection (214), metabolic disorders (215), and tumor development (204).

Necessary to understand the impact of tumor-borne signaling cues sent to immune infiltrate is the identification of the stimuli behind their polarization. We first reported that cancer cells undergoing ER stress can transmit ER stress to naïve bone marrow derived macrophages (136) and dendritic cells (137). These cells, in addition to undergoing a UPR, acquire pro-inflammatory and immune suppressive characteristics. This TERS mediated “mixed” phenotype also leads to poor antigen presentation to $CD8^+$ T cells. The cumulative consequences of such remodeling lead to a tumor promoting phenotype both

in vitro and in vivo. Here we investigated whether this mixed phenotype is present in vivo and elucidated the underlying signaling mechanism behind this phenomenon.

RESULTS

Tumor infiltrating myeloid cells display the TERS polarized genes in vivo

Recent reports find that both myeloid derived suppressor cells (MDSCs) (126) and dendritic cells (DCs) (129) that infiltrate the tumor microenvironment upregulate the UPR relative to the corresponding cells found outside of the tumor. Separately, we were the first to report that macrophages and dendritic cells were targets of cancer cell borne ER stress, a phenomenon termed transmissible ER stress (TERS) (216, 217). TERS conditioned medium (CM) treated myeloid cells transcriptionally upregulate UPR associated genes, as well as pro-inflammatory and immune suppressive genes. In light of these findings, we posited that $CD11b^+$ myeloid cells which infiltrate the tumor microenvironment undergo TERS polarization, and therefore express TERS responsive genes, while myeloid cells localized in healthy tissue would not.

We first sought to demonstrate that myeloid cells infiltrating the tumor microenvironment undergo ER stress. To that end, we implanted murine melanoma B16.F10 cells s.c. into mice transgenic for the ER stress activated indicator (ERAI), which express the fluorescent protein Venus upon *Xbp-1* splicing (218). Three weeks after implantation, palpable tumors were excised from tumor bearing ERAI mice, along with the spleen and bone marrow from the tumor-proximal and tumor-distal femurs, to account for any difference in extravasated myeloid cells in peripheral sites. We first determined the relative percent of $CD11b^+$ cellular infiltrate at each of the three sites (Fig. 3.1.A) and found that approximately 2-5% of the tumor infiltrate were $CD11b^+$. We then compared the Venus expression of $CD11b^+$ cells derived from the tumor versus that of the bone marrow and

spleen (Fig. 3.1, B and C). Strikingly, $CD11b^+$ cells within the tumor microenvironment had undergone substantial *Xbp-1* splicing activity relative to the myeloid cells resident in the spleen and the bone marrow. Moreover, Venus expression of tumor-infiltrating myeloid cells was normally distributed, suggesting that all $CD11b^+$ infiltrates had undergone ER stress. These results provide evidence that tumor infiltrating myeloid cells undergo ER stress while those resident in the spleen and bone marrow do not.

We next sought to determine if these same myeloid cells also preferentially expressed other genes affected by TERS CM. To that end, we injected B16.F10 cells s.c. into C57BL/6 mice, harvested tumors three weeks post implantation, and isolated the $CD11b^+$ cells from the tumor, spleen, and bone marrow of tumor-bearing hosts. Transcriptional analysis of isolated myeloid cells revealed that those infiltrating the tumor microenvironment not only had an upregulation of *Xbp1-s*, confirming the Venus expression results, but also of other related UPR related genes (*Grp78* and *Chop*) (Fig. 3.2.A). Beside a UPR, tumor-infiltrating myeloid cells also had transcriptional increases in pro-inflammatory (*Il-23p19*) and immune suppression (*Arg1*) genes relative to spleen and bone marrow resident myeloid cells (Fig. 3.2, A and B). These findings demonstrate that the tumor microenvironment promotes infiltrating myeloid cells to undergo a UPR and acquire a mixed pro-inflammatory/immune suppressive phenotype.

Encouraged by these findings, we next probed the expression of TERS-associated genes in a more physiologic, less aggressive form of tumorigenesis. At about one month of age, mice with mutations in the adenomatous polyposis coli (APC) gene develop adenomas along the small intestine (219). We pooled the $CD11b^+$ infiltrate of adenomas from APC mice (n=5) and probed their gene expression for TERS CM responsive genes relative to splenic and bone marrow controls (Fig. 3.2, C and D). In accordance with the B16.F10 results, adenoma infiltrating myeloid cells underwent a UPR and had increased

gene transcription for *Il23p19* and *Arg1*. Collectively, these data suggest that myeloid cells infiltrating the tumor microenvironment undergo ER stress and are influenced by the TME to acquire pro-inflammatory and immune suppressive features.

TLR4$^{-/-}$ myeloid infiltrate do not undergo TERS polarization

Previously, we reported that TLR4 facilitated TERS CM induced gene expression in receiver macrophages in vitro, while TLR2 and IL6R were dispensable (216). As such, we reasoned that tumor infiltrating myeloid cells deficient in TLR4 (TLR4$^{-/-}$) would be less responsive to tumor microenvironmental signals. To that end, we implanted B16.F10 cells s.c. into TLR4$^{-/-}$ or WT mice as a control. Isolated TLR4$^{-/-}$ myeloid cells present in the tumor had no significant upregulation in UPR genes (Fig. 3.3.A) or in pro-inflammation (Fig. 3.3.B), but, interestingly, were still immune suppressive (Fig. 3.3.C) relative to splenic derived myeloid cells. These results led us to conclude that TLR4 signaling was partially involved in TERS-responsive genes. Interestingly, B16.F10 tumors grew at slower rates in TLR4$^{-/-}$ hosts than in WT hosts (Fig. 3.3.D), and TLR4$^{-/-}$ hosts had significantly improved survival (Fig. 3.3.E). From this data, we conclude that TLR4 facilitates TERS responsive genes in vivo but does not entirely mediate the TERS phenotype.

IRE1α, but not PERK, signaling is necessary for TERS CM polarization of myeloid cells

In macrophages, TLR4 signaling is linked with UPR signaling through its activation of IRE1α, and its downstream effector XBP-1, during infection (99) and in rheumatoid arthritis (220). Based on these reports, we reasoned that IRE1α signaling could serve as a bridge between the myeloid polarization caused by transmissible ER stress and the role of TLR4 in vivo. We used the small molecule 4μ8c, which inhibits IRE1α RNase activity

by binding to the K907 residue of the protein at high specificity (221), to test the hypothesis that IRE1α signaling is involved in TERS activity. We confirmed that 4μ8c inhibited *Xbp-1* splicing by measuring Venus expression in B16.F10 tumor cells transduced with the ERAI construct (Fig. 3.4).

Next, we treated bone marrow derived macrophages (BMDM) with TERS CM in the absence or presence of 4μ8c, and analyzed the expression of TERS responsive genes. Strikingly, the inhibition of IRE1α signaling in BMDM treated with TERS CM substantially reduced UPR activation (Fig. 3.5.A) as well as the expression pro-inflammatory (Fig. 3.5.B) and immune suppressive genes (Fig. 3.5.C). These results suggest that polarization of myeloid cells driven by cues produced by ER stressed tumor cells is IRE1α dependent. IRE1α dependence for the TERS phenotype was not limited to the transcriptional profile because 4μ8c also inhibited the surface expression of several known TERS targets: CD80 and CD86 (Fig. 3.5.D).

We previously found that TERS promoted the surface expression of PD-L1 in bone marrow derived dendritic cells (BMDC) (216). We postulated that PD-L1 was similarly affected in TERS CM treated macrophages and that IRE1α signaling too mediates its expression. The addition of 4μ8c during TERS CM treatment substantially inhibited the surface expression of PD-L1 in TERS CM treated BMDM (Fig. 3.5.E), effectively restoring baseline expression. Collectively, these results demonstrate that the TERS mediated effects on macrophages are dependent on IRE1α signaling.

We next sought to determine if beside IRE1α, other arms of the UPR were also involved in promoting a pro-tumorigenic phenotype in myeloid cells. The small molecule GSK2656157 prevents kinase activity of activated PERK signaling at very high affinity (IC_{50} ~1 nM) by occupying its kinase P loop domain near the V606 residue (222). We first titrated GSK2656157 using B16.ERAI reporter cells to confirm that PERK inhibition did not

affect IRE1α activity (Fig. 3.6.A). Interestingly, GSK2656157 concentrations greater than 10 nM inhibited *Xbp-1* splicing activity, suggesting that saturating concentrations of the molecule affected other UPR pathways. We confirmed that at 10 nM concentration, GSK2656157 inhibited PERK signaling through the detection of phosphorylated PERK (pPERK) in BMDM treated with thapsigargin for 24 hours (Fig. 3.6.B). Importantly, 4μ8c had no effect on pPERK. We then analyzed BMDM treated with TERS CM in the absence or presence of the PERK inhibitor. GSK2656157 did not significantly inhibit increases in UPR, pro-inflammation, or immune suppression gene transcription (Fig. 3.6.C). GSK2656157 similarly had little to no effect on TERS CM driven surface expression of CD86 and PD-L1 (Fig. 3.6.D).

The role of IRE1α in TERS generation

The IRE1α-dependent mechanism in TERS CM mediated polarization in receiver myeloid cells led us to investigate if a specific arm of the UPR was responsible for transmitting ER stress. To that end, we treated BMDC with TERS CM generated from mouse embryonic fibroblasts (MEFs) carrying a deletion in the IRE1α (Fig. 3.7.A), PERK (Fig. 3.7.B), or ATF6 (Fig. 3.7.C) genes. Strikingly, TERS CM generated in IRE1α KO MEFs had less ER stress inducing activity than their respective wild-type (WT) MEF control line. There was no loss in TERS induced ER stress activity in PERK or ATF6 KO MEFs relative to their WT controls. In fact, ATF6 KO MEF TERS CM appeared to be more active than their WT counterpart. Importantly, BMDC treated with IRE1α KO TERS CM had less gene transcription for pro-inflammation than those treated with WT TERS CM (Fig. 3.7.D).

We reasoned that if IRE1α was involved for the transmission of ER stress, myeloid cells treated with the TERS conditioned medium of IRE1α KO MEFs would be less

effective to facilitate tumor growth in vivo than their WT TERS CM treated counterparts. To that end, we treated BMDC for 24 hours with Veh or TERS CM generated by WT or IRE1α KO MEFs. BMDCs were then harvested, add mixed with B16.F10 tumor cells at a 1:3 ratio, and implanted s.c. into immunocompetent C57BL/6 mice (n=4). Mice implanted with BMDC treated WT TERS CM grew tumors at markedly faster rates than those implanted with just B16.F10 cells alone or those add-mixed with WT Veh CM, consistent with an earlier observation (137). However, mice implanted with IRE1α KO TERS CM treated BMDC grew tumors at reduced rates (Fig. 3.7.E). This suggests that the pro-tumorigenic phenotype TERS imparts to myeloid cells is IRE1α-dependent.

The sum of these findings suggests that IRE1α may be involved both in the transmission and receipt of TERS. To substantiate this hypothesis, we generated TERS CM using WT and IRE1α KO MEFs. The resulting supernatants were then loaded onto naïve WT or IRE1α KO MEFs as receiver cells. Analysis of the UPR in receiver MEFs confirmed that TERS generated in IRE1α KO MEFs was less active than WT TERS CM in WT MEFs. However, WT TERS CM loaded onto receiver IRE1a KO MEFs had reduced activity for both *Grp78* and *Chop* gene expression (Fig. 3.8). These findings suggest that IRE1α is involved in both the production and receipt of TERS.

DISCUSSION

Here, we report that tumor-borne signals originating in cancer cells undergoing ER stress polarize receiver myeloid cells. We found that this polarization is dependent on IRE1α. Strikingly, myeloid polarization for both pro-inflammation and immune suppression was restricted to the tumor microenvironment in various tumor models. On further dissection, we found that the pro-inflammatory effect was dependent on TLR4 signaling.

Tumor-infiltrating myeloid cells are thought to play tumor facilitative roles by triggering pro-inflammation, angiogenesis, and immune suppression. Such a mixed phenotype suggests that the canonical clear-cut distinction of myeloid cells into M1 and M2 types does not apply to myeloid cells treated with transmissible ER stress (223). Since we first reported the occurrence of this phenotype, others have confirmed our findings.

That myeloid cells may not be of the classical M1, M2 type has revamped interest in the field of immunology, prompting a search for ligands effective in driving a mixed phenotype. For instance, human monocytes during sepsis become plastic and display a mixed pro-inflammatory/immune suppressive phenotype (224). Interestingly, this phenotype was found to be dependent on HIF1α, a known target of spliced XBP-1 (72). However, our experiments performed using bone marrow derived macrophages from HIF1α KO mice (225) failed to reveal any involvement on the part of HIF1α in the TERS phenomenon (unpublished data).

Importantly, tumor infiltrating myeloid cells displaying a mixed phenotype also experience increased expression of UPR associated genes. Previous reports showed that a UPR could occur in tumor infiltrating dendritic cells (129) and MDSCs (126). In contrast, our findings show that TERS can affect a broader range of host myeloid cells, suggesting that TERS polarization does not favor a specific myeloid subpopulation. Further, we found this profile to be consistently expressed in two independent tumor models, demonstrating our findings are not constrained to a specific tissue. The tumor infiltrating myeloid mixed expression of pro-inflammation and immune suppression was recently reported using an LLC tumor model (226).

The role of TLR4 signaling in myeloid cells is intriguing. The loss of MyD88 leads to a reduction in the number of induced skin papillomas by 7,12-dimethylbenz[a]anthracene (DMBA)/12-O-tetradecanoylphorbol 13-acetate (TPA) as well

as sarcomas induced by 3'-methylcholanthrene (MCA) (227). Intriguingly, those reports demonstrated that TNF-α-deficient mice were more susceptible to papilloma and sarcoma development, therefore emphasizing the role of host immunity and pro-inflammation in tumorigenesis independent of TNF-α signaling. These results are consistent with our findings that TLR4 facilitated ER stress and pro-inflammation in TERS CM treated macrophages (136). Similarly, TLR4 mediated pro-inflammation enhances tumor burden in colitis-associated models of cancer (228). The mechanism(s) behind TLR4-mediated facilitation of tumorigenesis via stromal cells remains to be fully elucidated. However, our findings emphasize its role in ER stress-mediated signaling.

The role of IRE1α in innate immunity during infection is well established, though its contributions to tumor immunity remain less understood. To the best of our knowledge, the involvement of IRE1α at the tumor-immune interface has only been reported once (129). The authors of this report speculated the existence of a factor of unidentified origin within the tumor microenvironment, but consistently emphasized the role of XBP-1 splicing. Through chemical inhibition of IRE1α during TERS CM induced activity, we demonstrate the tumor promoting roles of immune suppression and pro-inflammation were dependent on IRE1α mediated signaling. Importantly, PERK inhibition did not yield similar results. The surface expression of TERS affected molecules like CD86 also appeared to be dependent on IRE1α.

Our findings that IRE1α potentially facilitates PD-L1 surface expression is important. The current wave of enthusiasm behind checkpoint inhibitors necessitates further insight into the underlying mechanisms of action but also the regulation of the inhibitor targets on myeloid and tumor cells. The expression of PD-L1 in plasma cells from multiple myeloma patients is induced by IFN-γ and TLR agonism (229). Importantly, this report found that MyD88 inhibition prevents PD-L1 expression driven by the MEK/ERK

pathway. Of note, the UPR is centrally involved in the oncogenic activation of the MEK/ERK pathway (230, 231). Given our findings that TERS driven activity is dependent on TLR4 and IRE1α, our results are consistent with the published reports but also are the first to demonstrate that PD-L1 expression can be modulated by inhibiting the UPR, specifically IRE1α.

A validation of the chemical inhibition studies presented herein using genetic models, specifically the conditional deletion of IRE1α in myeloid cells, could not be done in time to include into this dissertation. However, genetic crosses using *ERN1* floxed and *XBP-1* floxed mice with lysozyme M-cre recombinase (LysM cre) mice have been done. We expect that macrophages from mice in which IRE1α or XBP-1 have been conditionally deleted will confirm the conclusions reached so far, which implicate the IRE1α pathway, but will also distinguish the relative contribution of these two proteins. Current IRE1α chemical inhibition studies could not differentiate between XBP-1 dependent or independent activity of IRE1α as 4μ8c also inhibits RIDD activity. Moreover, it was previously reported that the siRNA targeting of IRE1α in tumor infiltrating dendritic cells yielded significantly better survival in tumor bearing hosts than those similarly targeted for XBP-1, suggesting that pro-tumorigenic myeloid cell function operates beyond the role of IRE1α RNase activity (204). We anticipate that these mice will conclusively demonstrate that IRE1α signaling is indispensable in the polarization of tumor infiltrating myeloid cells and will better distinguish its role extends beyond its RNase functions. Importantly, this will provide deeper insight in the design of chemical inhibitors for future treatment of myeloid cell polarizations.

Our finding that IRE1α was responsible for TERS CM production is very interesting as it suggests that targets affected in this pathway are responsible for the production of molecules to hijack host immunity. A confounding piece of our analysis, however, is that

these findings could not be reproduced using IRE1α KO MEFs generated from separate target exons (232). This may suggest further specificity of the phenomenon or that the manipulation of MEF during immortalization affects the targeted signaling pathways. These results will require further investigation.

In sum, this report validates that the phenotype which transmissible ER stress imparts to myeloid cells can be found using unique in vivo models. This polarization appears to be TLR4 and IRE1α dependent but operate independently of PERK signaling. Further elucidation into this pathway will provide deeper insights into innate immunity and the role of IRE1α in the polarization of these cells.

FIGURES

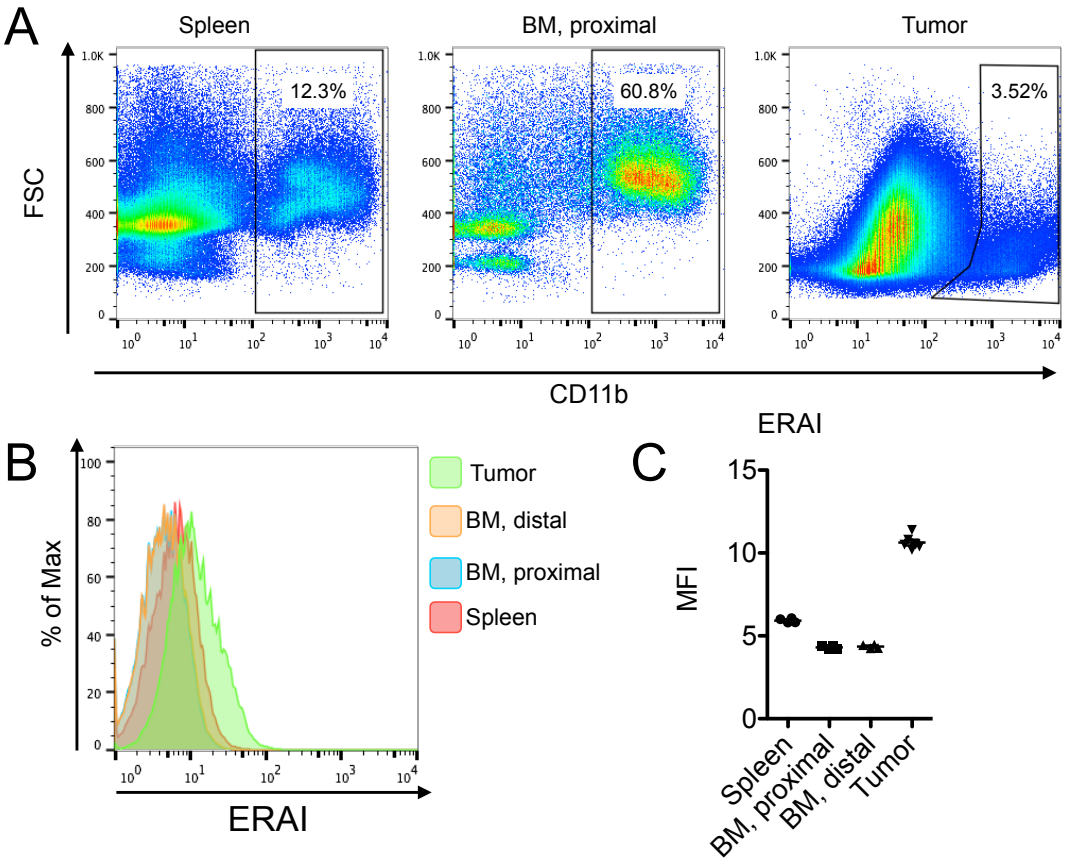

Figure 3.1. CD11b$^+$ myeloid cells undergo ER stress when occupying the tumor microenvironment (A) Relative percent CD11b$^+$ population of specified tissue as determined by flow cytometry. **(B)** Representative histogram and **(C)** Mean fluorescent intensity (MFI) expression of ERAI expression as determined by abundance of Venus fluorescent protein of CD11b$^+$ cells that occupy the tumor, spleen, and bone marrow both distally and proximally located (n=4).

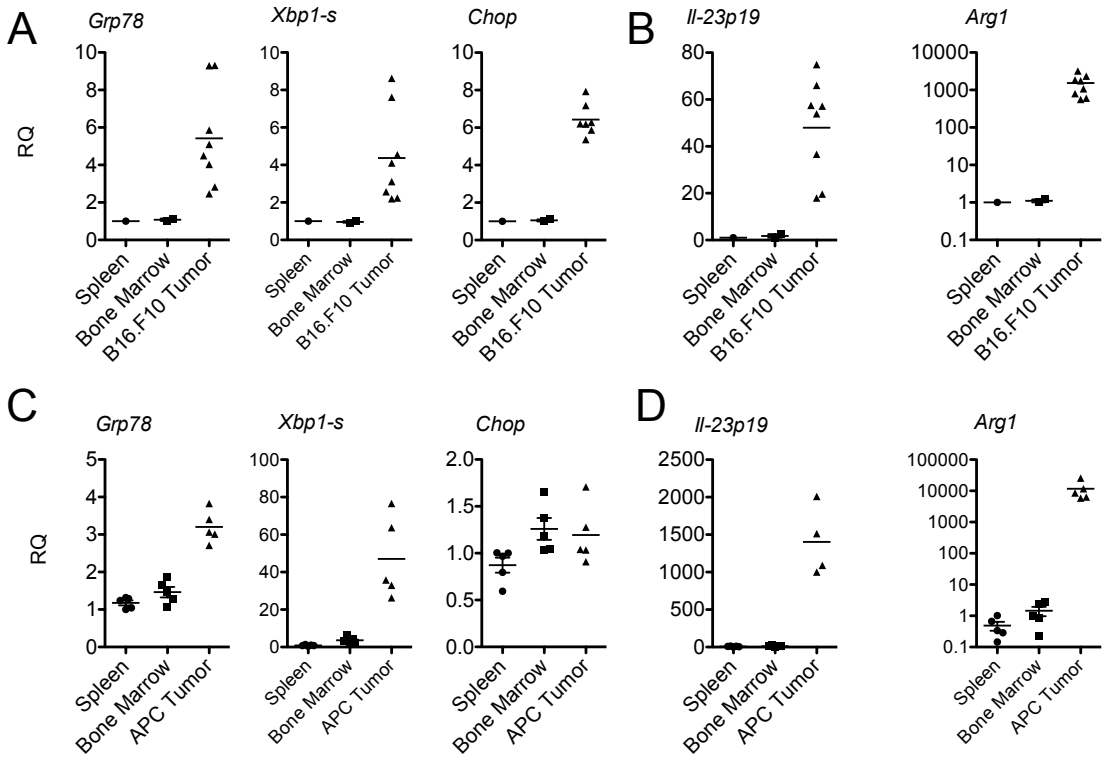

Figure 3.2. Tumor infiltrating myeloid cells express TERS responsive genes. Gene expression of myeloid cells contained within **(A,B)** B16.F10 tumors or **(C,D)** APC adenomas, and respective splenic and bone marrow counterparts (n≥4 per group). RNA isolated for myeloid cells were analyzed by RT-qPCR and probed for gene expression of (**A,C**) UPR (*Grp78, Xbp1-s, Chop)* genes and (**B,D)** pro-inflammation (*Il-23p19*)/immune suppression (*Arg1*). Gene expression was arbitrarily normalized to one splenic sample and values represent relative quantification (RQ) fold transcription expression.

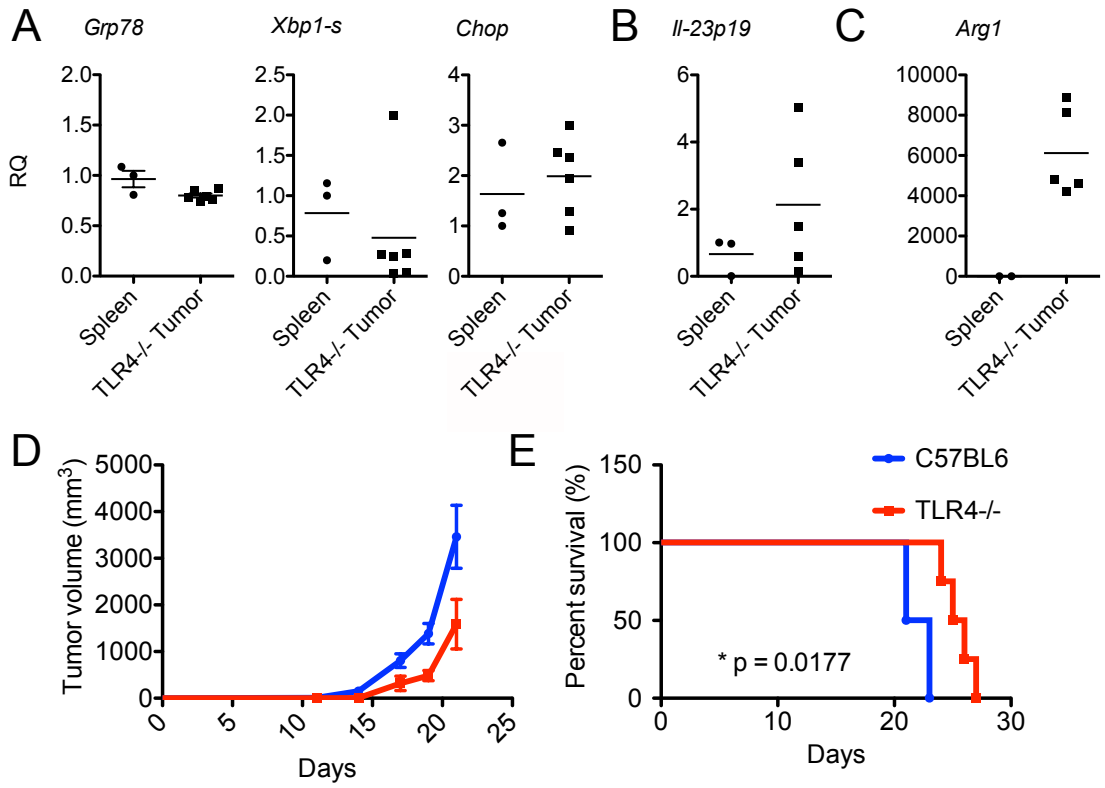

Figure 3.3. **TLR4 partially mediates TERS myeloid polarization in vivo.** Gene expression for **(A)** UPR, **(B)** pro-inflammatory, and **(C)** immune suppressive associated genes of myeloid cells contained within TLR4$^{-/-}$ hosts. **(D)** Tumor volume of B16.F10 tumors implanted into WT or TLR4$^{-/-}$ host mice (n=4). **(E)** Survival of WT or TLR4$^{-/-}$ tumor bearing hosts (n=4). *P<0.05, unpaired two-tailed t test. Error bars are representative of SEM.

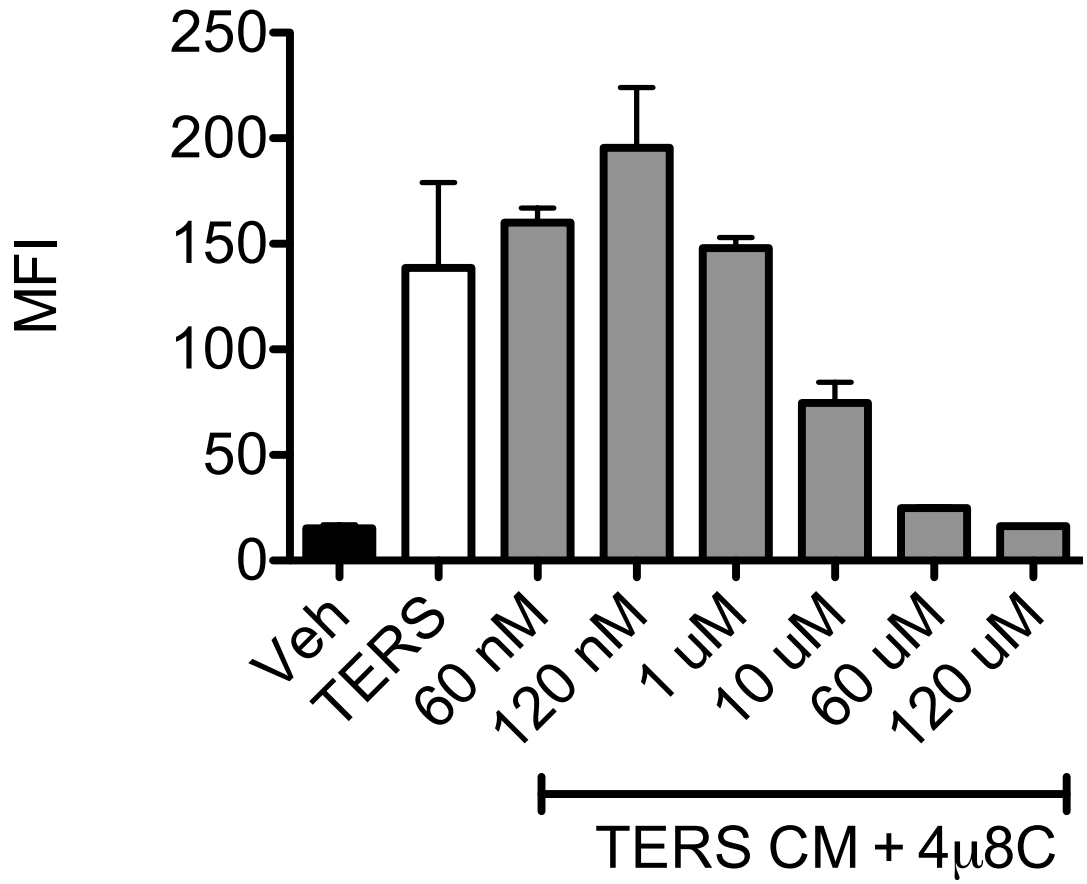

Figure 3.4. **Optimization of 4μ8C to inhibit *Xbp-1* splicing.** Venus protein expression as determined by flow cytometry of B16.ERAI cells treated with TERS CM with the addition of 4μ8C at specified concentration (n=2). Error bars are representative of SEM.

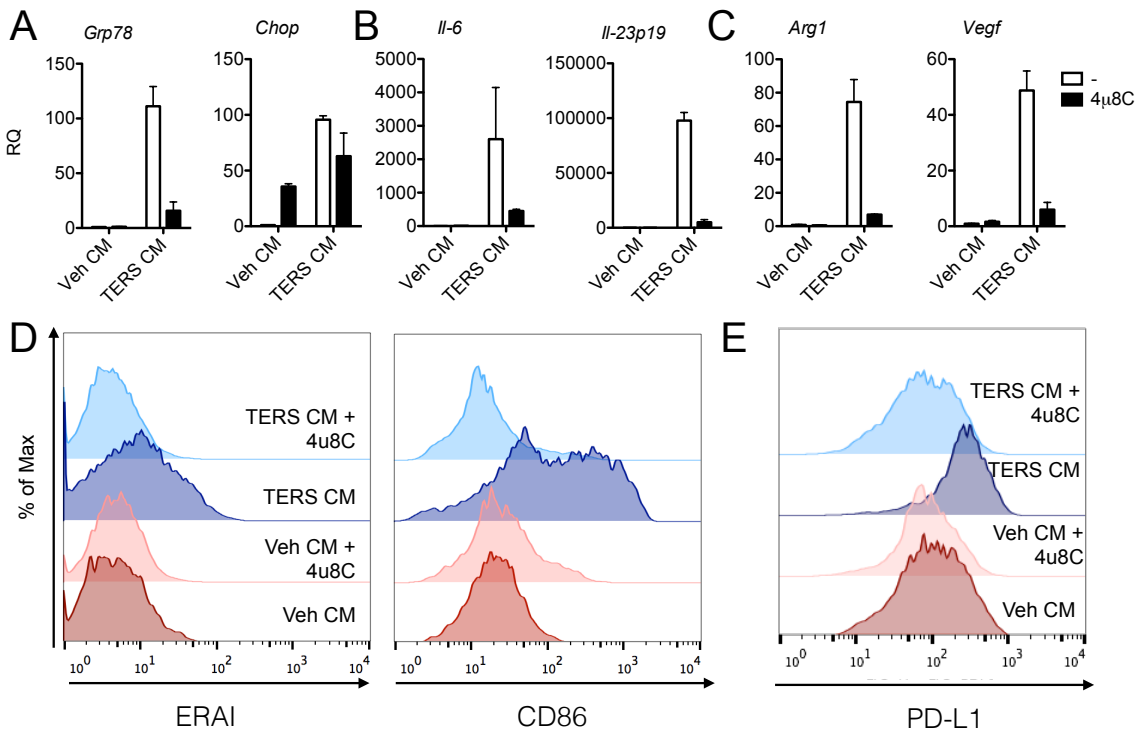

Figure 3.5. **IRE1α inhibition prevents TERS polarization in vitro.** RT-qPCR detection of TERS CM treated BMDM in the absence of presence of 4u8C (60 μM) for the expression of **(A)** UPR **(B)** pro-inflammatory and **(C)** immune suppressive associated genes (n=2). Relative quantification (RQ) was determined by arbitrarily normalizing gene expression to a Veh CM condition. Error bars are representative of SEM. **(D)** and **(E)** Flow cytometry analysis of the intracellular expression of Venus protein (ERAI) or surface expression of CD86 or PD-L1 of BMDM treated with TERS CM in in the absence of presence of 4u8C.

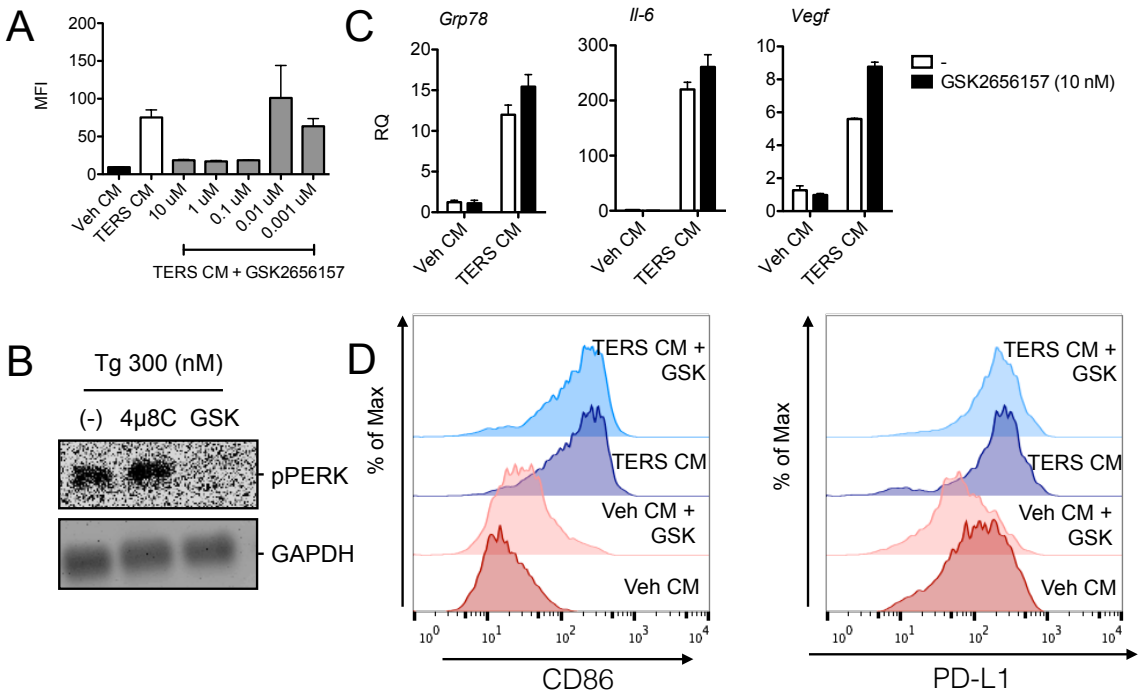

Figure 3.6. **PERK signaling does not mediate TERS CM activity in BMDM. (A)** Mean fluorescence intensity of Venus protein in B16.ERAI cells treated with TERS CM in the absence (white) or presence of a titration of GSK2656157 (n=2). **(B)** Western blot analysis for phosphorylated PERK (pPERK) in whole-cell lysates from BMDM treated with thapsigargin (Tg) in the absence (-) or presence of 4μ8C (30 μM) or GSK2656156 (GSK, 10 nM). **(C)** Expression of indicated mRNA by RT-qPCR of BMDM treated with Veh CM or TERS CM in the absence of presence of GSK2656157 (n=2). **(D)** Flow cytometry analysis of specified surface protein of BMDM treated with Veh or TERS CM in the absence or presence of GSK2656157 (GSK, 10 nM). Error bars are representative of SEM.

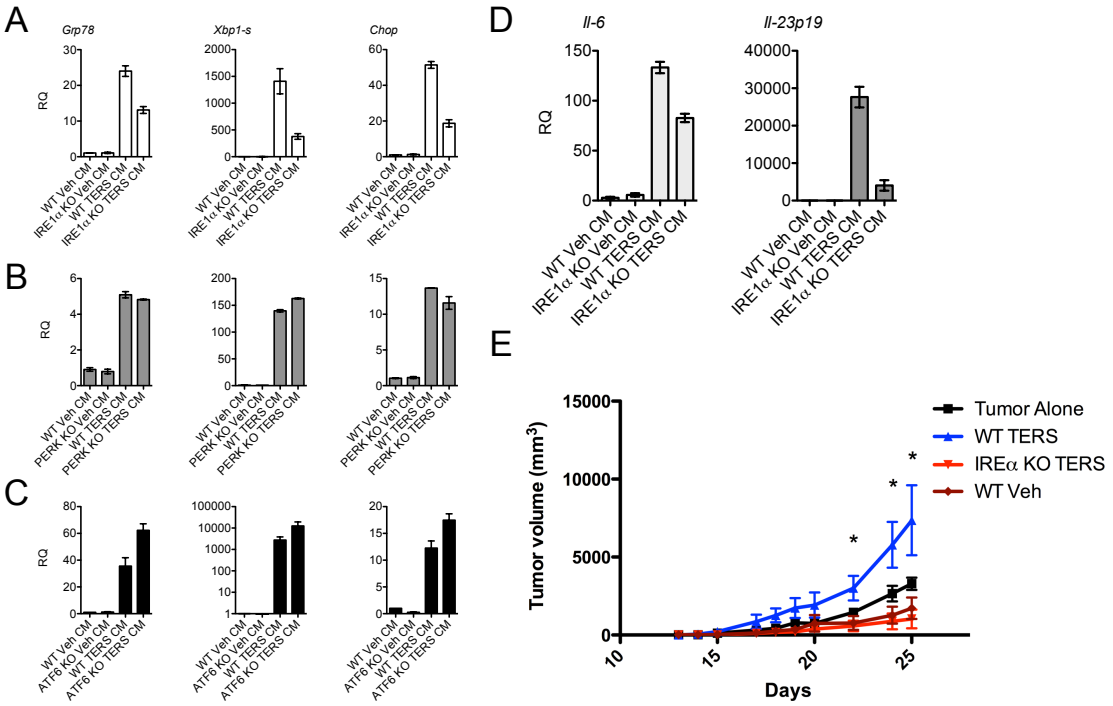

Figure 3.7. **IRE1α, but not PERK or ATF6, is responsible for TERS generation on BMDC.** RT-qPCR analysis of UPR associated genes of BMDC (n=2) treated for 24 hours with Veh or TERS CM generated by **(A)** IRE1α KO MEFs, **(B)** PERK KO MEFs, or **(C)** ATF6 KO MEFs, or their respective WT control MEF. Relative gene expression was normalized arbitrarily to a WT Veh CM condition. **(D)** Gene expression of pro-inflammatory genes of BMDC treated with WT or IRE1α Veh or TERS CM (n=2). Relative gene expression was normalized arbitrarily to a WT Veh CM condition. **(E)** Growth kinetics of B16.F10 tumors add mixed with BMDC pretreated for 24 hours with specified CM (n=4). *P<0.05, unpaired two-tailed t test. Error bars represent SEM.

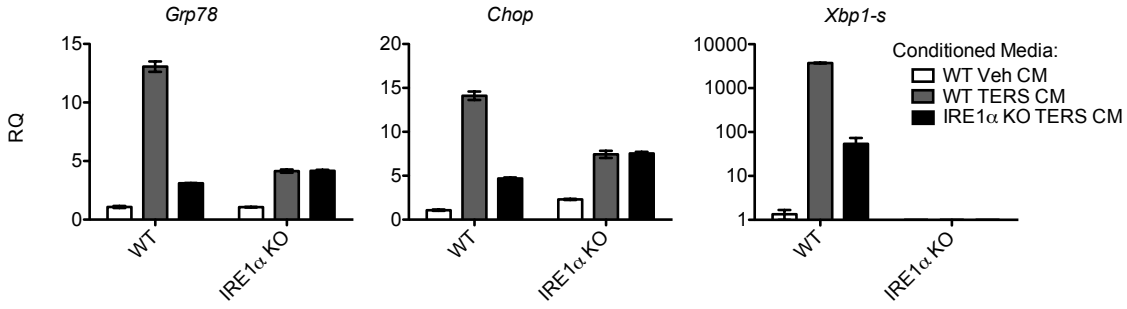

Figure 3.8. **IRE1α mediates TERS transmission and UPR activation.** RT-qPCR analysis of UPR associated gene expression in receiver WT MEFs (left) or IRE1α KO MEFs (right) treated for 24 hours with the conditioned medium generated by WT or IRE1α KO MEFs (n=2). Gene expression was normalized to WT KO MEF, Veh CM treated. Error bars represent SEM.

MATERIALS AND METHODS:

In vivo studies

For orthotropic tumor implantation model, B16.F10 cancer cells (n=4) were detached from plastic, washed twice with cold PBS, and resuspended at a concentration of 3e5cells/ml in PSB. Host C57BL/6 or transgenic ERAI mice (a kind gift from Dr. T. Iwawaki (Gunma University)) were subcutaneously injected with 100 µl (3e4 cells) of cell suspension into the right hind flank. After approximately 22 days, mice bearing tumors greater than 1 cm were sacrificed. For tumor growth studies, B16.F10 were subcutaneously injected in C57BL/6 (WT) or TLR4 KO mice (a kind gift from Dr. M. Corr (UCSD)). Tumor establishment was first determined by palpation and size was then measured in two dimensions using calipers. When tumors reached > 20 mm in any one dimension or after 30 days post implantation, whichever came first, mice were sacrificed. Tumor volume was calculated using the ellipsoid volume formula, $V = ½ (H \times W^2)$.

Myeloid cell isolation:

For B16.F10 model: B16.F10 cancer cells (n=5) were subcutaneously injected (3e4) into the right hind flank of C57BL/6 mice. After approximately 22 days, mice bearing tumors greater than 1 cm were sacrificed. For APC model: APC mice were genotyped for *APC* mutation to confirmed homozygosity of transgene. At approximately 12-15 weeks of age, APC mice were sacrificed. The small intestine was removed from host and cut longitudinally, running parallel to the intestinal lining. Adenomas lining the intestine were excised using an open blade and pooled, respective to the host, in ice cold PBS supplemented with 0.5% (w/v) bovine serum albumin (BSA). For both model systems: once the tumor, spleen, and bone marrow were isolated from tumor bearing hosts, tissues were dissociated through enzymatic digestion (TrypLE) at 37°C for 30 min on a rocker

plate, followed by cell straining through a 22 μm filter in ice cold PBS + 0.5% (w/v) BSA. Cell suspensions were then stained for CD11b+ positivity using a CD11b-biotin conjugated antibody (BD Biosciences) and incubated for 15 min at 4°C. Cells were then washed twice with PBS + 0.5% BSA and positively selected by magnetic separation using a biotin isolation kit (Stem Cell) according to manufacturer's specifications.

RT-qPCR:

mRNA was isolated and purified from myeloid cells after isolation or culture treatment using the RNA II Nucleospin Kit (Macherey-Nagel). The concentration and purity of RNA were determined by analysis on a NanoDrop spectrophotometer (ThermoScientific). cDNA generation occurred using the High Capacity cDNA Synthesis kit (Life Technologies/Applied Biosystems). RT-qPCR was performed on an ABI 7300 Real Time Real Time PCR machine using TaqMan reagents (Kapa Biosystems) for 50 cycles using universal cycling conditions. Validated FAM- labeled mouse *Il-23p19*(a), *Il-6*, *Ddit3* (*Chop*), *Hspa5* (*Grp78*), *Arg1*, *Vegf*, and VIC-labeled mouse *β-actin* TaqMan primer/probe sets (Life Technologies/Applied Biosystems) were used. Target gene expression was normalized to *β-actin*, and then calculated using the –ΔΔCT relative quantification method. FAM-labeled qPCR probe/primer sets specific for the spliced form of mouse Xbp-1 was obtained from Integrated DNA Technologies.

BMDM and BMDC generation:

Bone marrow derived cells were procured by isolating the femur and tibia of specified host and flushing out the bone marrow using cold, unsupplemented RPMI growth media (Corning) using a 27 gauge needle and syringe. Hemolysis was performed using ACK Lysis buffer (Bio Whittaker). For macrophage differentiation, bone marrow cells were

incubated one week in standard growth medium supplemented with 30% L929 conditioned medium (LCM). For dendritic cell differentiation, standard growth medium was supplemented with 10% mGM-CSF-producing hybridoma cells (GCM) as described in (233) and resupplemented every two days throughout one week.

Cell lines and cell culture

Human cells lines colon carcinoma DLD1 and prostate PC3 and murine cell lines prostate TC1 and melanoma B16.F10 cancer cells were grown in RPMI or DMEM (Corning) supplemented with 10% FBS (HyClone) and 1% penicillin/streptomycin/L-glutamine, NEAA, sodium pyruvate, HEPES. All cells were maintained at 37°C incubation with 5% O_2. All cell lines were mycoplasma free as determined PCR assay (Southern Biotech).

ERAI activity assay

Cancer cell line reporter cells were transduced with the ERAI construct, originally described (234). Briefly, the pCAX-F-XBP1ΔDBD-venus (a kind gift from Dr. Iwawaki, Gunma University) underwent PCR using following primers: F: ctaccggactcagatctcgagccaccATGGACTACAAGGACGACG, R: gaattatctagagtcgcggccgcTTACTTGTACAGCTCGTCC. PCR fragments were cloned into pLVX-puro (Clontech) lentivirus vector with Gibson Assembly Mixture (NEB) according to manufacturer's instruction. Stbl3 competent cells were transformed to produce the plasmid insert, whose presence was confirmed by sequencing. For production of lentivirus, 293FT (Invitorgen) cells were seeded in 10 cm dish and transfected with a plasmid mixture of ERAI plasmid and psPAX2 and pMD2G viral packaging plasmids. The supernatant of virus–producing transfected cells was collected every 24 hrs for three days post

transfection. Viral supernatant was concentrated by 10% PEG-8000 and pelleted with 2000 x g for 40 min at 4C and re-suspended PBS. Target cancer cells were transduced with lentivirus by adding supplementing with polybrene (8 μg/mL) to virus containing solution and loaded onto B16.F10 cancer cell line. Lines were transduced for 48 hours. Following, cells were washed twice with PBS and positively selected for using puromycin (2 μg/mL) for two weeks. In some instances, positively transduced cells were then stimulated for Venus expression and were sorted by FACS (BD) to isolate high expressing clones. Lines were maintained under puromycin.

Flow cytometry

Single cell suspensions of myeloid cells were separated and stained for CD80 (B7-1) (BD Biosciences), PD-L1 (CD274) (BD Biosciences), and CD86 (BD Biosciences). Viable cells were determined by 7AAD exclusion and data were acquired using a FACScalibur flow cytometer (BD). Flow results were analyzed using CellQuest Pro (BD) and Flow JO (Tree Star) software.

Western blotting

Cells were scraped using ice cold PBS, pooled, and lysed using RIPA lysis buffer (Thermo) supplemented with Halt Protease Inhibitor Cocktail (Thermo). Protein was quantified using BCA Protein Assay Kit (Pierce). Lysates were reduced with β-mercaptoethanol added to NuPage LDS sample buffer (Thermo) and denatured by incubating for 15 minutes at 95°C. Samples were normalized by concentration and separated using a 4-20% SDS-Page (BioRad) gel. Gels were transferred to blotting membrane using Trans-Blot Turbo Transfer system (BioRad). Blots were blocked using 5% nonfat milk powder in Tris-buffer saline with Tween (TBST) for 30 minutes. Primary

antibody incubation of phosphorylated PERK (Cell Signaling) occurred overnight at 4°C. Stained blots were then washed twice with TBST to remove excess antibody and subsequently stained for HRP conjugated antibody. Bands were visualized using Chemidoc-It Imaging System (UVP).

MEF KO studies

Mouse embryonic fibroblast lines were derived from the respective papers PERK KO (208), IRE1 KO (49), and ATF6 KO (209) and were cultured in standard DMEM conditions. For in vivo studies, BMDC were exposed to Veh or TERS CM generated from WT or IRE1α KO MEF for 24 hrs. B16.F10 tumor cells and treated BMDC were harvested, washed twice with PBS, and admixed at a 3:1 ratio, specifically 3e5 B16.F10 cell:1e5 BMDC per mL. Admixed cell suspensions were implanted as previously described into C57BL/6 hosts. Tumor size was determined as previously described. All in vivo studies were carried out under strict accordance with recommendations from National Institutes of Health under protocol No. S00023, as approved by the UCSD Institutional Animal Care and Use Committee.

ACKNOWLEDGEMENTS

Chapter 3 is a manuscript in preparation. J.J. Rodvold, N. Hiramatsu, K.T. Chiu, T. Iwawaki, J.H. Lin, M. Zanetti, IRE1α signaling mediates tumor mediated polarization of myeloid cells. The dissertation author is the lead investigator and author of this paper.

CHAPTER 4

Tumor cells undergoing ER stress produce a novel lipid that drives cell extrinsic myeloid immune dysfunction

Jeffrey J. Rodvold[1], Inho Yang[2], Nobuhiko Hiramatsu[3], Kevin T. Chiu[1], Oswald Quehenberger[4], Takeo Iwawaki[5], Jonathan H. Lin[3], William Fenical[2], Maurizio Zanetti[1]

[1] The Laboratory of Immunology

Department of Medicine and Moores Cancer Center

University of California, San Diego

[2] Center for Marine Biotechnology and Biomedicine

Scripps Institution of Oceanography

University of California, San Diego

[3] Department of Pathology and Ophthalmology

University of California, San Diego

La Jolla, California, USA

[4] Department of Pharmacology

University of California, San Diego

La Jolla, CA, USA

[5] Division of Cell Medicine

Medical Research Institute, Kazanawa Medical University

Ishikawa, Japan

PREFACE TO CHAPTER 4

Chapter 4 is a manuscript in preparation. The focus of the work featured in this chapter relates to the third and final aim of this dissertation: To identify the molecule or molecules responsible for transmissible ER stress. Here, we investigated the components of TERS conditioned medium utilizing standard and advanced biologic and chemical isolation techniques. These results reveal that the activity behind TERS can be ascribed to a stress-dependent lipid compartment. Importantly, this body of work identifies a novel monounsaturated fatty acid produced by tumor cells as the molecule responsible for the initiation of a UPR in receiver cells.

ABSTRACT

The role of endoplasmic reticulum (ER) stress in tumorigenesis is largely viewed as gains in cell intrinsic features such as chemoresistance and cell survival. Recently, we reported that ER stressed cancer cells can also transmit an unfolded protein response (UPR) to recipient cancer cells and myeloid cells, which in turn further enhance tumorigenic features. Here, we sought to identify the molecule responsible for this event, termed transmissible ER stress (TERS). We report that TERS activity can be ascribed to two unique lipid compartments: eicosanoids and a monounsaturated fatty acid. Compared to vehicle conditioned medium, TERS conditioned medium contained increased abundance of 30 eicosanoids that provided immune suppressive features to primary derived myeloid cells. Separately, a molecule that remains to be fully characterized is a monounsaturated fatty acid, which is responsible for transmitting ER stress to receiver cells. This molecule also triggers the polarization of myeloid cells, promotes pro-inflammation, and PD-L1 expression. This molecule is unique and distinct from other signaling molecules already reported to have allegedly similar functions as TERS.

INTRODUCTION

Cooperativity is key for successful tumorigenesis. While early theories posited that tumor cells do not communicate with each other within the tumor microenvironment (TME) (235), more recent reports demonstrated that tumor cells rely on intercellular cooperation to facilitate tumor outgrowth (236). There is no single class of molecules responsible for the multifaceted aspects of intratumoral signaling; molecules with signaling properties include proteins, lipids, glycans, DNA, and microvesicles (237). All can potentially contribute in some manner to tumor facilitation. Paracrine communication within the TME facilitates angiogenesis, immune suppression, pro-inflammation, metastasis, and chemoresistance, among other various pro-tumoral processes.

Signaling between neoplastic tumor cells and nontransformed cellular infiltrate is of key importance at both the primary site and distal metastasis and has been discussed previously at length (89). Because the signaling within the TME creates a type of intercellular communication that ultimately facilitates tumor growth, there exists much interest in understanding the nature of the overall consequences of this phenomenon.

Localized in the tumor microenvironment are a variety of *noxae* that can create endoplasmic reticulum (ER) stress. These stimuli include TME endogenous insults like hypoxia and scant access to nutrients. Within the cancer cell, insults like aberrant metabolism, ploidy status, and viral infection too can create ER stress. To cope with the accumulation of misfolded protein that creates ER stress, cells initiate the evolutionarily conserved signaling pathway termed the unfolded protein response (UPR). The UPR is coordinated by three ER transmembrane proteins that attempt to restore ER protein homeostasis through a) the reduction of protein synthesis and b) the selective upregulation of a variety of chaperone molecules. The UPR is incriminated as a mechanism to enhance cellular survival as well as host of tumorigenic functions (66).

We recently reported that cancer cells of various origin can transmit ER stress to target cells such as macrophages (136), dendritic cells (137), and other cancer cells (138). This event, termed transmissible ER stress (TERS), provides for tumor promotion via pro-inflammation, angiogenesis, immune suppression, and cancer cell chemoresistance. Our findings demonstrate that the creation of a UPR in receiver cells facilitates a pro-tumor phenotype in vivo for myeloid and cancer cells. Here, we dissected TERS conditioned medium to identify the molecule(s) responsible for ER stress signaling, the co-option of immunity, and the acquisition of resistance to chemotherapy in cancer cells.

RESULTS

TERS is a lipophilic molecule

We first sought to establish a cell reporter system for the accurate and rapid detection of UPR induction. To this end, murine TRAMP C1 (TC1) and B16.F10, and the human DLD1 colon cancer lines were transduced with the ER stress activated-indicator (ERAI) gene construct described in (218). ERAI reports ER stress via IRE1α mediated endonuclease activity of the *XBP-1* mRNA transcript, which occurs upon ER stress. Specifically, the ERAI construct contains a *Venus* transcript after the stop-codon contained in the spliced region of *XBP-1,* allowing translation of the fluorescent protein to only occur when the *XBP-1* mRNA is spliced by IRE1α endonuclease activity (Fig. 4.1.A). We first confirmed that these reporter cell lines accurately reported ER stress when treated with the sarco/endoplasmic reticulum calcium ATPase (SERCA) inhibitor thapsigargin over a broad dose range or with TERS conditioned medium (CM) (Fig. 4.1.B).

To probe for the possibility that the factor responsible for ER stress transmission was a protein, we generated TERS CM through our standard technique (138, 217). Vehicle (Veh) conditioned medium served as control. The conditioned media were

incubated in a 95°C water bath for 15 or 30 minutes. As a control, other Veh and TERS CM was separately left at room temperature. Reporter ERAI cells were then treated with the heat-inactivated solutions for 24 hours (Fig. 4.1.C). We found that heat-inactivated TERS CM retained its ER stress-inducing activity, leading us to believe that the ER stress-inducing molecule in TERS CM was not a protein, given its thermostability. To confirm this conclusion, we performed an acidified acetone total protein extraction, precipitating all proteins out of the CM solution. The protein pellet was then air dried, resolubilized in standard growth medium, and loaded onto ERAI reporter cells. The protein enriched material had no ER stress activity (Fig. 4.1.D). Because the protein enriched portion of TERS CM lacked ER stress activity, we conclude that the responsible transmitted molecule is not a protein.

Given the thermostable nature of TERS, we reasoned that the molecule behind its activity could be lipophilic in nature. To that end, we added ethyl acetate to CM to separate lipophilic (contained in the organic phase) and lipophobic (contained within the aqueous phase) molecules. The TERS CM organic and aqueous partitions were separated, evaporated, resolubilized in standard growth media, and treated on the ERAI reporter cells. We found that ER stress activity resided exclusively in the organic phase of the TERS CM while the aqueous phase had no ER stress activity (Fig. 4.1.E). These findings indicated that TERS is a lipophilic molecule. Reproducibly, the use of an alternative organic solvent, chloroform, always yielded similar results (Fig. 4.1.F). The conclusion of these studies is that ER stress activity in TERS is assignable to a lipophilic molecule.

Eicosanoids are enriched in TERS

Our finding that TERS is likely a lipid led us to hypothesize that it could be an arachidonic acid derivative. These products are broadly identified as eicosanoids,

including prostaglandins, and have biologic activities very similar to that of TERS, namely they can induce Arginase 1 (238) and facilitate chemoresistance (239). We probed for the abundance of 154 known eicosanoids contained within generated TERS and Veh CM using tandem mass spectroscopy (Lipid Maps). Of the probed analytes, 71 eicosanoids were detected in both TERS and Veh CM. TERS CM contained 30 eicosanoids that were at least 1.5 fold higher in concentration over Veh CM, while 35 eicosanoids were similarly expressed and 6 were decreased (Fig. 4.2.A) (Complete data, Table 4.1 - 4.4). We noted the most abundant eicosanoid present in TERS CM was PGE2 (~10 nM) while the eicosanoid most increased relative to Veh CM was PGA2 (~25 fold).

We next wanted to see if any of these eicosanoids enriched in TERS CM could be responsible for its ER stress activity. We defined six key eicosanoids as the most enriched or dynamic in TERS CM (PGA2, PDG1, PGE2, 8-iso-15k PGF2b, PGJ2, 11-HETE) (Fig. 4.2.B) and formed a synthetic mixture of these moieties, termed prostaglandin cocktail (PG cocktail). We treated reporter ERAI cells with artificially pooled PGA2, PDG1, PGE2, 8-iso-15k PGF2b, PGJ2, 11-HETE at various concentrations and found that the PG cocktail did not cause ER stress even when tested at a concentration of 1 μM for each eicosanoid (Fig. 4.2.C). These concentrations are at least 100 times greater than what is detected in the TERS CM, suggesting that eicosanoids are not responsible for ER stress transmission. To confirm this conclusion, we generated TERS CM in the presence of the nonselective Cox inhibitor flurbiprofen. Cox inhibition did not diminish Venus expression in transmitting TC1.ERAI cells nor in receiver bone marrow derived macorophages (BMDM) ERAI cells (Fig. 4.2.D). The addition of flurbiprofen in TERS CM treated BMDM did not have any effect on transcription for *Grp78* (Fig. 4.2.E) but did decrease *Il-23p19* transcription. The inhibition of *Il-23* was to be expected because flurbiprofen inhibits Cox activation and its downstream inflammatory targets like IL-23. In essence flurbiprofen

inhibited downstream signaling of activated UPR signaling. These findings demonstrate that TERS driven ER stress is not dependent on eicosanoids.

Because the PG cocktail did not create ER stress, we next probed what effects, if any, these eicosanoids imparted on receiver myeloid cells. We treated BMDM with the PG cocktail, reconstituted at approximately the concentration detected in TERS CM, and probed for BMDM transcriptional polarization 24 hours after later. The PG cocktail did not cause any change in UPR or pro-inflammatory genes. However, it did promote increased gene expression of the immune suppressive genes *Arg1* and *Vegf* (Fig. 4.3.A). These enriched eicosanoids did not affect ERAI expression or CD86 expression in BMDM (Fig. 4.3.B). The conclusion of these studies is that TERS CM is enriched in eicosanoids, which can promote immune suppression while not causing ER stress or driving pro-inflammation.

Tumor cells secrete a novel monounsaturated fatty acid to transmit ER stress

Because the enriched eicosanoid compartment of TERS CM could not account for its UPR inducing features, we hypothesized the existence of a separate lipophilic moiety. To that end, we used chromatographic techniques to fractionate the ER stress related compartment of TERS starting from ethyl actetate extraction (Fig. 4.4.A). The separated organic phase was then passed through a C18 HPLC column, yielding 6 retention time fractions and one unique peak of absorption (Fig. 4.4.B). These fractions were loaded onto B16.ERAI reporter cells where we found that one specific peak of fractionated TERS CM caused robust ER stress activity, termed Peak 6 (P6) (Fig. 4.4.C). This peak was then analyzed using NMR (Fig. 4.4.D). We recognized that the spectra of this molecule had features consistent with that of a monounsaturated fatty acid and, therefore, compared its spectra with that of a known monounsaturated fatty acid, erucic acid (22:1ω9) (Fig. 4.4.E). Strikingly, the two molecules share near identical ^{1}H NMR spectra. However, further 13-C

analysis revealed P6 has a δ_C of 176.8 ppm versus erucic acid's value of 179.3 ppm (Fig. 4.4.F). This difference in absorption led us to conclude that P6 contains a modified carboxylic acid moiety at its C1 position. We subsequently performed various chemical techniques to identify a value consistent with P6 C1 chemical shift. Using this approach, we eliminated the possibility that P6 contained anhydride dimers, peroxide dimers, and amide groups. At the time this dissertation goes to press, the identity of P6 remains to be conclusively resolved. What can be concluded, however, is that P6 is a monounsaturated fatty acid with a double-bond at its center and most likely has a *cis* formation. Importantly, P6 appears to be unique from other related molecules.

We then sought to demonstrate P6 biologic activity. BMDM treated with P6 underwent ER stress, pro-inflammation, and angiogenic transcriptional responses (Fig. 4.5.A). While the induction of *Vegf* was relatively similar to that caused by the PG cocktail, *Arg1* expression was only increased (~2 fold) by P6. Subsequently we went on to probe whether P6 provided additional TERS-associated activity not accounted for by the PG cocktail by analyzing the expression of ERAI, PD-L1, and CD86 in BMDM (Fig. 4.5.B). P6 caused macrophages to increase expression of all three targets (ERAI, PD-L1, and CD86). These findings suggest that P6 is the complement of the eicosanoid compartment, and that the two combined (P6 and PG cocktail) recapitulate the full TERS activity.

To probe whether the ER stress inducing activity was privileged to P6 versus similar molecules, we tested a variety of other monounsaturated fatty acids for their ER stress inducing capability. Specifically, ERAI cells were treated with increasing concentrations of erucic acid (C22), oleic acid (C18), and their respective amide analogues (erucamide and oleamide) (Fig. 4.6, A and B). None of these compounds tested at a nanomolar to micromolar concentration generated a UPR in receiver ERAI cells. These findings are consistent with other reports in the literature that find that

monounsaturated fatty acids do not create ER stress (240). Unlike unsaturated fatty acids, saturated fatty acids are known to cause ER stress (215). To that end, we treated reporter ERAI cells with a series of standard saturated fatty acids, including stearic (C18), lauric (C12), myristic (C14), and heptadecanoic (C17) acids. While ER stress activity could be detected, it was only induced at high (~100 μM) concentrations (Fig. 4.7), which are far greater than the estimated low nanomolar concentration of P6.

A previous report showed that lactic acid (LA) is allegedly responsible for the immune suppressive characteristics of tumor infiltrating macrophages (241). In repeat experiments, we found that lactic acid at published concentrations (30 mM) did not cause ER stress in reporter ERAI cells (Fig. 4.8.A). LA similarly did not create ER stress or drive CD86 expression in primary derived macrophages from ERAI mice (Fig. 4.8.B). However, it did drive immune suppressive features, albeit reduced from TERS CM or the PG cocktail (Fig. 4.8.C).

DISCUSSION

Here, we provide evidence that the biologic activity of TERS is assignable to two lipid-associated molecules: eicosanoids and a novel monounsaturated fatty acid. We demonstrate that eicosanoids drive immune suppression but not ER stress or pro-inflammation in bone marrow derived myeloid cells. Separately, the novel monounsaturated fatty acid provisionally termed Peak 6 (P6) initiates a UPR in receiver cancer and myeloid cells, drives pro-inflammation and the surface expression of PD-L1 and costimulatory molecule CD86.

While the role of eicosanoids in cancer is established (Reviewed in (242)), the stimuli responsible for their production remains unclear. Our finding that eicosanoids are produced by tumor cells undergoing ER stress provides a possible explanation. Of the

154 eicosanoids probed, 30 were increased in TERS CM. While the biologic significance of each of these hits remains to be fully characterized, some are already established contributors to tumor development, i.e. PGE2. Enhanced prostanoid production correlates with poor prognosis in several malignancies including colon (243), breast (244), and lung (245). Once produced, prostanoids, including PGE2, endow the tumor microenvironment with a variety of functional gains. For example, increased endogenous PGE2 production in $APC^{Min/+}$ mice leads to increased carcinogenesis (246), while its deletion curbs tumor development (247). Importantly, the immune infiltrate of APC mice display a TERS like signature, as discussed in Chapter 3. Therefore, it is likely that PGE2 produced in response to TME ER stress plays a vital role in polarizing infiltrating myeloid cells. PGE2 induced two key tumor developmental features in myeloid cells: immune suppression and angiogenesis. Rodriquez et al. demonstrated that tumor cells constitutively express cyclooxygenase 1 and 2 (COX-1 and COX-2) to produce high levels of PGE2, which induces myeloid suppressor cells to produce Arginase 1 (248). The authors concluded that tumor-derived PGE2 is responsible for immune suppression, yet were unable to determine the stimulus driving its production. Importantly, the PGE2 concentration detected in this model (< 28 nM) is comparably similar to that detected in TERS CM (~ 10 nM). PGE2 can drive the differentiation of cytotoxic T cells to become Tregs through the promotion of *FOXP3* expression (249). The inhibition of PGE2 secretion promotes anti-tumor clearance by T cells by favoring IL-12 production over IL-10 (250). In addition to restraining anti-tumor immunity, prostanoids promote angiogenesis. PGE2 promotes the expression of CDCL1 in colorectal cancer cells, initiating endothelial cell migration and vascularization of the TME both in vitro and in vivo (251). Concordantly, PGE2 drives the expression of VEGF in various tumor models including breast (252) and prostate (253). We too found that the TERS CM enriched eicosanoids drive *Vegf* expression in BMDM.

Similarly, eicosanoids have profound effects on receiver cancer cells. For example, PGE2 promotes cellular proliferation by driving Ras-Erk signaling and GSK3B-β-catenin in cancers of various origin (reviewed in (242)). It is important to note that TERS CM provided the stabilization of β-catenin and promoted its nuclear translocation to drive Wnt signaling in treated cancer cells (138). Separate reports find that PGE2 is produced by chemotherapy-induced apoptotic cancer cells, stimulating the proliferation of surviving cancer stem cells and leading to tumor repopulation (239). While TERS transmitting cancer cells do not actively undergo apoptosis (136), it is reasonable to postulate that dying cells experience considerable ER stress, thereby enhancing the production of signaling molecules like prostanoids. These observations are not limited to colorectal and bladder cancer. Myeloma cells that have RAS mutations also undergo increased COX-2 expression, leading to enhanced eicosanoid production and chemoresistance (254). Stopping the production of eicosanoids through COX-2 blockade, for instance with the inhibitor Celecoxib, has been shown to be therapeutically valuable in a variety of cancers including breast, lung, and colon cancers (Reviewed in (255)). Moreover, aspirin use was found to reduce the risk of colorectal cancer-specific mortality, particularly when tumors overexpressed COX-2 (256). Contextually, our results provide insight into a mechanism whereby eicosanoids are produced by tumor cells undergoing ER stress, thereby promoting chemoresistance, angiogenesis, and immune suppression.

The second, and most elusive, molecular component of TERS CM was identified as a monounsaturated fatty acid, provisionally termed Peak 6. P6 was found to be the complement of the prostanoid compartment as it endows receiver cancer cells and myeloid cells alike with ER stress and pro-inflammation. NMR analysis revealed that P6 has a very similar spectra to that of the monounsaturated fatty acid erucic acid. However,

there exists no literature to suggest monounsaturated fatty acids cause ER stress at any threshold. To the contrary, oleate resolves ER stress created by saturated fatty acids like palmitate in diabetes models (257). Our findings are consistent with these reports.

The significance of P6 must also be seen in the broader context of recent reports suggesting that other molecules are responsible for “TERS-like” polarization of myeloid cells. Most notably, 4-hydroxynonal (4-HNE) reportedly affects ovarian cancer infiltrating dendritic cells by creating protein abducts, leading to increased ER stress. This ER stress subsequently dysregulates lipid metabolism and enables poor antigen presentation, thereby restraining adaptive anti-tumor immunity (204). The authors of this report found that ovarian cancer ascites contains a factor or factors that generate 4-HNE-protein abducts in dendritic cells. They speculate, without demonstrating so, that the responsible factors are reactive oxygen species. 4-HNE was not detected in cell-free ascites, per se arguing that 4-HNE is not involved in intercellular signaling within the TME. Interestingly, the retention time of P6 and 4-HNE are different, suggesting that P6 is not 4-HNE.

Other reports suggested that tumor derived lactic acid is responsible for myeloid cell dysfunction (241). This report found that macrophages are polarized to an immune suppressive phenotype in a HIF1α dependent manner through tumor secreted lactic acid. Our findings demonstrate that lactic acid does not account for the ER stress and pro-inflammation in myeloid cells, though it induces immune suppressive activity. Finally, oxidized lipids are known to create lipid dysfunction and lead to defective antigen presentation in tumor infiltrating dendritic cells (32). Using oxidized LDL, we were able to create ER stress in BMDM, but only if used at 50 μg/ml, a concentration far greater than the effective concentration of P6 (< 0.0002 μg/ml).

Our identification of P6 also excludes the potential that TERS, as a phenomenon, is an artifact, e.g. due to thapsigargin carryover. Thapsigargin has several key chromophores, such as aromatic rings and acetate esters. Importantly, these types of chromophores are not present on P6, as determined by NMR analysis. Thapsigargin metabolites, as identified using rat hepatocytes (258), include chromophores like ketones, which again are absent from the P6 spectra. Therefore, we conclude that based off of our mass spectrometry and NMR spectra analysis, the activity of TERS is not due to thapsigargin carryover or to a known thapsigargin metabolite.

While we have almost resolved the chemical nature of TERS CM through the identification of Peak 6, additional aspects surrounding this molecule remain to be understood. Foremost, what is the mechanism behind its action at the level of the target cell? Presently, it appears that there are no phosphate groups on P6, which would suggest that P6 activity is unique and distinct from signaling molecules such as sphingosine 1 phosphate (S1P), which is not only produced by tumor cells undergoing ER stress (259), but also evokes lymphoangiogenesis in receiver macrophages (260). Also, the relative stability of P6 argues against the presence of a phosphate group. Should P6 not contain a phosphate group, its activity might best be attributed to the presence of a reactive aldehyde and/or hydroxyl group attached to its C1. This activity would be similar to that of 4-HNE, which is known to create reactive oxygen species (ROS) and drive ER stress. It is interesting to consider P6 as a related compound to 4-HNE. 4-HNE is associated with other stress related phenomenon including Rett syndrome (261) and ischemic stroke (262). Should P6 be similarly secreted as 4-HNE, it may serve as a valuable biomarker since P6 is bioactive at two logs lower concentration than 4-HNE.

Collectively, we identified the molecules responsible for the TERS activity as 1) eicosanoids, which induce an immune suppressive phenotype and 2) a novel

monounsaturated fatty acid, which triggers a UPR and activates pro-inflammatory genes. The results of this work provide the basis for the interrogation of clinical biospecimens and further studies to precisely identify the mechanisms responsible for the generation of P6 and its mode of action at the level of the target cell.

FIGURES

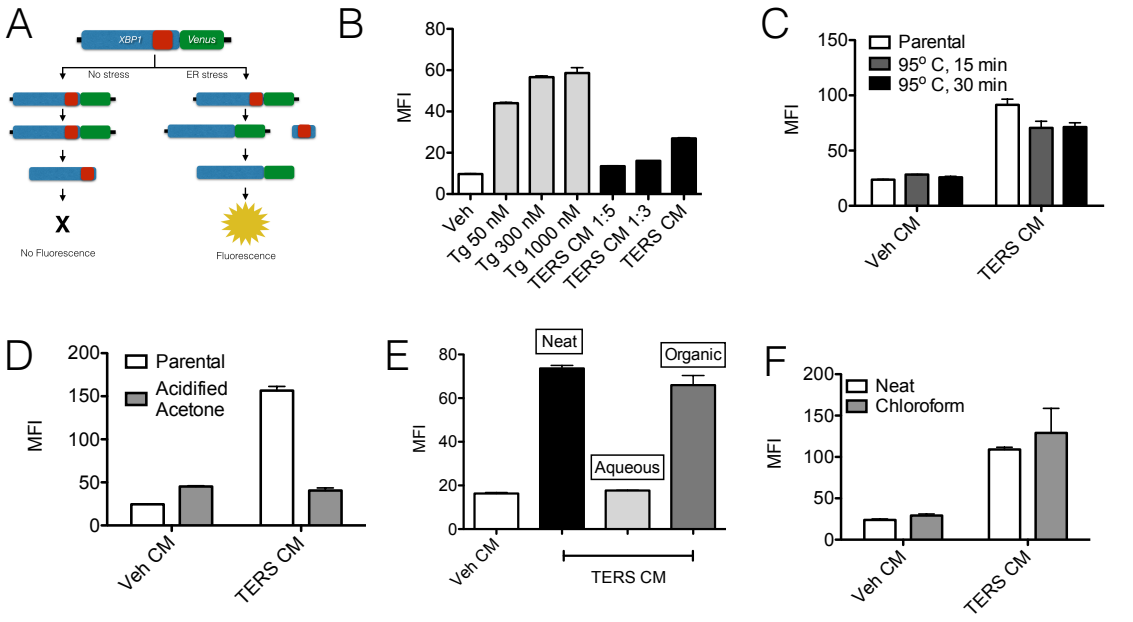

Figure 4.1. TERS is a lipophilic molecule. **(A)** Model of the ERAI reporter system. **(B)** Flow cytometric determination of mean fluorescence intensity (MFI) of Venus protein expression in TC1.ERAI reporter cells treated for 24 hours with specified concentration of thapsigargin (Tg) or TERS CM (n=2)**. (C)** ERAI reporter activity TERS and Veh CM after being kept at room temperature (parental) or being heat inactivated for specified time (n=2). **(D)** Standard Veh or TERS CM (neat) or acidified acetone extracted protein material from TERS and Veh CM loaded onto ERAI reporter cells (n=2). **(E)** ERAI activity of TC1.ERAI cells treated with Veh CM or TERS CM before (neat) and after ethyl acetate extraction to partition TERS CM into aqueous and organic phases (n=2). **(F)** ERAI activity caused by standard Veh or TERS CM (neat) or from organic phase of chloroform extract (n=2). Error bars represent SEM.

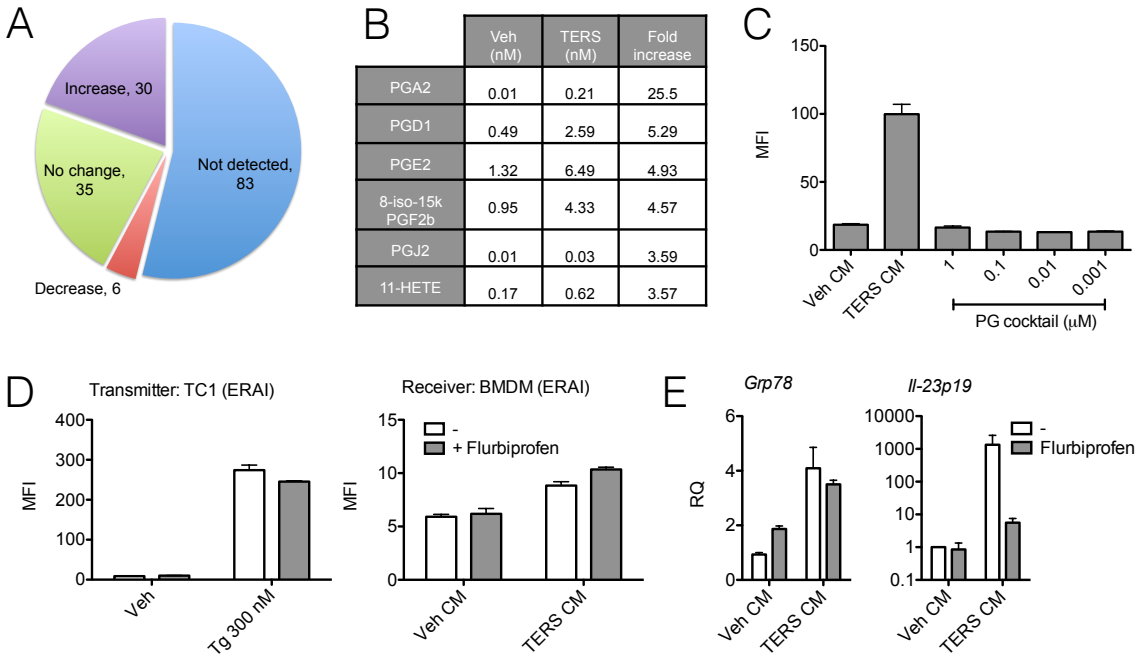

Figure 4.2. TERS is enriched in eicosanoids. **(A)** Distribution of relative abundance of probed eicosanoids in TERS CM to Veh CM eicosanoids. **(B)** Table of representative eicosanoids enriched in TERS CM, composing prostaglandin (PG) cocktail. **(C)** Flow cytometric analysis of ERAI reporter cells treated with PG cocktail at specified concentrations for 24 hours (n=2). **(D)** Flow cytometric analysis of TERS CM transmitting TC1.ERAI cells and receiver BMDM.ERAI cells (n=2) with or without flurbiprofen (10 μM). **(E)** RT-qPCR detection of BMDM treated with TERS CM in the absence or presence of flubiprofen (n=2). Relative quantification (RQ) was determined by arbitrarily normalizing gene expression to Veh CM treated condition. Error bars represent SEM.

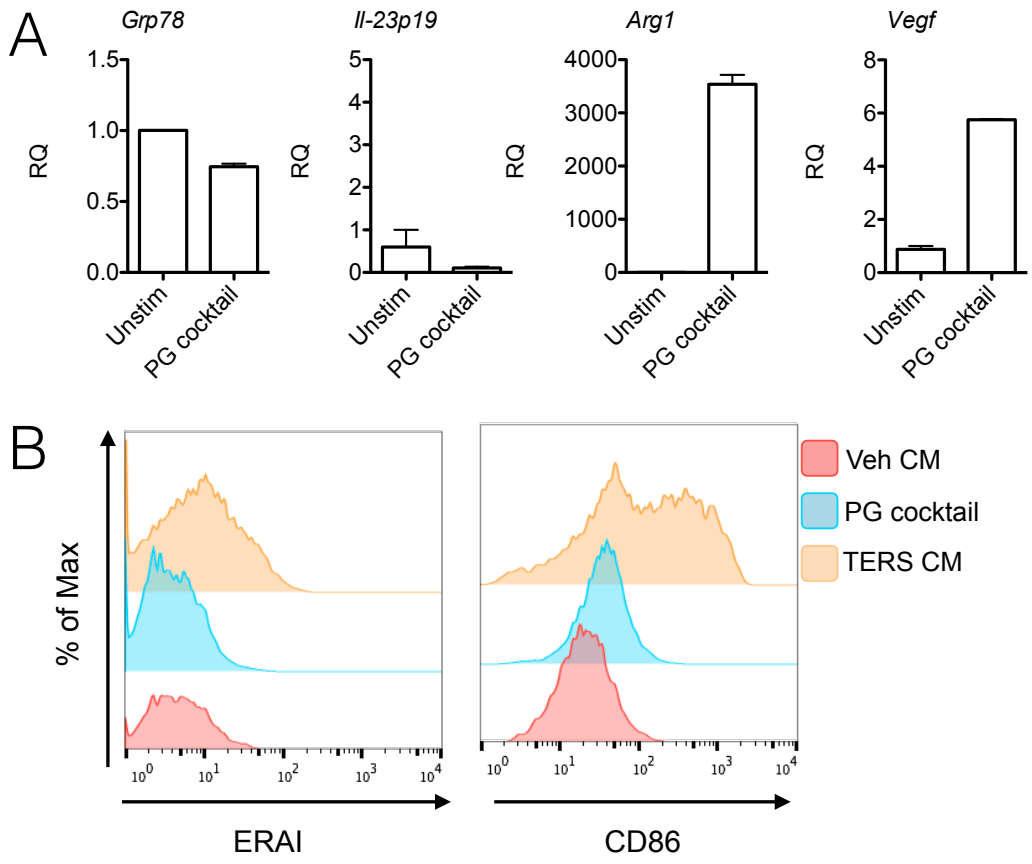

Figure 4.3. TERS associated eicosanoids promote immunesuppression. (A) Gene expression of BMDM treated with PG cocktail for 24 hours (n=2). Gene expression was normalized to unstimulated (Unstim) condition. **(B)** Flow cytometric analysis of BMDM.ERAI treated with PG cocktail or TERS CM for 24 hours detecting Venus fluorescence expression and CD86 surface expression.

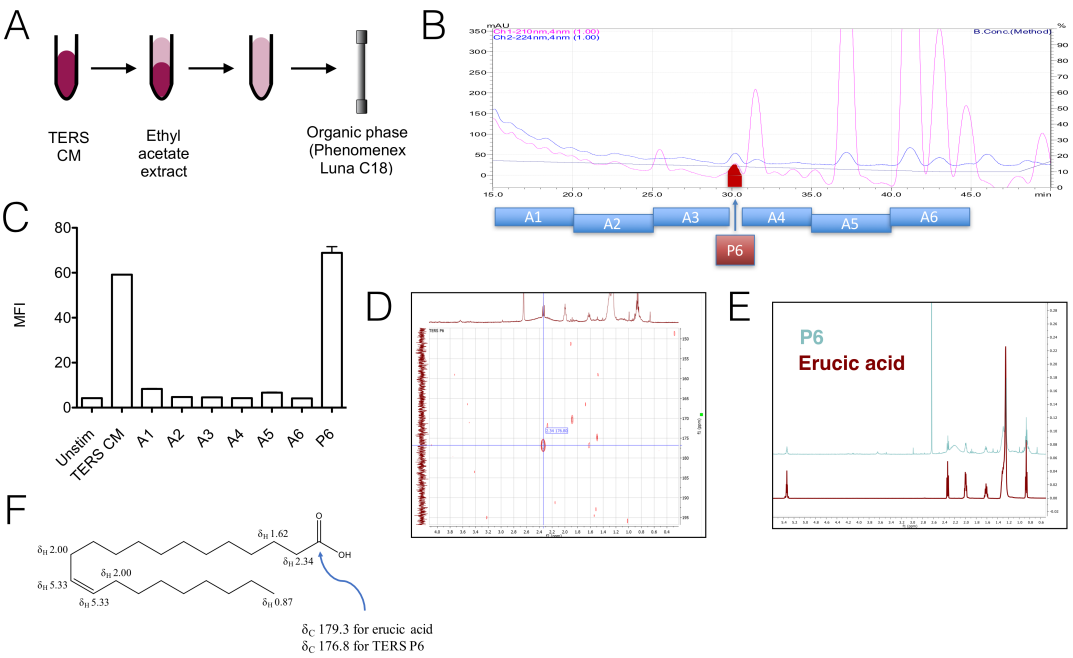

Figure 4.4. TERS is a monounsaturated fatty acid. (A) Model of isolation technique of TERS CM. **(B)** Chromatograph of ethyl acetate extract of TERS CM passed through C18 column. **(C)** Flow cytometric detection of Venus protein expression of B16.ERAI treated with TERS CM or generated retention fractions (A1-A6) and isolated peak 6 (P6), respective to chromatograph (n=2). **(D)** Partial HMBC spectra of P6. **(E)** Comparative ^{1}H NMR spectra of P6 and erucic acid. **(F)** Molecular structure of erucic acid and noted spectra difference between it and P6.

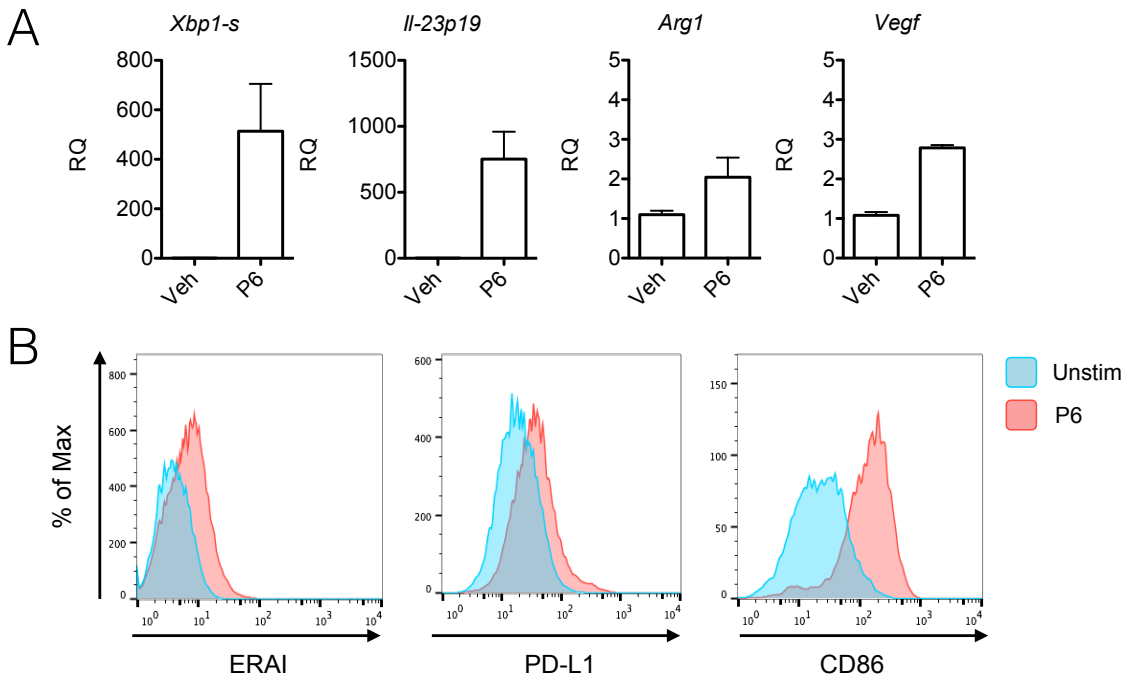

Figure 4.5. Peak 6 causes ER stress, pro-inflammation, and angiogenesis. (A) Gene expression of BMDM treated with Peak 6 (P6) samples analyzed by RT-qPCR for UPR status (*Xbp-1s*), pro-inflammation (*Il-23p19*), and immune suppression (*Arg1*, *Vegf*) and normalized to Veh condition to determine relative quantification (RQ) of gene expression (n=2/condition). **(B)** Flow cytometric analysis of expression for Venus protein in BMDM.ERAI and surface expression for PD-L1 and CD86.

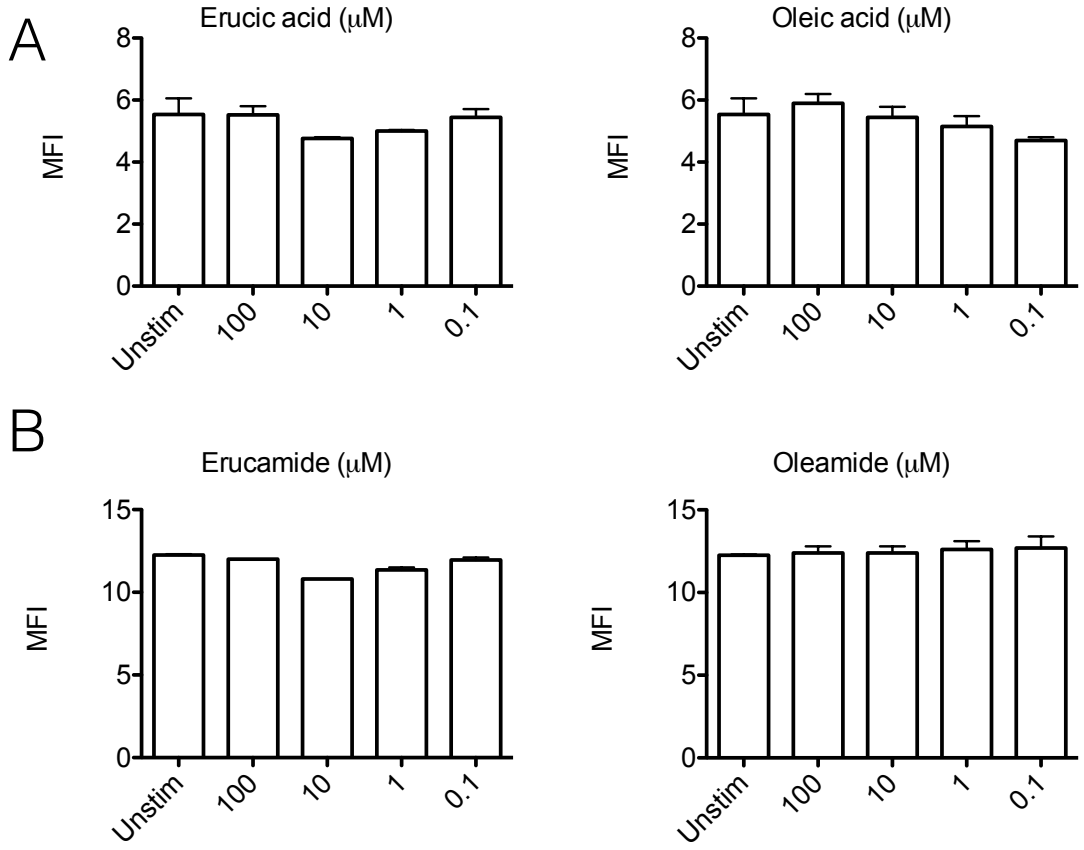

Figure 4.6. Monounsaturated fatty acids do not cause ER stress. Venus protein expression evaluated by flow cytometry for ER stress activity of **(A)** Erucic acid and oleic acid or **(B)** their amide analogues, erucamide and oleamide, treated onto reporter B16.ERAI cells for 24 hours (n=2).

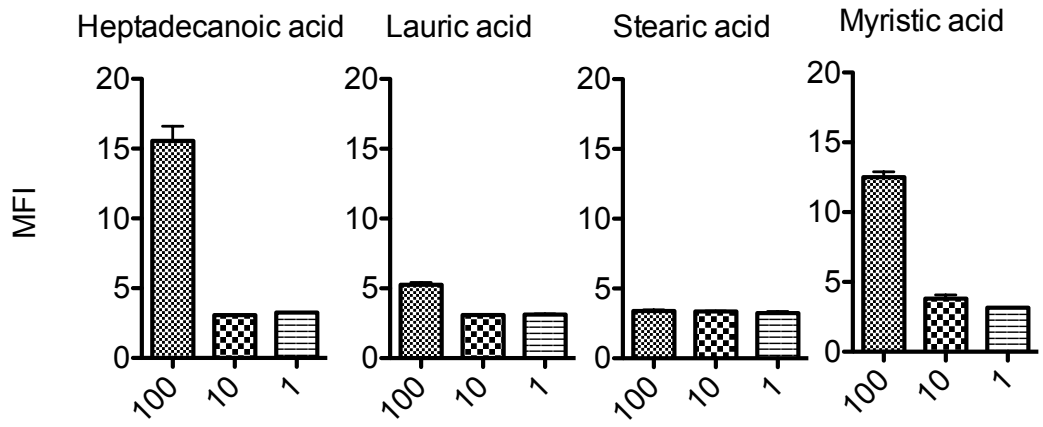

Figure 4.7. Saturated fatty acids do not cause ER stress at low concentrations. Venus protein expression evaluated by flow cytometry for ER stress activity of specified saturated fatty acid treated onto B16.ERAI cells (n=2) at specified μM concentration for 24 hours. Error bars represent SEM.

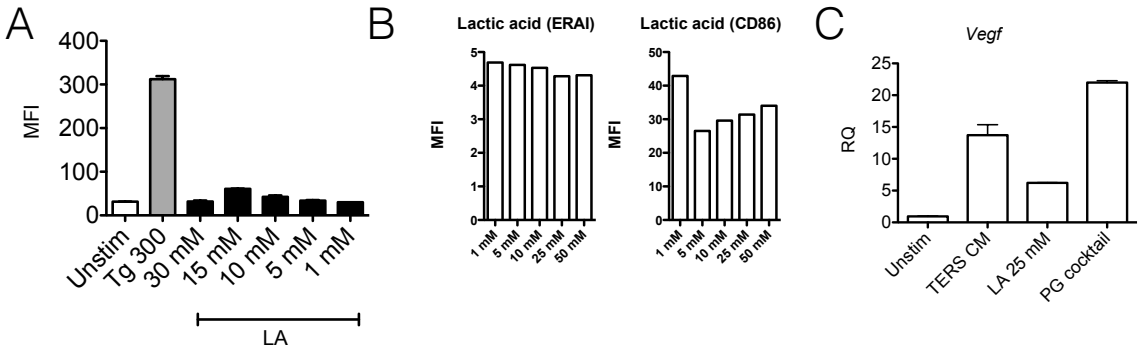

Figure 4.8. Lactic acid does not cause ER stress. (A) ER stress activity of B16.ERAI cells (n=2) treated with thapsigargin (Tg) or specified concentration of lactic acid (LA). **(B)** Flow cytometric analysis of Venus protein (ERAI) or surface expression of CD86 of BMDM.ERAI treated with increasing concentrations of lactic acid. **(C)** RT-qPCR as determined by the mean fluorescence intensity (MFI) of Venus protein expression**.** Relative quantification (RQ) was normalized to unstimulated (unstim) condition. Error bars represent SEM.

Table 4.1. Eicosanoids not detected in TERS or Veh CM.

Protectin D1	15t-Protectin D1	10S-Protectin D1	8,15-diHETE	5-iso PGF2a VI	8-iso PGF2a III	2,3 dinor-6k PGF1a	11d-TXB2	14,15-EET	
PGD2	11b PGF2a	TXB1	d17 6k PGF1a	TXB3	PGF3a	PGE3	PGD3	11b dhk PGF2a	
dihomo PGE2	dihomo PGD2	dihomo PGJ2	dihomo 15d PGD2	6k PGE1	6,15 dk-,dh-PGF1a	15k PGF1a	15k PGF2a	15k PGE2	
20oh PGF2a	19oh PGE2	20oh PGE2	2,3 dinor 11b PGF2a	PGFM	11b PGE2	PGK2	15d PGD2	15d PGJ2	
5,15-diHETE	6R-LXA4	6S-LXA4	15R-LXA4	LXA5	PGB2	15d PGA2	Resolvin E1	Resolvin D1	
20oh LTB4	20cooh LTB4	5,6-diHETE	6t LTB4	12epi LTB4	6t,12epi LTB4	12oxo LTB4	LTC4	LTD4	
13-HOTrE	8-HEPE	14,15 LTC4	14,15 LTD4	14,15 LTE4	HXA3	12-oxoETE	15 oxoEDE	17k DPA	
2,3 dinor TXB2	5,6-EET	8,9-EET	11,12-EET	LTE4	11t LTC4	11t LTD4	11t LTE4	14(15) EpETE	16(17) EpDPE
15k PGD2	dh PGF2a	PGK1	8-iso PGF3a	9-Nitrooleate	10-Nitrooleate	tetranor-PGDM	7(R) Maresin-1	17(18) EpETE	11,12-diHETrE

Table 4.2. Eicosanoids that are decreased in TERS CM over Veh CM.

	tetranor 12-HETE	18-HETE	bicyclo PGE2	dhk PGF2a	18-HEPE	dhk PGD2
Veh CM	0.37	0.03	0.02	0.06	0.04	0.05
TERS CM	0.07	0.01	0.01	0.04	0.03	0.04
Ratio	0.19	0.43	0.74	0.77	0.79	0.79

Table 4.3. Eicosanoids not differentially expressed between Veh CM and TERS CM.

	16-HETE	15-HEPE	19-HETE	17 HDoHE	20-HETE	PGEM	9,10 EpOME	17-HETE	9,10 diHOME
Veh CM	0.48	0.04	1.46	0.35	5.42	0.17	0.05	0.02	0.02
TERS CM	0.39	0.04	1.23	0.30	4.73	0.15	0.04	0.02	0.02
Ratio	0.81	0.84	0.84	0.84	0.87	0.91	0.94	0.97	0.97

	11-HEPE	12,13 EpOME	TxB2	PGF 2a	12,13 diHOME	PGF1a	6k PGF1a	9-HEPE	HXB3
Veh CM	0.02	0.04	1.43	0.98	0.02	0.39	0.14	0.06	0.20
TERS CM	0.02	0.04	1.54	1.06	0.02	0.43	0.16	0.07	0.24
Ratio	1.07	1.08	1.08	1.09	1.10	1.10	1.13	1.14	1.17

	5-oxoETE	20 HDoHE	PGE1	13-HODE	12-HETE	9-HOTrE	19oh PGF2a	12-HHTrE	8-HETrE
Veh CM	0.01	0.17	0.06	0.13	4.53	0.00	4.38	0.71	0.07
TERS CM	0.01	0.23	0.08	0.17	6.07	0.00	6.17	1.04	0.11
Ratio	1.27	1.29	1.32	1.32	1.34	1.38	1.41	1.45	1.50

	15-oxoETE	16 HDoHE	2,3 dinor 8-iso PGF2a	12-HEPE	14 HDoHE	14,15-diHETrE	19,20 DiHDPA	LTB 4
Veh CM	0.03	0.13	0.73	0.15	0.34	0.01	0.02	0.05
TERS CM	0.03	0.16	0.91	0.20	0.34	0.01	0.02	0.05
Ratio	1.21	1.23	1.25	1.27	1.00	1.01	1.02	1.04

Table 4.4. Eicosanoids increased in abundance in TERS CM over Veh CM.

	13 HDoHE	8-HETE	13-oxoODE	9-HODE	11 HDoHE	13-HOTrE(y)	8 HDoHE	10 HDoHE
Veh CM	0.09	0.17	0.05	0.08	0.14	0.01	0.17	0.06
TERS CM	0.15	0.28	0.09	0.15	0.24	0.01	0.33	0.12
Ratio	1.64	1.69	1.70	1.73	1.74	1.91	1.94	1.99

	19(20) EpDPE	8,9-diHETrE	LXB4	5,6-diHETrE	4 HDoHE	5-HEPE	11-HETE	PGJ2
Veh CM	0.03	0.00	0.24	0.00	0.15	0.02	0.17	0.01
TERS CM	0.08	0.01	0.75	0.01	0.49	0.08	0.62	0.03
Ratio	2.86	2.91	3.07	3.12	3.20	3.30	3.57	3.59

	15-HETE	15-HETrE	9-HETE	5-HETE	5-HETrE	dhk PGE2	8-iso-15k PGF2b	PGE2
Veh CM	0.53	0.19	0.09	0.16	0.02	0.04	0.95	1.32
TERS CM	1.06	0.40	0.21	0.44	0.06	0.16	4.33	6.49
Ratio	2.01	2.09	2.43	2.67	2.71	3.64	4.57	4.93

	PGA2	20cooh AA	9-oxoODE	7 HDoHE	dihomo PGF2a	PGD1
Veh CM	0.01	0.31	0.09	0.09	0.01	0.49
TERS CM	0.21	0.48	0.13	0.13	0.04	2.59
Ratio	25.52	1.52	1.53	1.53	4.98	5.29

METHODS

Cell lines and cell culture

Human cancer cells lines colon carcinoma DLD1 and prostate PC3 and murine cancer cell lines prostate TC1 and melanoma B16.F10 cancer cells were grown in RPMI or DMEM (Corning) supplemented with 10% FBS (HyClone) and 1% penicillin/streptomycin/L-glutamine, NEAA, sodium pyruvate, HEPES. All cells were maintained at 37°C incubation with 5% O_2. All cell lines were mycoplasma free as determined PCR assay (Southern Biotech).

Establishment of ERAI reporter cells

Cancer cell line reporter cells were transduced with the ERAI construct, originally described (234). Briefly, the pCAX-F-XBP1ΔDBD-venus (a kind gift from Dr. Iwawaki (Gunma University)) underwent PCR using following primers: F: ctaccggactcagatctcgagccaccATGGACTACAAGGACGACG, R: gaattatctagagtcgcggccgcTTACTTGTACAGCTCGTCC. PCR fragments were cloned into pLVX-puro (Clontech) lentivirus vector with Gibson Assembly Mixture (NEB) according to manufacturer's instruction. Stbl3 competent cells were transformed to produce the plasmid insert, whose presence was confirmed by sequencing. For production of lentivirus, 293FT (Invitrogen) cells were seeded in 10 cm dish and transfected with a plasmid mixture of ERAI plasmid and psPAX2 and pMD2G viral packaging plasmids. The supernatant of virus–producing transfected cells was collected every 24 hours for three days post transfection. Viral supernatant was concentrated by 10% PEG-8000 and pelleted with 2000 x g for 40 min at 4°C and re-suspended PBS. Cancer cell lines were transduced with lentivirus by adding concentrated virus solution, supplemented with polybrene (8 μg/mL). Lines were transduced for 48 hours. Transduced cells were then washed twice with PBS

and positively selected for using puromycin (2 μg/mL) for two weeks. In some instances, positively transduced cells were then stimulated for Venus expression and were sorted by FACS (BD) to isolate high expressing clones. Lines were grown under standard growth medium supplemented with puromycin (2 μg/mL).

Flow cytometry

ERAI activity assays were performed on single cell suspensions. Briefly, treated reporter cells were enzymatically detached for plastic, and washed twice with PBS (Corning) supplemented with 0.5% BSA (w:v) and 0.05% NaN_3 (v:v). For surface staining, BMDM/DC were stained with fluorphore conjugated anti-PD-L1- (BD Biosciences), anti-CD80 (BD Biosceinces), or anti-CD96 (BD Biosciences). Data were acquired on a FACSCalibur flow cytometer (Becton Dickinson) and analyzed using CellQuest Pro (BD Biosciences) and FlowJo software (Tree Star). Analyzed cells were washed resuspended in 7AAD staining buffer and analyzed via flow cytometry with 7AAD exclusion.

TERS conditioned media (CM) generation

DLD1 cancer cells were induced to undergo ER stress through treatment of 300 nM thapsigargin (Tg) (Enzo Life Sciences) for 2 hours. Control cells were similarly treated with an equal volume of vehicle (0.02% ethanol). Cells were washed twice with Dulbecco's PBS (Corning), and then incubated in fresh, standard growth medium for 16 hrs. Conditioned medium was then harvested, centrifuged for 10 min at 2,000 RPM, filtered through a 0.22-μm filter (Millipore), and treated to cells, stored at -80°C until use, or used for specified chemical techniques.

BMDM and BMDC generation:

Bone marrow derived cells were procured by isolating the femur and tibia of specified host and flushing out the bone marrow using cold, unsupplemented RPMI growth media (Corning) using a 27 gauge needle and syringe. Hemolysis was performed using ACK Lysis buffer (Bio Whittaker). For macrophage differentiation, bone marrow cells were incubated one week in standard growth medium supplemented with 30% L929 conditioned medium (LCM). For dendritic cell differentiation, standard growth medium was supplemented with 10% mGM-CSF-producing hybridoma cells (GCM) as described in (233) and resupplemented every two days throughout one week.

Lipid Maps eicosanoid analysis

TERS and Veh CM was generated plating PC3 cells at 5e5/well in a 6 well plate. Conditioned medium was generated in 2 mL. Bioactive TERS CM was then provided to Lipid Maps core (UCSD). Briefly, eicosanoids were removed from media by loading methanol (MeOH) and 0.5% acetic acid to CM. The organic phase was then separated, lyophilized, and resuspended in MeOH solvent and passed through a Synergi reverse-phase C18 column. Abundances of eicosanoids were then determined using an ABI/SCiex 4000 QTRAP hybrid, triple quadrupole, linear ion trap mass spectrometer. Quantitation of c.m. contained eicosanoids were then determined based off of established curves of commercially purchased standards (Cayman). Detailed methods are described (263). For PG cocktail, all synthetic eicosanoids and flurbiprofen were purchased through Cayman.

Acidified acetone total protein extraction

Acetone was supplemented with HCl to create a 1 mM solution. For every unit of CM, four units of ice cold acidified acetone was added (v:v). Solutions were mixed and kept on ice for 10 minutes. Following, precipitate was pelleted by centrifugation at 2,500 x

g for 15 minutes at 4^{o}C. Supernatant was then gently poured off and residual organic solvent was evaporated by speed-vac. Dried pellet was resuspended with standard growth medium at same starting volume of CM.

Ethyl acetate and chloroform extraction

Lipid soluble material was extracted from TERS CM by first adding equal parts ethyl acetate or chloroform (v:v). After 2 hours of gentle stirring, carefully to avoid emersion formation, the organic layer was isolated and dried under vacuum. Dried material was solubilized into acetonitrile and ethyl acetate and transferred into a smaller vial. Solvents were removed under nitrogen gas flow. Generally, 100 ml of TERS yielded 4 mg of extract material. For studies probing aqueous phase of ethyl acetate extraction, aqueous phase as lyophilized before resolubilized in standard growth medium.

HPLC isolation

Ethyl acetate extract of TERS CM was solubilized with 1 ml of acetonitrile. No other filter or pretreatment method were used. Two Shimadzu LC-6AD pumps and SPD-M10A diode array detectors were connected with SCL-10A controller module. Solvents were degassed with DGU-14A degasser. Phenomenex Luna C18(2) 100 Å 250 x 10 mm reverse phased column was used. HPLC grade solvents, water and acetonitrile (Fisher Scientific), were used. Tetrafluoroacetic (TFA) acid (Sigma Aldrich) was added at 0.05% (v/v). Gradient run condition was ran at 2 mL/min solvent flow and used as follows; 80% acetonitrile maintained for 3 minutes, acetonitrile concentration raised to 90% till 43 minute, 90% acetonitrile and maintained until minute 48.

HPLC fraction generation

Beginning at minute 5 minutes and ending at minute 45, retention fractions were gathered every 5 minutes to generates fractions A1 to A6. Each fraction was separately dried under air flow. Chromatograph were recorded using UV absorbance of 210, 224, and 254 nm.

NMR equipment

NMR spectra were recorded on a Jeol 500 MHz NMR spectrometer (500 and 125 MHz for ^{1}H and ^{13}C NMR respectively), using the signals of the residual solvent protons carbons as internal references (δ_H 7.24 and δ_C 77.0 ppm for $CDCl_3$).

RT-qPCR

RNA was harvested from cells using Nucleospin II Kit (Macherey-Nagel). Concentration and purity of RNA was quantified the NanoDrop (ND-1000) spectrophotometer (Thermo Scientific) and analyzed with NanoDrop Software v3.8.0. RNA was normalized between conditions and cDNA generated using the High Capacity cDNA Synthesis kit (Life Technologies). RT-qPCR was performed on ABI 7300 Real-Time PCR system using TaqMan reagents for 50 cycles using universal cycling conditions. Cycling conditions followed manufacturer's specifications (KAPA Biosystems). Target gene expression was normalized to *β-actin*, and relative expression determined by using the –ΔΔCt relative quantification method. Validated FAM-labeled mouse *Hspa5*, *Ddit3*, *Il-6*, *Il-23p19*, *Arg1, Vegf*, and VIC-labeled mouse *β-actin* TaqMan primer/probe sets (Life Technologies, Catalog # 4326315E) were used. FAM-labeled qPCR primer set specific for the mouse *Xbp-1* spliced isoform was generated from Integrated DNA Technologies.

ACKNOWLEDGEMENTS

Chapter 4 is a portion from a manuscript in preparation that will be submitted as: Rodvold, J.J., Yang, I., Hiramatsu, N., Chiu K.T., Quehenberger, O., Iwawaki, T., Lin, J.H., Fenical, W., Zanetti, M.. Tumor cells undergoing ER stress produce a novel lipid that drives cell extrinsic myeloid immune dysfunction. The dissertation author is the primary author of this manuscript.

Chapter 5

CONCLUSION

This project was borne out of investigations to explain one of the most outstanding questions in tumor immunology: “What cues produced by the tumor microenvironment are necessary to coerce immune cells to abandon their role of tumor rejection and facilitate tumor growth?” Investigation into this question has led to a wealth of new knowledge as to how the tumor microenvironment operates in a cell non-autonomous manner to ensure tumor outgrowth. The sum of these efforts, which includes several published reports, as well as the yet-to-be published data contained within this dissertation, is presented in Figure 5.1.

First I found that TERS affects cancer cells in a several ways. Recipient cancer cells undergo a global ER stress response, and upregulate GRP78 both intracellularly and translocate it to the cell surface. These activities are associated with chemoresistance, tumor cell survival, and are predictors of poor prognosis in variety of malignancies. More striking is that TERS experienced cancer cells have decreased expression of PERK associated proteins while having increased expression of Wnt signaling, suggesting that pathways known to be involved in tumorigenesis are targets of TERS mediated effects. My findings reveal that this cell nonautonomous reprogramming enhances cytoprotection against tumor microenvironmental (nutrient deprivation) and chemotherapeutic (bortezomib and paclitaxel) insults. This protection primarily relies on PERK/ATF4 signaling. The gains in cellular fitness were shown in cell tagging experiments, where it became evident that dominant TERS clones emerge only upon secondary challenge. This suggests that the tumor microenvironment may harbor tumor cells in a latent state until acquiring survival characteristics upon endogenous (nutrient starvation) or exogenous (chemotherapy) stimuli. This new behavior represents a concern for therapeutic

intervention as it is capable of driving functional tumor heterogeneity independent of genomic alterations.

Second, consistent with our earlier reports that myeloid cells treated with TERS in vitro acquire a ‘mixed’ pro-inflammatory/immune suppressive phenotype, I was able to provide evidence that myeloid cells that accumulate in tumors in vivo in immunocompetent mice are a faithful mimic to those generated in vitro. By analyzing two in vivo models of tumorigenesis in the mouse, I found that tumor infiltrating myeloid cells undergo ER stress and have increased gene expression for pro-inflammatory and immune suppressive genes relative to myeloid cells in healthy tissue. This demonstrates that TERS mediated immune gene expression is likely operative in vivo, is limited to the tumor microenvironment, and is not tissue specific. The mechanism behind TERS polarization in myeloid cells appears to be IRE1α dependent and PERK independent.

Third, I was able to determine that the characteristics of ER stress transmission imparted on myeloid cells or tumor cells are owed to two molecular species: eicosanoids and a monounsaturated fatty acid, provisionally termed Peak 6 (P6). The former endows immune suppressive features on myeloid cells while the latter creates ER stress and drives pro-inflammation. The isolation of P6 proved to be particularly vexing given its chemistry and low abundance despite robust activity. To the best of our knowledge, P6 is a novel molecule with unique chemistry.

A general consideration is that this new type of cell extrinsic signaling within the tumor microenvironment is like many other signaling systems that cancer cells artfully manipulate, coopting neighboring cells in a seemingly “altruistic” manner that, as demonstrated, only benefits tumor growth. If at all pertinent, a parallel can be drawn with C. elegans where XBP-1 driven activity of neuronal cells provides stress resistance and longevity to the organism in a cell nonautonomous manner (150, 264).

Where to go from here? A groundswell of research will be available once P6 is completely identified, which is well within reach. Foremost, development of a mass spectrometry bioassay will enable us to validate the presence of P6 in clinical specimens as a biomarker indicative of a process taking place in the tumor microenvironment and possibly as a predictor of clinical progression. At the biologic level, we can begin to elucidate the exact mechanism behind P6 generation, transmission, and action at the level of target cells.

Should ablating P6 curb tumor growth, it will be possible to contextualize its contributions to clonal heterogeneity in the setting of those signaling pathways known to be affected by TERS (Wnt, PERK, GRP78), and likewise determine the consequences on the myeloid cell compartment. This may lead to new forms of therapy specifically targeting the tumor microenvironment.

Two fertile areas of further inquiry in the field of TERS lay ahead. The first is to explore the relationship between the dysfunction within the tumor microenvironment resulting from ER stress transmission and T cell dysfunction. Does TERS affect T-lymphocytes? Does TERS promote the differentiation of Tregs? As the interplay among T cells and the TME is not only complex, but critical to the success of immunotherapy (e.g. immune check point blockage), shedding light on this aspect of the tumor:immune interface will prove incredibly informative.

The other is an inquiry into the relationship between aneuploidy and the ER stress based cell nonautonomous phenomenon, the object of the studies presented this dissertation. In Chapter 1 of this dissertation, I discussed Kroemer's proposal that aneuploidy induces ER stress and promotes anti-tumor T cell immunity (82). However, this model is in direct contrast with TERS mediated effects in the tumor microenvironment. Because the two theories are antithetic (265), I attempted to reconcile the two by predicting

that aneuploidy creates ER stress in cancer cells and, in turn, these cancer cells signal to myeloid cells via TERS. I obtained initial validation for this new idea in an experiment where nearly diploid colon cancer DLD1 cells were treated for 24 hours with reversine to induce aneuploidy (266). DLD1 cells underwent ER stress that lasted for one month (Fig. 5.2, A and B). The supernatant from these cells treated onto bone marrow derived macrophages increased CD86 and PD-L1 (two hallmarks of TERS) (Fig. 5.2.C). The implication of this study is that aneuploidy leads to ER stress and its cell nonautonomous effects. This connection may represent a new dimension in the study of the interface between cancer cell biology and immunity. This no doubt will have relevance for immunotherapy and the response to immune checkpoint inhibitors (267).

There likely will never be a silver bullet against cancer, but treatment instead will rely on a series of interventions targeting both cancer cells and the tumor microenvironment. Beyond what currently is under development, I propose that the phenomenon driving TERS is a worthy candidate of this consideration. This dissertation provides three possible novel lines of therapeutic intervention: 1) Chemical inhibition of IRE1α, which would impinge on TERS production (Fig. 3.8) as well as the polarization of myeloid cells (Fig. 3.5); 2) Blocking P6 itself, for example through use of antibodies; 3) Inhibit the production of immune suppressive prostaglandins produced by tumor cells undergoing ER stress. Affecting the mechanism or molecules responsible for TERS would disable a key mechanism of tumor escape and rescue anti-tumor immunity.

Certainly, research related to TERS and P6 is only in its infancy but ultimately, validating this mechanism in cancer patients will make TERS/P6 as a new biomarker of disease, and may open the path to novel forms of therapy that target the tumor microenvironment. Arguably, the impact of our work on patient management could be

huge, resulting in extending life for patients with aggressive or recurrent/progressive cancer.

FIGURES

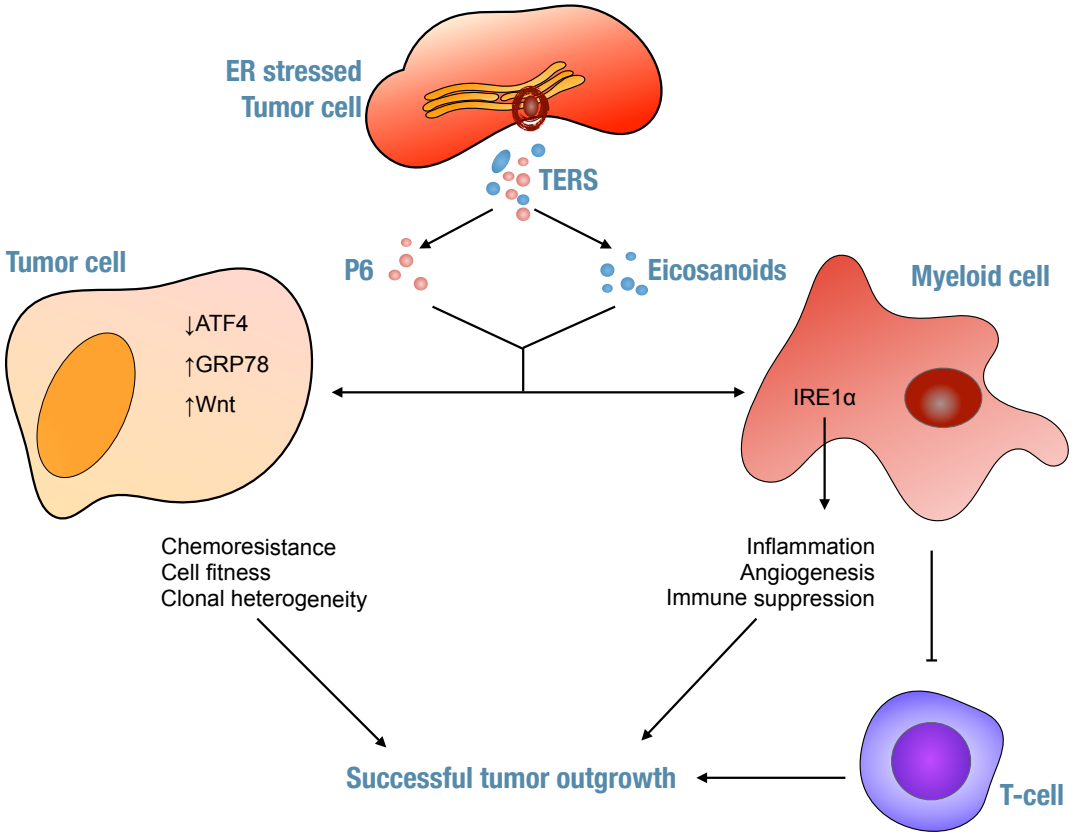

Figure 5.1. Revised model of TERS and its mediated effects on tumor outgrowth. A tumor cell undergoing ER stress produces transmissible ER stress, or TERS. TERS consists two molecules: a monounsaturated fatty acid provisionally termed Peak 6 (P6) and a variety of eicosanoids. Together, these molecules affect both recipient tumor cells and myeloid cells. **(Right)** TERS experienced tumor cells increase expression in GRP78 and in Wnt signaling while decreasing expression of ATF4. This reprogramming provides the tumor cell with chemoresistance, cellular fitness, and clonal heterogeneity. These events appear to be PERK dependent. **(Left)** Recipient myeloid cells undergo a polarization in a IRE1α dependent manner that lead to the production of pro-tumorigenic cytokines that are inflammatory, angiogenic, and immune suppressive. These effects in sum lead to successful tumor outgrowth.

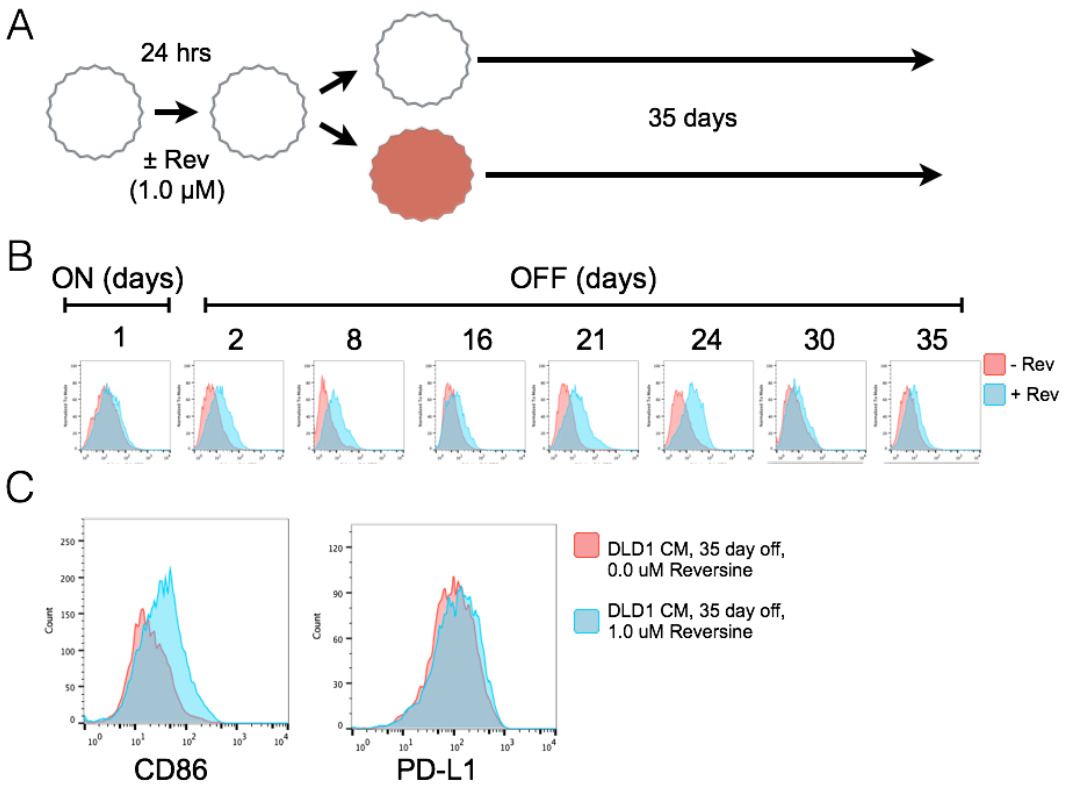

.

Figure 5.2. Induced aneuploidy leads to durable ER stress and production of factors that polarize BMDM. (A) DLD1.ERAI cells were treated with (blue) or without (red) 1.0 μM reversine (Cayman) for 24 hours. Subsequently, cells were washed twice to remove any excess molecule and cells were maintained under standard cell culture passaging techniques. **(B)** At specified days, cells were analyzed by flow cytometry for Venus expression. **(C)** For conditioned medium, parental DLD1.ERAI or reversine treated DLD1.ERAI cells were plated at 5e5 cells/well in a six well plate for 48 hours. The resulting conditioned medium was filtered and treated onto BMDM for 24 hours. Recipient BMDM were analyzed by flow cytometry for surface expression of CD86 and PD-L1.

REFERENCES

1. **Burnet FM.** 1970. The concept of immunological surveillance. Prog Exp Tumor Res **13:**1-27.

2. **Schreiber RD, Old LJ, Smyth MJ.** 2011. Cancer immunoediting: integrating immunity's roles in cancer suppression and promotion. Science (New York, NY) **331:**1565-1570.

3. **Virchow RKL.** 1865. Die Krankhaften Geschwülste A. Hirschwald, Berlin.

4. **Grivennikov SI, Greten FR, Karin M.** 2010. Immunity, inflammation, and cancer. Cell **140:**883-899.

5. **Silverstein AM.** 1989. A history of immunology. Academic Press, San Diego, Inc.

6. **Burnet FM.** 1971. Immunological surveillance in neoplasia. Transplant Rev **7:**3-25.

7. **Prehn RT.** 1972. The immune reaction as a stimulator of tumor growth. Science **176:**170-171.

8. **Grivennikov S, Karin E, Terzic J, Mucida D, Yu G-Y, Vallabhapurapu S, Scheller J, Rose-John S, Cheroutre H, Eckmann L, Karin M.** 2009. IL-6 and Stat3 Are Required for Survival of Intestinal Epithelial Cells and Development of Colitis-Associated Cancer. Cancer cell **15:**103-113.

9. **Langowski JL, Zhang X, Wu L, Mattson JD, Chen T, Smith K, Basham B, McClanahan T, Kastelein RA, Oft M.** 2006. IL-23 promotes tumour incidence and growth. Nature **442:**461-465.

10. **Sakaguchi S.** 2003. Control of immune responses by naturally arising CD4+ regulatory T cells that express toll-like receptors. J Exp Med **197:**397-401.

11. **Sakaguchi S, Yamaguchi T, Nomura T, Ono M.** 2008. Regulatory T cells and immune tolerance. Cell **133:**775-787.

12. **de Visser KE, Korets LV, Coussens LM.** 2005. De novo carcinogenesis promoted by chronic inflammation is B lymphocyte dependent. Cancer Cell **7:**411-423.

13. **Andreu P, Johansson M, Affara NI, Pucci F, Tan T, Junankar S, Korets L, Lam J, Tawfik D, DeNardo DG, Naldini L, de Visser KE, De Palma M, Coussens LM.** 2010. FcRgamma activation regulates inflammation-associated squamous carcinogenesis. Cancer Cell **17:**121-134.

14. **Ammirante M, Luo JL, Grivennikov S, Nedospasov S, Karin M.** 2010. B-cell-derived lymphotoxin promotes castration-resistant prostate cancer. Nature **464:**302-305.

15. **Ostrand-Rosenberg S, Sinha P.** 2009. Myeloid-derived suppressor cells: linking inflammation and cancer. J Immunol **182:**4499-4506.

16. **Gabrilovich DI, Ostrand-Rosenberg S, Bronte V.** 2012. Coordinated regulation of myeloid cells by tumours. Nat Rev Immunol **12:**253-268.

17. **Willimsky G, Blankenstein T.** 2005. Sporadic immunogenic tumours avoid destruction by inducing T-cell tolerance. Nature **437:**141-146.

18. **Dunn GP, Bruce AT, Ikeda H, Old LJ.** 2002. Cancer immunoediting: from immunosurveillance to tumor escape. Nature.

19. **Shankaran V, Ikeda H, Bruce AT, White JM, Swanson PE, Old LJ, Schreiber RD.** 2001. IFN[gamma] and lymphocytes prevent primary tumour development and shape tumour immunogenicity : Abstract : Nature. Nature **410:**1107-1111.

20. **Simson L, Ellyard JI, Dent LA, Matthaei KI, Rothenberg ME, Foster PS, Smyth MJ, Parish CR.** 2007. Regulation of carcinogenesis by IL-5 and CCL11: a potential role for eosinophils in tumor immune surveillance. Journal of immunology (Baltimore, Md : 1950) **178:**4222-4229.

21. **Vesely MD, Kershaw MH, Schreiber RD, Smyth MJ.** 2011. Natural innate and adaptive immunity to cancer. Annual review of immunology **29:**235-271.

22. **Seliger B, Schreiber K, Delp K, Meissner M, Hammers S, Reichert T, Pawlischko K, Tampe R, Huber C.** 2001. Downregulation of the constitutive tapasin expression in human tumor cells of distinct origin and its transcriptional upregulation by cytokines. Tissue Antigens **57:**39-45.

23. **Topalian SL, Hodi FS, Brahmer JR, Gettinger SN, Smith DC, McDermott DF, Powderly JD, Carvajal RD, Sosman JA, Atkins MB, Leming PD, Spigel DR, Antonia SJ, Horn L, Drake CG, Pardoll DM, Chen L, Sharfman WH, Anders RA, Taube JM, McMiller TL, Xu H, Korman AJ, Jure-Kunkel M, Agrawal S, McDonald D, Kollia GD, Gupta A, Wigginton JM, Sznol M.** 2012. Safety, activity, and immune correlates of anti-PD-1 antibody in cancer. N Engl J Med **366:**2443-2454.

24. **Hamilton MJ, Bosiljcic M, Lepard NE, Halvorsen EC, Ho VW, Banáth JP, Krystal G, Bennewith KL.** 2014. Macrophages are more potent immune suppressors ex vivo than immature myeloid-derived suppressor cells induced by metastatic murine mammary carcinomas. Journal of immunology (Baltimore, Md : 1950) **192:**512-522.

25. **Almand B, Resser JR, Lindman B, Nadaf S, Clark JI, Kwon ED, Carbone DP, Gabrilovich DI.** 2000. Clinical Significance of Defective Dendritic Cell Differentiation in Cancer. Clinical cancer research : an official journal of the American Association for Cancer Research **6:**1755-1766.

26. **Almand B, Clark JI, Nikitina E, van Beynen J, English NR, Knight SC, Carbone DP, Gabrilovich DI.** 2001. Increased production of immature myeloid cells in

cancer patients: a mechanism of immunosuppression in cancer. J Immunol **166:**678-689.

27. **Prendergast GC.** 2008. Immune escape as a fundamental trait of cancer: focus on IDO. Oncogene **27:**3889-3900.

28. **Thomas DA, Massague J.** 2005. TGF-beta directly targets cytotoxic T cell functions during tumor evasion of immune surveillance. Cancer Cell **8:**369-380.

29. **Gabrilovich DI, Ishida T, Nadaf S, Ohm JE, Carbone DP.** 1999. Antibodies to Vascular Endothelial Growth Factor Enhance the Efficacy of Cancer Immunotherapy by Improving Endogenous Dendritic Cell Function. Clinical cancer research : an official journal of the American Association for Cancer Research **5:**2963-2970.

30. **Zea AH, Rodriguez PC, Atkins MB, Hernandez C, Signoretti S, Zabaleta J, McDermott D, Quiceno D, Youmans A, O'Neill A, Mier J, Ochoa AC.** 2005. Arginase-Producing Myeloid Suppressor Cells in Renal Cell Carcinoma Patients: A Mechanism of Tumor Evasion. Cancer research **65:**3044-3048.

31. **Rodriguez PC, Quiceno DG, Zabaleta J, Ortiz B, Zea AH, Piazuelo MB, Delgado A, Correa P, Brayer J, Sotomayor EM, Antonia S, Ochoa JB, Ochoa AC.** 2004. Arginase I production in the tumor microenvironment by mature myeloid cells inhibits T-cell receptor expression and antigen-specific T-cell responses. Cancer research **64:**5839-5849.

32. **Herber DL, Cao W, Nefedova Y, Novitskiy SV, Nagaraj S, Tyurin VA, Corzo A, Cho H-I, Celis E, Lennox B, Knight SC, Padhya T, McCaffrey TV, McCaffrey JC, Antonia S, Fishman M, Ferris RL, Kagan VE, Gabrilovich DI.** 2010. Lipid accumulation and dendritic cell dysfunction in cancer. Nature medicine **16:**880-886.

33. **Chen ML.** 2005. Regulatory T cells suppress tumor-specific CD8 T cell cytotoxicity through TGF- signals in vivo. PNAS **102:**419-424.

34. **Langowski JL, Kastelein RA, Oft M.** 2007. Swords into plowshares: IL-23 repurposes tumor immune surveillance. Trends Immunol **28:**207-212.

35. **Grivennikov SI, Wang K, Mucida D, Stewart CA, Schnabl B, Jauch D, Taniguchi K, Yu G-Y, Osterreicher CH, Hung KE, Datz C, Feng Y, Fearon ER, Oukka M, Tessarollo L, Coppola V, Yarovinsky F, Cheroutre H, Eckmann L, Trinchieri G, Karin M.** 2012. Adenoma-linked barrier defects and microbial products drive IL-23/IL-17-mediated tumour growth. Nature **491:**254-258.

36. **Teng MW, Andrews DM, McLaughlin N, von Scheidt B, Ngiow SF, Moller A, Hill GR, Iwakura Y, Oft M, Smyth MJ.** 2010. IL-23 suppresses innate immune response independently of IL-17A during carcinogenesis and metastasis. Proc Natl Acad Sci U S A **107:**8328-8333.

37. **Smyth MJ, Cretney E, Kershaw MH, Hayakawa Y.** 2004. Cytokines in cancer immunity and immunotherapy. Immunological reviews **202:**275-293.

38. **Tsukamoto H, Senju S, Matsumura K, Swain SL, Nishimura Y.** 2015. IL-6-mediated environmental conditioning of defective Th1 differentiation dampens antitumour immune responses in old age. Nature Communications **6:**6702.

39. **Balkwill FR, Lee A, Aldam G, Moodie E, Thomas JA, Tavernier J, Fiers W.** 1986. Human Tumor Xenografts Treated with Recombinant Human Tumor Necrosis Factor Alone or in Combination with Interferons. Cancer research **46:**3990-3993.

40. **Moore RJ, Owens DM, Stamp G, Arnott C, Burke F, East N, Holdsworth H, Turner L, Rollins B, Pasparakis M, Kollias G, Balkwill F.** 1999. Mice deficient in tumor necrosis factor-|[alpha]| are resistant to skin carcinogenesis. Nature medicine **5:**828-831.

41. **Cordero JB, Macagno JP, Stefanatos RK, Strathdee KE, Cagan RL, Vidal M.** 2010. Oncogenic Ras Diverts a Host TNF Tumor Suppressor Activity into Tumor Promoter. Developmental cell **18:**999-1011.

42. **Rosenberg SA, Restifo NP.** 2015. Adoptive cell transfer as personalized immunotherapy for human cancer. Science **348:**62-68.

43. **Boutros C, Tarhini A, Routier E, Lambotte O, Ladurie FL, Carbonnel F, Izzeddine H, Marabelle A, Champiat S, Berdelou A, Lanoy E, Texier M, Libenciuc C, Eggermont AM, Soria JC, Mateus C, Robert C.** 2016. Safety profiles of anti-CTLA-4 and anti-PD-1 antibodies alone and in combination. Nat Rev Clin Oncol **13:**473-486.

44. **Warburg O.** 1956. On the origin of cancer cells. Science **123:**309-314.

45. **Heazlewood CK, Cook MC, Eri R, Price GR, Tauro SB, Taupin D, Thornton DJ, Png CW, Crockford TL, Cornall RJ, Adams R, Kato M, Nelms KA, Hong NA, Florin THJ, Goodnow CC, McGuckin MA.** 2008. Aberrant Mucin Assembly in Mice Causes Endoplasmic Reticulum Stress and Spontaneous Inflammation Resembling Ulcerative Colitis. PLOS Medicine **5:**e54.

46. **Schröder M, Kaufman RJ.** 2005. ER stress and the unfolded protein response. Mutation Research/Fundamental and Molecular Mechanisms of Mutagenesis **569:**29-63.

47. **Walter P, Ron D.** 2011. The unfolded protein response: from stress pathway to homeostatic regulation. Science **334:**1081-1086.

48. **Bertolotti A, Wang X, Novoa I, Jungreis R, Schlessinger K, Cho JH, West AB, Ron D.** 2001. Increased sensitivity to dextran sodium sulfate colitis in IRE1beta-deficient mice. J Clin Invest **107:**585-593.

49. **Urano F, Wang X, Bertolotti A, Zhang Y, Chung P, Harding HP, Ron D.** 2000. Coupling of stress in the ER to activation of JNK protein kinases by transmembrane protein kinase IRE1. Science **287:**664-666.

50. **Hollien J, Lin JH, Li H, Stevens N, Walter P, Weissman JS.** 2009. Regulated Ire1-dependent decay of messenger RNAs in mammalian cells. J Cell Biol **186:**323-331.

51. **Vattem KM, Wek RC.** 2004. Reinitiation involving upstream ORFs regulates ATF4 mRNA translation in mammalian cells. Proc Natl Acad Sci U S A **101:**11269-11274.

52. **Lin JH, Walter P, Yen TS.** 2008. Endoplasmic reticulum stress in disease pathogenesis. Annu Rev Pathol **3:**399-425.

53. **Marciniak SJ, Ron D.** 2006. Endoplasmic reticulum stress signaling in disease. Physiol Rev **86:**1133-1149.

54. **Pagliassotti MJ.** 2012. Endoplasmic reticulum stress in nonalcoholic fatty liver disease. Annu Rev Nutr **32:**17-33.

55. **Ribeiro CM, Boucher RC.** 2010. Role of endoplasmic reticulum stress in cystic fibrosis-related airway inflammatory responses. Proc Am Thorac Soc **7:**387-394.

56. **Fernandez PM, Tabbara SO, Jacobs LK, Manning FC, Tsangaris TN, Schwartz AM, Kennedy KA, Patierno SR.** 2000. Overexpression of the glucose-regulated stress gene GRP78 in malignant but not benign human breast lesions. Breast Cancer Res Treat **59:**15-26.

57. **Uramoto H, Sugio K, Oyama T, Nakata S, Ono K, Yoshimastu T, Morita M, Yasumoto K.** 2005. Expression of endoplasmic reticulum molecular chaperone Grp78 in human lung cancer and its clinical significance. Lung Cancer **49:**55-62.

58. **Shuda M, Kondoh N, Imazeki N, Tanaka K, Okada T, Mori K, Hada A, Arai M, Wakatsuki T, Matsubara O, Yamamoto N, Yamamoto M.** 2003. Activation of the ATF6, XBP1 and grp78 genes in human hepatocellular carcinoma: a possible involvement of the ER stress pathway in hepatocarcinogenesis. J Hepatol **38:**605-614.

59. **Xing X, Lai M, Wang Y, Xu E, Huang Q.** 2006. Overexpression of glucose-regulated protein 78 in colon cancer. Clin Chim Acta **364:**308-315.

60. **Daneshmand S, Quek ML, Lin E, Lee C, Cote RJ, Hawes D, Cai J, Groshen S, Lieskovsky G, Skinner DG, Lee AS, Pinski J.** 2007. Glucose-regulated protein GRP78 is up-regulated in prostate cancer and correlates with recurrence and survival. Hum Pathol **38:**1547-1552.

61. **Pyrko P, Schönthal AH, Hofman FM, Chen TC, Lee AS.** 2007. The Unfolded Protein Response Regulator GRP78/BiP as a Novel Target for Increasing Chemosensitivity in Malignant Gliomas. Cancer research **67:**9809-9816.

62. **Arap MA, Lahdenranta J, Mintz PJ, Hajitou A, Sarkis ÁS, Arap W, Pasqualini R.** 2004. Cell surface expression of the stress response chaperone GRP78 enables tumor targeting by circulating ligands. Cancer cell **6:**275-284.

63. **Davidson DJ, Haskell C, Majest S, Kherzai A, Egan DA, Walter KA, Schneider A, Gubbins EF, Solomon L, Chen Z, Lesniewski R, Henkin J.** 2005. Kringle 5 of human plasminogen induces apoptosis of endothelial and tumor cells through surface-expressed glucose-regulated protein 78. Cancer Res **65:**4663-4672.

64. **Li J, Lee AS.** 2006. Stress induction of GRP78/BiP and its role in cancer. Curr Mol Med **6:**45-54.

65. **Lee AS.** 2014. Glucose-regulated proteins in cancer: molecular mechanisms and therapeutic potential. Nat Rev Cancer **14:**263-276.

66. **Wang M, Kaufman RJ.** 2014. The impact of the endoplasmic reticulum protein-folding environment on cancer development. Nat Rev Cancer **14:**581-597.

67. **Fu Y, Wey S, Wang M, Ye R, Liao C-P, Roy-Burman P, Lee AS.** 2008. Pten null prostate tumorigenesis and AKT activation are blocked by targeted knockout of ER chaperone GRP78/BiP in prostate epithelium. PNAS **105:**19444-19449.

68. **Lin YG, Shen J, Yoo E, Liu R, Yen HY, Mehta A, Rajaei A, Yang W, Mhawech-Fauceglia P, DeMayo FJ, Lydon J, Gill P, Lee AS.** 2015. Targeting the glucose-regulated protein-78 abrogates Pten-null driven AKT activation and endometrioid tumorigenesis. Oncogene doi:10.1038/onc.2015.4.

69. **Romero-Ramirez L, Cao H, Regalado MP, Kambham N, Siemann D, Kim JJ, Le QT, Koong AC.** 2009. X box-binding protein 1 regulates angiogenesis in human pancreatic adenocarcinomas. Transl Oncol **2:**31-38.

70. **Romero-Ramirez L, Cao H, Nelson D, Hammond E, Lee AH, Yoshida H, Mori K, Glimcher LH, Denko NC, Giaccia AJ, Le QT, Koong AC.** 2004. XBP1 is essential for survival under hypoxic conditions and is required for tumor growth. Cancer Res **64:**5943-5947.

71. **Drogat B, Auguste P, Nguyen DT, Bouchecareilh M, Pineau R, Nalbantoglu J, Kaufman RJ, Chevet E, Bikfalvi A, Moenner M.** 2007. IRE1 signaling is essential for ischemia-induced vascular endothelial growth factor-A expression and contributes to angiogenesis and tumor growth in vivo. Cancer Res **67:**6700-6707.

72. **Chen X, Iliopoulos D, Zhang Q, Tang Q, Greenblatt MB, Hatziapostolou M, Lim E, Tam WL, Ni M, Chen Y, Mai J, Shen H, Hu DZ, Adoro S, Hu B, Song M, Tan C, Landis MD, Ferrari M, Shin SJ, Brown M, Chang JC, Liu XS, Glimcher LH.** 2014. XBP1 promotes triple-negative breast cancer by controlling the HIF1α pathway. Nature **508:**103-107.

73. **Mani SA, Guo W, Liao M-J, Eaton EN, Ayyanan A, Zhou AY, Brooks M, Reinhard F, Zhang CC, Shipitsin M, Campbell LL, Polyak K, Brisken C, Yang**

J, Weinberg RA. 2008. The Epithelial-Mesenchymal Transition Generates Cells with Properties of Stem Cells. Cell **133:**704-715.

74. **Yu M, Bardia A, Wittner BS, Stott SL, Smas ME, Ting DT, Isakoff SJ, Ciciliano JC, Wells MN, Shah AM, Concannon KF, Donaldson MC, Sequist LV, Brachtel E, Sgroi D, Baselga J, Ramaswamy S, Toner M, Haber DA, Maheswaran S.** 2013. Circulating breast tumor cells exhibit dynamic changes in epithelial and mesenchymal composition. Science **339:**580-584.

75. **Idowu MO, Kmieciak M, Dumur C, Burton RS, Grimes MM, Powers CN, Manjili MH.** 2012. CD44(+)/CD24(-/low) cancer stem/progenitor cells are more abundant in triple-negative invasive breast carcinoma phenotype and are associated with poor outcome. Hum Pathol **43:**364-373.

76. **Bi M, Naczki C, Koritzinsky M, Fels D, Blais J, Hu N, Harding H, Novoa I, Varia M, Raleigh J, Scheuner D, Kaufman RJ, Bell J, Ron D, Wouters BG, Koumenis C.** 2005. ER stress-regulated translation increases tolerance to extreme hypoxia and promotes tumor growth. EMBO J **24:**3470-3481.

77. **Lin JH, Li H, Yasumura D, Cohen HR, Zhang C, Panning B, Shokat KM, Lavail MM, Walter P.** 2007. IRE1 signaling affects cell fate during the unfolded protein response. Science **318:**944-949.

78. **Tam AB, Koong AC, Niwa M.** 2014. Ire1 has distinct catalytic mechanisms for XBP1/HAC1 splicing and RIDD. Cell Rep **9:**850-858.

79. **Han D, Lerner AG, Vande Walle L, Upton JP, Xu W, Hagen A, Backes BJ, Oakes SA, Papa FR.** 2009. IRE1alpha kinase activation modes control alternate endoribonuclease outputs to determine divergent cell fates. Cell **138:**562-575.

80. **Chen Y, Brandizzi F.** 2013. IRE1: ER stress sensor and cell fate executor. Trends Cell Biol **23:**547-555.

81. **Chitnis NS, Pytel D, Bobrovnikova-Marjon E, Pant D, Zheng H, Maas NL, Frederick B, Kushner JA, Chodosh LA, Koumenis C, Fuchs SY, Diehl JA.** 2012. miR-211 is a prosurvival microRNA that regulates chop expression in a PERK-dependent manner. Mol Cell **48:**353-364.

82. **Senovilla L, Vitale I, Martins I, Tailler M, Pailleret C, Michaud M, Galluzzi L, Adjemian S, Kepp O, Niso-Santano M, Shen S, Mariño G, Criollo A, Boilève A, Job B, Ladoire S, Ghiringhelli F, Sistigu A, Yamazaki T, Rello-Varona S, Locher C, Poirier-Colame V, Talbot M, Valent A, Berardinelli F, Antoccia A, Ciccosanti F, Fimia GM, Piacentini M, Fueyo A, Messina NL, Li M, Chan CJ, Sigl V, Pourcher G, Ruckenstuhl C, Carmona-Gutierrez D, Lazar V, Penninger JM, Madeo F, López-Otín C, Smyth MJ, Zitvogel L, Castedo M, Kroemer G.** 2012. An immunosurveillance mechanism controls cancer cell ploidy. Science (New York, NY) **337:**1678-1684.

83. **Boilève A, Senovilla L, Vitale I, Lissa D, Martins I, Métivier D, van den Brink S, Clevers H, Galluzzi L, Castedo M, Kroemer G.** 2013. Immunosurveillance

against tetraploidization-induced colon tumorigenesis. Cell cycle (Georgetown, Tex) **12:**473-479.

84. **Fucikova J, Becht E, Iribarren K, Goc J, Remark R, Damotte D, Alifano M, Devi P, Biton J, Germain C, Lupo A, Fridman WH, Dieu-Nosjean M-C, Kroemer G, Sautès-Fridman C, Cremer I.** 2016. Calreticulin Expression in Human Non-Small Cell Lung Cancers Correlates with Increased Accumulation of Antitumor Immune Cells and Favorable Prognosis. Cancer research **76:**1746-1756.

85. **Beroukhim R, Mermel CH, Porter D, Wei G, Raychaudhuri S, Donovan J, Barretina J, Boehm JS, Dobson J, Urashima M, Mc Henry KT, Pinchback RM, Ligon AH, Cho YJ, Haery L, Greulich H, Reich M, Winckler W, Lawrence MS, Weir BA, Tanaka KE, Chiang DY, Bass AJ, Loo A, Hoffman C, Prensner J, Liefeld T, Gao Q, Yecies D, Signoretti S, Maher E, Kaye FJ, Sasaki H, Tepper JE, Fletcher JA, Tabernero J, Baselga J, Tsao MS, Demichelis F, Rubin MA, Janne PA, Daly MJ, Nucera C, Levine RL, Ebert BL, Gabriel S, Rustgi AK, Antonescu CR, Ladanyi M, Letai A, Garraway L., Loda M., Beer DG, True LD, Okamoto A, Pomeroy SL, Singer S, Golub TR, Lander ES, Getz G, Sellers WR, Meyerson M.** 2010. The landscape of somatic copy-number alteration across human cancers. Nature **463:**899-905.

86. **Varetti G, Pellman D, Gordon DJ.** 2014. Aurea mediocritas: the importance of a balanced genome. Cold Spring Harb Perspect Biol **6:**a015842.

87. **Davoli T, Uno H, Wooten EC, Elledge SJ.** 2017. Tumor aneuploidy correlates with markers of immune evasion and with reduced response to immunotherapy. Science **355**.

88. **Balkwill F, Charles KA, Mantovani A.** 2005. Smoldering and polarized inflammation in the initiation and promotion of malignant disease. Cancer Cell **7:**211-217.

89. **Hanahan D, Weinberg RA.** 2011. Hallmarks of cancer: the next generation. Cell **144:**646-674.

90. **Wheeler MC, Rizzi M, Sasik R, Almanza G, Hardiman G, Zanetti M.** 2008. KDEL-Retained Antigen in B Lymphocytes Induces a Proinflammatory Response: A Possible Role for Endoplasmic Reticulum Stress in Adaptive T Cell Immunity. J Immunol **181:**256-264.

91. **Mahadevan NR, Fernandez A, Rodvold J, Almanza G, Zanetti M.** 2010. Prostate cancer cells undergoing ER stress in vitro and in vivo activate transcription of pro-inflammatory cytokines. Journal of inflammation research **3:**99-103.

92. **Goodall JC, Wu C, Zhang Y, McNeill L, Ellis L, Saudek V, Gaston JS.** 2010. Endoplasmic reticulum stress-induced transcription factor, CHOP, is crucial for dendritic cell IL-23 expression. Proc Natl Acad Sci U S A **107:**17698-17703.

93. **Chen L, Jarujaron S, Wu X, Sun L, Zha W, Liang G, Wang X, Gurley EC, Studer EJ, Hylemon PB, Pandak WM, Jr., Zhang L, Wang G, Li X, Dent P, Zhou H.** 2009. HIV protease inhibitor lopinavir-induced TNF-alpha and IL-6 expression is coupled to the unfolded protein response and ERK signaling pathways in macrophages. Biochem Pharmacol **78:**70-77.

94. **Tam AB, Mercado EL, Hoffmann A, Niwa M.** 2012. ER stress activates NF-κB by integrating functions of basal IKK activity, IRE1 and PERK. PloS one **7:**e45078.

95. **Deng J, Lu PD, Zhang Y, Scheuner D, Kaufman RJ, Sonenberg N, Harding HP, Ron D.** 2004. Translational repression mediates activation of nuclear factor kappa B by phosphorylated translation initiation factor 2. Mol Cell Biol **24:**10161-10168.

96. **Jiang HY, Wek SA, McGrath BC, Scheuner D, Kaufman RJ, Cavener DR, Wek RC.** 2003. Phosphorylation of the alpha subunit of eukaryotic initiation factor 2 is required for activation of NF-kappaB in response to diverse cellular stresses. Mol Cell Biol **23:**5651-5663.

97. **Hu P, Han Z, Couvillon AD, Kaufman RJ, Exton JH.** 2006. Autocrine tumor necrosis factor alpha links endoplasmic reticulum stress to the membrane death receptor pathway through IRE1alpha-mediated NF-kappaB activation and down-regulation of TRAF2 expression. Mol Cell Biol **26:**3071-3084.

98. **Yamazaki H, Hiramatsu N, Hayakawa K, Tagawa Y, Okamura M, Ogata R, Huang T, Nakajima S, Yao J, Paton AW, Paton JC, Kitamura M.** 2009. Activation of the Akt-NF-kappaB pathway by subtilase cytotoxin through the ATF6 branch of the unfolded protein response. J Immunol **183:**1480-1487.

99. **Martinon F, Chen X, Lee A-H, Glimcher LH.** 2010. TLR activation of the transcription factor XBP1 regulates innate immune responses in macrophages. Nature immunology **11:**411-418.

100. **DeLay ML, Turner MJ, Klenk EI, Smith JA, Sowders DP, Colbert RA.** 2009. HLA-B27 misfolding and the unfolded protein response augment interleukin-23 production and are associated with Th17 activation in transgenic rats. Arthritis Rheum **60:**2633-2643.

101. **Eletto D, Dersh D, Argon Y.** 2010. GRP94 in ER quality control and stress responses. Semin Cell Dev Biol **21:**479-485.

102. **Yang Y, Liu B, Dai J, Srivastava PK, Zammit DJ, Lefrançois L, Li Z.** 2007. Heat shock protein gp96 is a master chaperone for toll-like receptors and is important in the innate function of macrophages. Immunity **26:**215-226.

103. **Yang Y, Li Z.** 2005. Roles of heat shock protein gp96 in the ER quality control: redundant or unique function? Mol Cells **20:**173-182.

104. **Liu B, Yang Y, Qiu Z, Staron M, Hong F, Li Y, Wu S, Li Y, Hao B, Bona R, Han D, Li Z.** 2010. Folding of Toll-like receptors by the HSP90 paralogue gp96 requires a substrate-specific cochaperone. Nat Commun **1:**79.

105. **Morales C, Rachidi S, Hong F, Sun S, Ouyang X, Wallace C, Zhang Y, Garret-Mayer E, Wu J, Liu B, Li Z.** 2014. Immune chaperone gp96 drives the contributions of macrophages to inflammatory colon tumorigenesis. Cancer Res **74:**446-459.

106. **Zhang Y, Wu BX, Metelli A, Thaxton JE, Hong F, Rachidi S, Ansa-Addo E, Sun S, Vasu C, Yang Y, Liu B, Li Z.** 2015. GP96 is a GARP chaperone and controls regulatory T cell functions. J Clin Invest **125:**859-869.

107. **Jensen PE.** 2007. Recent advances in antigen processing and presentation. Nature immunology **8:**1041-1048.

108. **de Almeida SF, Fleming JV, Azevedo JE, Carmo-Fonseca M, de Sousa M.** 2007. Stimulation of an unfolded protein response impairs MHC class I expression. J Immunol **178:**3612-3619.

109. **Granados DP, Tanguay P-L, Hardy M-P, Caron E, de Verteuil D, Meloche S, Perreault C.** 2009. ER stress affects processing of MHC class I-associated peptides. BMC immunology **10:**10.

110. **Pellicciotta I, Cortez-Gonzalez X, Sasik R, Reiter Y, Hardiman G, Langlade-Demoyen P, Zanetti M.** 2008. Presentation of telomerase reverse transcriptase, a self-tumor antigen, is down-regulated by histone deacetylase inhibition. Cancer Res **68:**8085-8093.

111. **Bartoszewski R, Brewer JW, Rab A, Crossman DK, Bartoszewska S, Kapoor N, Fuller C, Collawn JF, Bebok Z.** 2011. The unfolded protein response (UPR)-activated transcription factor X-box-binding protein 1 (XBP1) induces microRNA-346 expression that targets the human antigen peptide transporter 1 (TAP1) mRNA and governs immune regulatory genes. J Biol Chem **286:**41862-41870.

112. **Osorio F, Tavernier SJ, Hoffmann E, Saeys Y, Martens L, Vetters J, Delrue I, De Rycke R, Parthoens E, Pouliot P, Iwawaki T, Janssens S, Lambrecht BN.** 2014. The unfolded-protein-response sensor IRE-1α regulates the function of CD8α(+) dendritic cells. Nature immunology doi:10.1038/ni.2808.

113. **Leek RD, Lewis CE, Whitehouse R, Greenall M, Clarke J, Harris AL.** 1996. Association of macrophage infiltration with angiogenesis and prognosis in invasive breast carcinoma. Cancer Res **56:**4625-4629.

114. **Oskolkova OV, Afonyushkin T, Leitner A, von Schlieffen E, Gargalovic PS, Lusis AJ, Binder BR, Bochkov VN.** 2008. ATF4-dependent transcription is a key mechanism in VEGF up-regulation by oxidized phospholipids: critical role of oxidized sn-2 residues in activation of unfolded protein response. Blood **112:**330-339.

115. **Blais JD, Filipenko V, Bi M, Harding HP, Ron D, Koumenis C, Wouters BG, Bell JC.** 2004. Activating transcription factor 4 is translationally regulated by hypoxic stress. Molecular and cellular biology **24:**7469-7482.

116. **Urra H, Hetz C.** 2014. A novel ER stress-independent function of the UPR in angiogenesis. Molecular cell **54:**542-544.

117. **Karali E, Bellou S, Stellas D, Klinakis A, Murphy C, Fotsis T.** 2014. VEGF Signals through ATF6 and PERK to promote endothelial cell survival and angiogenesis in the absence of ER stress. Molecular cell **54:**559-572.

118. **Auf G, Jabouille A, Guérit S, Pineau R, Delugin M, Bouchecareilh M, Magnin N, Favereaux A, Maitre M, Gaiser T, von Deimling A, Czabanka M, Vajkoczy P, Chevet E, Bikfalvi A, Moenner M.** 2010. Inositol-requiring enzyme 1α is a key regulator of angiogenesis and invasion in malignant glioma. Proceedings of the National Academy of Sciences of the United States of America **107:**15553-15558.

119. **Cullen SJ, Fatemie S, Ladiges W.** 2013. Breast tumor cells primed by endoplasmic reticulum stress remodel macrophage phenotype. Am J Cancer Res **3:**196-210.

120. **Mei Y, Thompson MD, Shiraishi Y, Cohen RA, Tong X.** 2014. Sarcoplasmic/endoplasmic reticulum Ca2+ ATPase C674 promotes ischemia- and hypoxia-induced angiogenesis via coordinated endothelial cell and macrophage function. Journal of molecular and cellular cardiology **76:**275-282.

121. **Apte RN, Dotan S, Elkabets M, White MR, Reich E, Carmi Y, Song X, Dvozkin T, Krelin Y, Voronov E.** 2006. The involvement of IL-1 in tumorigenesis, tumor invasiveness, metastasis and tumor-host interactions. Cancer metastasis reviews **25:**387-408.

122. **Shenderov K, Riteau N, Yip R, Mayer-Barber KD, Oland S, Hieny S, Fitzgerald P, Oberst A, Dillon CP, Green DR, Cerundolo V, Sher A.** 2014. Cutting edge: Endoplasmic reticulum stress licenses macrophages to produce mature IL-1β in response to TLR4 stimulation through a caspase-8- and TRIF-dependent pathway. Journal of immunology (Baltimore, Md : 1950) **192:**2029-2033.

123. **Kim S, Joe Y, Kim HJ, Kim Y-S, Jeong SO, Pae H-O, Ryter SW, Surh Y-J, Chung HT.** 2015. Endoplasmic Reticulum Stress-Induced IRE1α Activation Mediates Cross-Talk of GSK-3β and XBP-1 To Regulate Inflammatory Cytokine Production. Journal of immunology (Baltimore, Md : 1950) **194:**4498-4506.

124. **Dong D, Dubeau L, Bading J, Nguyen K, Luna M, Yu H, Gazit-Bornstein G, Gordon EM, Gomer C, Hall FL, Gambhir SS, Lee AS.** 2004. Spontaneous and controllable activation of suicide gene expression driven by the stress-inducible grp78 promoter resulting in eradication of sizable human tumors. Human gene therapy **15:**553-561.

125. **Chittezhath M, Dhillon MK, Lim JY, Laoui D, Shalova IN, Teo YL, Chen J, Kamaraj R, Raman L, Lum J, Thamboo TP, Chiong E, Zolezzi F, Yang H, Van**

Ginderachter JA, Poidinger M, Wong ASC, Biswas SK. 2014. Molecular profiling reveals a tumor-promoting phenotype of monocytes and macrophages in human cancer progression. Immunity **41:**815-829.

126. **Condamine T, Kumar V, Ramachandran IR, Youn J-I, Celis E, Finnberg N, El-Deiry WS, Winograd R, Vonderheide RH, English NR, Knight SC, Yagita H, McCaffrey JC, Antonia S, Hockstein N, Witt R, Masters G, Bauer T, Gabrilovich DI.** 2014. ER stress regulates myeloid-derived suppressor cell fate through TRAIL-R-mediated apoptosis. The Journal of clinical investigation **124:**2626-2639.

127. **Thevenot PT, Sierra RA, Raber PL, Al-Khami AA, Trillo-Tinoco J, Zarreii P, Ochoa AC, Cui Y, Del Valle L, Rodriguez PC.** 2014. The stress-response sensor chop regulates the function and accumulation of myeloid-derived suppressor cells in tumors. Immunity **41:**389-401.

128. **Condamine T, Gabrilovich DI.** 2014. Can the suppressive activity of myeloid-derived suppressor cells be "chop"ped? Immunity **41:**341-342.

129. **Cubillos-Ruiz JR, Silberman PC, Rutkowski MR, Chopra S, Perales-Puchalt A, Song M, Zhang S, Bettigole SE, Gupta D, Holcomb K, Ellenson LH, Caputo T, Lee A-H, Conejo-Garcia JR, Glimcher LH.** 2013. ER Stress Sensor XBP1 Controls Anti-tumor Immunity by Disrupting Dendritic Cell Homeostasis. Cell **0**.

130. **Ramakrishnan R, Tyurin VA, Tuyrin VA, Veglia F, Condamine T, Amoscato A, Mohammadyani D, Johnson JJ, Zhang LM, Klein-Seetharaman J, Celis E, Kagan VE, Gabrilovich DI.** 2014. Oxidized lipids block antigen cross-presentation by dendritic cells in cancer. Journal of immunology (Baltimore, Md : 1950) **192:**2920-2931.

131. **Varn FS, Mullins DW, Arias-Pulido H, Fiering S, Cheng C.** 2017. Adaptive immunity programmes in breast cancer. Immunology **150:**25-34.

132. **Scheu S, Stetson DB, Reinhardt RL, Leber JH, Mohrs M, Locksley RM.** 2006. Activation of the integrated stress response during T helper cell differentiation. Nat Immunol **7:**644-651.

133. **Kamimura D, Bevan MJ.** 2008. Endoplasmic reticulum stress regulator XBP-1 contributes to effector CD8+ T cell differentiation during acute infection. J Immunol **181:**5433-5441.

134. **García-Navas R, Munder M, Mollinedo F.** 2012. Depletion of L-arginine induces autophagy as a cytoprotective response to endoplasmic reticulum stress in human T lymphocytes. Autophagy **8:**1557-1576.

135. **Franco A, Almanza G, Burns JC, Wheeler M, Zanetti M.** 2010. Endoplasmic reticulum stress drives a regulatory phenotype in human T-cell clones. Cell Immunol **266:**1-6.

136. **Mahadevan NR, Rodvold J, Sepulveda H, Rossi S, Drew AF, Zanetti M.** 2011. Transmission of endoplasmic reticulum stress and pro-inflammation from tumor cells to myeloid cells. Proc Natl Acad Sci U S A **108:**6561-6566.

137. **Mahadevan NR, Anufreichik V, Rodvold J, Chiu KT, Sepulveda H, Zanetti M.** 2012. Cell-Extrinsic Effects of Tumor ER Stress Imprint Myeloid Dendritic Cells and Impair CD8(+) T Cell Priming. PloS one **7:**e51845.

138. **Rodvold J, Chiu KT, Hiramatsu N, Nussbacher JK, Galimberti V, Mahadevan NR, Willert K, Lin JH, Zanetti M.** 2017. Intercellular transmission of the unfolded protein response promotes survival and drug resistance in cancer cells. Science Signaling **10**.

139. **Heazlewood CK, Cook MC, Eri R, Price GR, Tauro SB, Taupin D, Thornton DJ, Png CW, Crockford TL, Cornall RJ, Adams R, Kato M, Nelms KA, Hong NA, Florin TH, Goodnow CC, McGuckin MA.** 2008. Aberrant mucin assembly in mice causes endoplasmic reticulum stress and spontaneous inflammation resembling ulcerative colitis. PLoS Med **5:**e54.

140. **He B.** 2006. Viruses, endoplasmic reticulum stress, and interferon responses. Cell Death Differ **13:**393-403.

141. **Yamamoto K, Sato T, Matsui T, Sato M, Okada T, Yoshida H, Harada A, Mori K.** 2007. Transcriptional induction of mammalian ER quality control proteins is mediated by single or combined action of ATF6alpha and XBP1. Dev Cell **13:**365-376.

142. **Zinszner H, Kuroda M, Wang X, Batchvarova N, Lightfoot RT, Remotti H, Stevens JL, Ron D.** 1998. CHOP is implicated in programmed cell death in response to impaired function of the endoplasmic reticulum. Genes Dev **12:**982-995.

143. **Mahadevan NR, Zanetti M.** 2011. Tumor stress inside out: Cell-extrinsic effects of the unfolded protein response in tumor cells modulate the immunological landscape of the tumor microenvironment. J Immunol **187:**4403-4409.

144. **Mahadevan NR, Anufreichik V, Rodvold JJ, Chiu KT, Sepulveda H, Zanetti M.** 2012. Cell-Extrinsic Effects of Tumor ER Stress Imprint Myeloid Dendritic Cells and Impair CD8(+) T Cell Priming. PLoS One **7:**e51845.

145. **Rodvold JJ, Mahadevan NR, Zanetti M.** 2015. Immune modulation by ER stress and inflammation in the tumor microenvironment. Cancer Lett doi:10.1016/j.canlet.2015.09.009.

146. **Fu Y, Wey S, Wang M, Ye R, Liao CP, Roy-Burman P, Lee AS.** 2008. Pten null prostate tumorigenesis and AKT activation are blocked by targeted knockout of ER chaperone GRP78/BiP in prostate epithelium. Proc Natl Acad Sci U S A **105:**19444-19449.

147. **Ranganathan AC, Zhang L, Adam AP, Aguirre-Ghiso JA.** 2006. Functional coupling of p38-induced up-regulation of BiP and activation of RNA-dependent protein kinase-like endoplasmic reticulum kinase to drug resistance of dormant carcinoma cells. Cancer Res **66:**1702-1711.

148. **Misra UK, Deedwania R, Pizzo SV.** 2006. Activation and cross-talk between Akt, NF-kappaB, and unfolded protein response signaling in 1-LN prostate cancer cells consequent to ligation of cell surface-associated GRP78. J Biol Chem **281:**13694-13707.

149. **Zhang Y, Tseng CC, Tsai YL, Fu X, Schiff R, Lee AS.** 2013. Cancer cells resistant to therapy promote cell surface relocalization of GRP78 which complexes with PI3K and enhances PI(3,4,5)P3 production. PLoS One **8:**e80071.

150. **Taylor RC, Dillin A.** 2013. XBP-1 Is a Cell-Nonautonomous Regulator of Stress Resistance and Longevity. Cell **153:**1435-1447.

151. **Zanetti M, Rodvold JJ, Mahadevan NR.** 2015. The evolving paradigm of cell-nonautonomous UPR-based regulation of immunity by cancer cells. Oncogene doi:10.1038/onc.2015.108.

152. **Spiotto MT, Banh A, Papandreou I, Cao H, Galvez MG, Gurtner GC, Denko NC, Le QT, Koong AC.** 2010. Imaging the unfolded protein response in primary tumors reveals microenvironments with metabolic variations that predict tumor growth. Cancer Res **70:**78-88.

153. **Arap MA, Lahdenranta J, Mintz PJ, Hajitou A, Sarkis AS, Arap W, Pasqualini R.** 2004. Cell surface expression of the stress response chaperone GRP78 enables tumor targeting by circulating ligands. Cancer Cell **6:**275-284.

154. **Ray R, de Ridder GG, Eu JP, Paton AW, Paton JC, Pizzo SV.** 2012. The Escherichia coli subtilase cytotoxin A subunit specifically cleaves cell-surface GRP78 protein and abolishes COOH-terminal-dependent signaling. J Biol Chem **287:**32755-32769.

155. **Ni M, Zhang Y, Lee AS.** 2011. Beyond the endoplasmic reticulum: atypical GRP78 in cell viability, signalling and therapeutic targeting. Biochem J **434:**181-188.

156. **Quinones QJ, de Ridder GG, Pizzo SV.** 2008. GRP78: a chaperone with diverse roles beyond the endoplasmic reticulum. Histol Histopathol **23:**1409-1416.

157. **Shin BK, Wang H, Yim AM, Le Naour F, Brichory F, Jang JH, Zhao R, Puravs E, Tra J, Michael CW, Misek DE, Hanash SM.** 2003. Global profiling of the cell surface proteome of cancer cells uncovers an abundance of proteins with chaperone function. J Biol Chem **278:**7607-7616.

158. **Rutkowski DT, Arnold SM, Miller CN, Wu J, Li J, Gunnison KM, Mori K, Sadighi Akha AA, Raden D, Kaufman RJ.** 2006. Adaptation to ER stress is mediated by differential stabilities of pro-survival and pro-apoptotic mRNAs and proteins. PLoS Biol **4:**e374.

159. **Richardson PG, Sonneveld P, Schuster MW, Irwin D, Stadtmauer EA, Facon T, Harousseau JL, Ben-Yehuda D, Lonial S, Goldschmidt H, Reece D, San-Miguel JF, Blade J, Boccadoro M, Cavenagh J, Dalton WS, Boral AL, Esseltine DL, Porter JB, Schenkein D, Anderson KC, Assessment of Proteasome Inhibition for Extending Remissions I.** 2005. Bortezomib or high-dose dexamethasone for relapsed multiple myeloma. N Engl J Med **352:**2487-2498.

160. **Papandreou CN, Daliani DD, Nix D, Yang H, Madden T, Wang X, Pien CS, Millikan RE, Tu SM, Pagliaro L, Kim J, Adams J, Elliott P, Esseltine D, Petrusich A, Dieringer P, Perez C, Logothetis CJ.** 2004. Phase I trial of the proteasome inhibitor bortezomib in patients with advanced solid tumors with observations in androgen-independent prostate cancer. J Clin Oncol **22:**2108-2121.

161. **Papandreou CN, Logothetis CJ.** 2004. Bortezomib as a potential treatment for prostate cancer. Cancer Res **64:**5036-5043.

162. **Lee AH, Iwakoshi NN, Anderson KC, Glimcher LH.** 2003. Proteasome inhibitors disrupt the unfolded protein response in myeloma cells. Proc Natl Acad Sci U S A **100:**9946-9951.

163. **Armstrong JL, Flockhart R, Veal GJ, Lovat PE, Redfern CP.** 2010. Regulation of endoplasmic reticulum stress-induced cell death by ATF4 in neuroectodermal tumor cells. J Biol Chem **285:**6091-6100.

164. **Jeon YJ, Khelifa S, Ratnikov B, Scott DA, Feng Y, Parisi F, Ruller C, Lau E, Kim H, Brill LM, Jiang T, Rimm DL, Cardiff RD, Mills GB, Smith JW, Osterman AL, Kluger Y, Ronai ZA.** 2015. Regulation of glutamine carrier proteins by RNF5 determines breast cancer response to ER stress-inducing chemotherapies. Cancer Cell **27:**354-369.

165. **Jordan MA, Toso RJ, Thrower D, Wilson L.** 1993. Mechanism of mitotic block and inhibition of cell proliferation by taxol at low concentrations. Proc Natl Acad Sci U S A **90:**9552-9556.

166. **Woods CM, Zhu J, McQueney PA, Bollag D, Lazarides E.** 1995. Taxol-induced mitotic block triggers rapid onset of a p53-independent apoptotic pathway. Mol Med **1:**506-526.

167. **DiPaola RS.** 2002. To arrest or not to G(2)-M Cell-cycle arrest : commentary re: A. K. Tyagi et al., Silibinin strongly synergizes human prostate carcinoma DU145 cells to doxorubicin-induced growth inhibition, G(2)-M arrest, and apoptosis. Clin. cancer res., 8: 3512-3519, 2002. Clin Cancer Res **8:**3311-3314.

168. **Davidson G, Niehrs C.** 2010. Emerging links between CDK cell cycle regulators and Wnt signaling. Trends Cell Biol **20:**453-460.

169. **Willert K, Nusse R.** 1998. Beta-catenin: a key mediator of Wnt signaling. Curr Opin Genet Dev **8:**95-102.

170. **Clevers H, Nusse R.** 2012. Wnt/beta-catenin signaling and disease. Cell **149:**1192-1205.

171. **Ikeda S, Kishida S, Yamamoto H, Murai H, Koyama S, Kikuchi A.** 1998. Axin, a negative regulator of the Wnt signaling pathway, forms a complex with GSK-3beta and beta-catenin and promotes GSK-3beta-dependent phosphorylation of beta-catenin. EMBO J **17:**1371-1384.

172. **Veeman MT, Slusarski DC, Kaykas A, Louie SH, Moon RT.** 2003. Zebrafish prickle, a modulator of noncanonical Wnt/Fz signaling, regulates gastrulation movements. Curr Biol **13:**680-685.

173. **Fuerer C, Nusse R.** 2010. Lentiviral vectors to probe and manipulate the Wnt signaling pathway. PLoS One **5:**e9370.

174. **Fernandez A, Huggins IJ, Perna L, Brafman D, Lu D, Yao S, Gaasterland T, Carson DA, Willert K.** 2014. The WNT receptor FZD7 is required for maintenance of the pluripotent state in human embryonic stem cells. Proc Natl Acad Sci U S A **111:**1409-1414.

175. **Atilla-Gokcumen GE, Williams DS, Bregman H, Pagano N, Meggers E.** 2006. Organometallic compounds with biological activity: a very selective and highly potent cellular inhibitor for glycogen synthase kinase 3. Chembiochem **7:**1443-1450.

176. **Logan CY, Nusse R.** 2004. The Wnt signaling pathway in development and disease. Annu Rev Cell Dev Biol **20:**781-810.

177. **Cross BC, Bond PJ, Sadowski PG, Jha BK, Zak J, Goodman JM, Silverman RH, Neubert TA, Baxendale IR, Ron D, Harding HP.** 2012. The molecular basis for selective inhibition of unconventional mRNA splicing by an IRE1-binding small molecule. Proc Natl Acad Sci U S A **109:**E869-878.

178. **Axten JM, Romeril SP, Shu A, Ralph J, Medina JR, Feng Y, Li WH, Grant SW, Heerding DA, Minthorn E, Mencken T, Gaul N, Goetz A, Stanley T, Hassell AM, Gampe RT, Atkins C, Kumar R.** 2013. Discovery of GSK2656157: An Optimized PERK Inhibitor Selected for Preclinical Development. ACS Med Chem Lett **4:**964-968.

179. **Hoffmeyer K, Raggioli A, Rudloff S, Anton R, Hierholzer A, Del Valle I, Hein K, Vogt R, Kemler R.** 2012. Wnt/beta-catenin signaling regulates telomerase in stem cells and cancer cells. Science **336:**1549-1554.

180. **Hosoi T, Inoue Y, Nakatsu K, Matsushima N, Kiyose N, Shimamoto A, Tahara H, Ozawa K.** 2014. TERT attenuated ER stress-induced cell death. Biochem Biophys Res Commun **447:**378-382.

181. **Zhou J, Mao B, Zhou Q, Ding D, Wang M, Guo P, Gao Y, Shay JW, Yuan Z, Cong YS.** 2014. Endoplasmic reticulum stress activates telomerase. Aging Cell **13:**197-200.

182. **Bell RJ, Rube HT, Kreig A, Mancini A, Fouse SD, Nagarajan RP, Choi S, Hong C, He D, Pekmezci M, Wiencke JK, Wrensch MR, Chang SM, Walsh KM, Myong S, Song JS, Costello JF.** 2015. Cancer. The transcription factor GABP selectively binds and activates the mutant TERT promoter in cancer. Science **348:**1036-1039.

183. **Haendeler J, Hoffmann J, Brandes RP, Zeiher AM, Dimmeler S.** 2003. Hydrogen peroxide triggers nuclear export of telomerase reverse transcriptase via Src kinase family-dependent phosphorylation of tyrosine 707. Mol Cell Biol **23:**4598-4610.

184. **B'Chir W, Maurin AC, Carraro V, Averous J, Jousse C, Muranishi Y, Parry L, Stepien G, Fafournoux P, Bruhat A.** 2013. The eIF2alpha/ATF4 pathway is essential for stress-induced autophagy gene expression. Nucleic Acids Res **41:**7683-7699.

185. **Ye J, Kumanova M, Hart LS, Sloane K, Zhang H, De Panis DN, Bobrovnikova-Marjon E, Diehl JA, Ron D, Koumenis C.** 2010. The GCN2-ATF4 pathway is critical for tumour cell survival and proliferation in response to nutrient deprivation. EMBO J **29:**2082-2096.

186. **Notte A, Rebucci M, Fransolet M, Roegiers E, Genin M, Tellier C, Watillon K, Fattaccioli A, Arnould T, Michiels C.** 2015. Taxol-induced unfolded protein response activation in breast cancer cells exposed to hypoxia: ATF4 activation regulates autophagy and inhibits apoptosis. Int J Biochem Cell Biol **62:**1-14.

187. **Condamine T, Kumar V, Ramachandran IR, Youn JI, Celis E, Finnberg N, El-Deiry WS, Winograd R, Vonderheide RH, English NR, Knight SC, Yagita H, McCaffrey JC, Antonia S, Hockstein N, Witt R, Masters G, Bauer T, Gabrilovich DI.** 2014. ER stress regulates myeloid-derived suppressor cell fate through TRAIL-R-mediated apoptosis. J Clin Invest **124:**2626-2639.

188. **Nusse R, Fuerer C, Ching W, Harnish K, Logan C, Zeng A, ten Berge D, Kalani Y.** 2008. Wnt signaling and stem cell control. Cold Spring Harb Symp Quant Biol **73:**59-66.

189. **He TC, Sparks AB, Rago C, Hermeking H, Zawel L, da Costa LT, Morin PJ, Vogelstein B, Kinzler KW.** 1998. Identification of c-MYC as a target of the APC pathway. Science **281:**1509-1512.

190. **Tetsu O, McCormick F.** 1999. Beta-catenin regulates expression of cyclin D1 in colon carcinoma cells. Nature **398:**422-426.

191. **Du Q, Park KS, Guo Z, He P, Nagashima M, Shao L, Sahai R, Geller DA, Hussain SP.** 2006. Regulation of human nitric oxide synthase 2 expression by Wnt beta-catenin signaling. Cancer Res **66:**7024-7031.

192. **Miyamoto DT, Zheng Y, Wittner BS, Lee RJ, Zhu H, Broderick KT, Desai R, Fox DB, Brannigan BW, Trautwein J, Arora KS, Desai N, Dahl DM, Sequist LV, Smith MR, Kapur R, Wu CL, Shioda T, Ramaswamy S, Ting DT, Toner M,**

Maheswaran S, Haber DA. 2015. RNA-Seq of single prostate CTCs implicates noncanonical Wnt signaling in antiandrogen resistance. Science **349:**1351-1356.

193. **Ben-Sahra I, Hoxhaj G, Ricoult SJ, Asara JM, Manning BD.** 2016. mTORC1 induces purine synthesis through control of the mitochondrial tetrahydrofolate cycle. Science **351:**728-733.

194. **Walter F, Schmid J, Dussmann H, Concannon CG, Prehn JH.** 2015. Imaging of single cell responses to ER stress indicates that the relative dynamics of IRE1/XBP1 and PERK/ATF4 signalling rather than a switch between signalling branches determine cell survival. Cell Death Differ **22:**1502-1516.

195. **Bertolotti A, Zhang Y, Hendershot LM, Harding HP, Ron D.** 2000. Dynamic interaction of BiP and ER stress transducers in the unfolded-protein response. Nat Cell Biol **2:**326-332.

196. **Jamora C, Dennert G, Lee AS.** 1996. Inhibition of tumor progression by suppression of stress protein GRP78/BiP induction in fibrosarcoma B/C10ME. Proc Natl Acad Sci U S A **93:**7690-7694.

197. **Dong D, Ni M, Li J, Xiong S, Ye W, Virrey JJ, Mao C, Ye R, Wang M, Pen L, Dubeau L, Groshen S, Hofman FM, Lee AS.** 2008. Critical role of the stress chaperone GRP78/BiP in tumor proliferation, survival, and tumor angiogenesis in transgene-induced mammary tumor development. Cancer Res **68:**498-505.

198. **Lee AS.** 2007. GRP78 induction in cancer: therapeutic and prognostic implications. Cancer Res **67:**3496-3499.

199. **Gonzalez-Gronow M, Selim MA, Papalas J, Pizzo SV.** 2009. GRP78: a multifunctional receptor on the cell surface. Antioxid Redox Signal **11:**2299-2306.

200. **Gonzalez-Gronow M, Cuchacovich M, Llanos C, Urzua C, Gawdi G, Pizzo SV.** 2006. Prostate cancer cell proliferation in vitro is modulated by antibodies against glucose-regulated protein 78 isolated from patient serum. Cancer Res **66:**11424-11431.

201. **Preissler S, Rato C, Chen R, Antrobus R, Ding S, Fearnley IM, Ron D.** 2015. AMPylation matches BiP activity to client protein load in the endoplasmic reticulum. Elife **4:**e12621.

202. **Li Y, Tergaonkar V.** 2014. Noncanonical functions of telomerase: implications in telomerase-targeted cancer therapies. Cancer Res **74:**1639-1644.

203. **Sharma GG, Gupta A, Wang H, Scherthan H, Dhar S, Gandhi V, Iliakis G, Shay JW, Young CS, Pandita TK.** 2003. hTERT associates with human telomeres and enhances genomic stability and DNA repair. Oncogene **22:**131-146.

204. **Cubillos-Ruiz JR, Silberman PC, Rutkowski MR, Chopra S, Perales-Puchalt A, Song M, Zhang S, Bettigole SE, Gupta D, Holcomb K, Ellenson LH, Caputo T, Lee AH, Conejo-Garcia JR, Glimcher LH.** 2015. ER Stress Sensor XBP1

Controls Anti-tumor Immunity by Disrupting Dendritic Cell Homeostasis. Cell **161:**1527-1538.

205. **Ramakrishnan R, Tyurin VA, Veglia F, Condamine T, Amoscato A, Mohammadyani D, Johnson JJ, Zhang LM, Klein-Seetharaman J, Celis E, Kagan VE, Gabrilovich DI.** 2014. Oxidized lipids block antigen cross-presentation by dendritic cells in cancer. J Immunol **192:**2920-2931.

206. **Kreso A, O'Brien CA, van Galen P, Gan OI, Notta F, Brown AM, Ng K, Ma J, Wienholds E, Dunant C, Pollett A, Gallinger S, McPherson J, Mullighan CG, Shibata D, Dick JE.** 2013. Variable clonal repopulation dynamics influence chemotherapy response in colorectal cancer. Science **339:**543-548.

207. **Marusyk A, Tabassum DP, Altrock PM, Almendro V, Michor F, Polyak K.** 2014. Non-cell-autonomous driving of tumour growth supports sub-clonal heterogeneity. Nature doi:10.1038/nature13556.

208. **Harding HP, Zhang Y, Bertolotti A, Zeng H, Ron D.** 2000. Perk is essential for translational regulation and cell survival during the unfolded protein response. Mol Cell **5:**897-904.

209. **Wu J, Rutkowski DT, Dubois M, Swathirajan J, Saunders T, Wang J, Song B, Yau GD, Kaufman RJ.** 2007. ATF6alpha optimizes long-term endoplasmic reticulum function to protect cells from chronic stress. Dev Cell **13:**351-364.

210. **Hayashi MT, Cesare AJ, Fitzpatrick JA, Lazzerini-Denchi E, Karlseder J.** 2012. A telomere-dependent DNA damage checkpoint induced by prolonged mitotic arrest. Nat Struct Mol Biol **19:**387-394.

211. **Montague TG, Cruz JM, Gagnon JA, Church GM, Valen E.** 2014. CHOPCHOP: a CRISPR/Cas9 and TALEN web tool for genome editing. Nucleic Acids Res **42:**W401-407.

212. **Ran FA, Hsu PD, Wright J, Agarwala V, Scott DA, Zhang F.** 2013. Genome engineering using the CRISPR-Cas9 system. Nat Protoc **8:**2281-2308.

213. **Hanahan D, Coussens LM.** 2012. Accessories to the Crime: Functions of Cells Recruited to the Tumor Microenvironment. Cancer cell **21:**309-322.

214. **Cho JA, Lee A-H, Platzer B, Cross BCS, Gardner BM, De Luca H, Luong P, Harding HP, Glimcher LH, Walter P, Fiebiger E, Ron D, Kagan JC, Lencer WI.** 2013. The unfolded protein response element IRE1α senses bacterial proteins invading the ER to activate RIG-I and innate immune signaling. Cell host & microbe **13:**558-569.

215. **Robblee MM, Kim CC, Porter Abate J, Valdearcos M, Sandlund KLM, Shenoy MK, Volmer R, Iwawaki T, Koliwad SK.** 2016. Saturated Fatty Acids Engage an IRE1α-Dependent Pathway to Activate the NLRP3 Inflammasome in Myeloid Cells. Cell reports **14:**2611-2623.

216. **Mahadevan NR, Anufreichik V, Rodvold JJ, Chiu KT, Sepulveda H, Zanetti M.** 2012. Cell-extrinsic effects of tumor ER stress imprint myeloid dendritic cells and impair $CD8^+$ T cell priming. PloS one **7:**e51845.

217. **Mahadevan NR, Rodvold J, Sepulveda H, Rossi S, Drew AF, Zanetti M.** 2011. Transmission of endoplasmic reticulum stress and pro-inflammation from tumor cells to myeloid cells. PNAS **108:**6561-6566.

218. **Iwawaki T, Akai R, Kohno K, Miura M.** 2004. A transgenic mouse model for monitoring endoplasmic reticulum stress. Nature medicine **10:**98-102.

219. **McCart AE, Vickaryous NK, Silver A.** 2008. Apc mice: models, modifiers and mutants. Pathology, research and practice **204:**479-490.

220. **Qiu Q, Zheng Z, Chang L, Zhao Y-S, Tan C, Dandekar A, Zhang Z, Lin Z, Gui M, Li X, Zhang T, Kong Q, Li H, Chen S, Chen A, Kaufman RJ, Yang W-L, Lin H-K, Zhang D, Perlman H, Thorp E, Zhang K, Fang D.** 2013. Toll-like receptor-mediated IRE1α activation as a therapeutic target for inflammatory arthritis. The EMBO journal **32:**2477-2490.

221. **Cross BCS, Bond PJ, Sadowski PG, Jha BK, Zak J, Goodman JM, Silverman RH, Neubert TA, Baxendale IR, Ron D, Harding HP.** 2012. The molecular basis for selective inhibition of unconventional mRNA splicing by an IRE1-binding small molecule. PNAS **109:**E869-878.

222. **Axten JM, Romeril SP, Shu A, Ralph J, Medina JR, Feng Y, Li WHH, Grant SW, Heerding DA, Minthorn E, Mencken T, Gaul N, Goetz A, Stanley T, Hassell AM, Gampe RT, Atkins C, Kumar R.** 2013. Discovery of GSK2656157: An Optimized PERK Inhibitor Selected for Preclinical Development. ACS medicinal chemistry letters **4:**964-968.

223. **Mahadevan NR, Rodvold J, Zanetti M.** 2013. A Janus-faced role of the unfolded protein response in antitumor immunity. Oncoimmunology **2:**e23901.

224. **Shalova IN, Lim JY, Chittezhath M, Zinkernagel AS, Beasley F, Hernández-Jiménez E, Toledano V, Cubillos-Zapata C, Rapisarda A, Chen J, Duan K, Yang H, Poidinger M, Melillo G, Nizet V, Arnalich F, López-Collazo E, Biswas SK.** 2015. Human Monocytes Undergo Functional Re-programming during Sepsis Mediated by Hypoxia-Inducible Factor-1α. Immunity **42:**484-498.

225. **Peyssonnaux C, Datta V, Cramer T, Doedens A, Theodorakis EA, Gallo RL, Hurtado-Ziola N, Nizet V, Johnson RS.** 2005. HIF-1alpha expression regulates the bactericidal capacity of phagocytes. The Journal of clinical investigation **115:**1806-1815.

226. **Kaneda MM, Messer KS, Ralainirina N, Li H, Leem C, Gorjestani S, Woo G, Nguyen AV, Figueiredo CC, Foubert P, Schmid MC, Pink M, Winkler DG, Rausch M, Palombella VJ, Kutok J, McGovern K, Frazer KA, Wu X, Karin M, Sasik R, Cohen EEW, Varner JA.** 2016. PI3Kγ is a molecular switch that controls immune suppression. Nature **539:**437-442.

227. **Swann JB, Vesely MD, Silva A, Sharkey J, Akira S, Schreiber RD, Smyth MJ.** 2008. Demonstration of inflammation-induced cancer and cancer immunoediting during primary tumorigenesis. PNAS **105:**652-656.

228. **Fukata M, Hernandez Y, Conduah D, Cohen J, Chen A, Breglio K, Goo T, Hsu D, Xu R, Abreu MT.** 2009. Innate immune signaling by Toll-like receptor-4 (TLR4) shapes the inflammatory microenvironment in colitis-associated tumors. Inflammatory Bowel Diseases **15:**997-1006.

229. **Liu J, Hamrouni A, Wolowiec D, Coiteux V, Kuliczkowski K, Hetuin D, Saudemont A, Quesnel B.** 2007. Plasma cells from multiple myeloma patients express B7-H1 (PD-L1) and increase expression after stimulation with IFN-{gamma} and TLR ligands via a MyD88-, TRAF6-, and MEK-dependent pathway. Blood **110:**296-304.

230. **Beck D, Niessner H, Smalley KSM, Flaherty K, Paraiso KHT, Busch C, Sinnberg T, Vasseur S, Iovanna JL, Drießen S, Stork B, Wesselborg S, Schaller M, Biedermann T, Bauer J, Lasithiotakis K, Weide B, Eberle J, Schittek B, Schadendorf D, Garbe C, Kulms D, Meier F.** 2013. Vemurafenib potently induces endoplasmic reticulum stress-mediated apoptosis in BRAFV600E melanoma cells. Science Signaling **6:**ra7-ra7.

231. **Croft A, Tay KH, Boyd SC, Guo ST, Jiang CC, Lai F, Tseng H-Y, Jin L, Rizos H, Hersey P, Zhang XD.** 2014. Oncogenic activation of MEK/ERK primes melanoma cells for adaptation to endoplasmic reticulum stress. The Journal of investigative dermatology **134:**488-497.

232. **Lee K, Tirasophon W, Shen X, Michalak M, Prywes R, Okada T, Yoshida H, Mori K, Kaufman RJ.** 2002. IRE1-mediated unconventional mRNA splicing and S2P-mediated ATF6 cleavage merge to regulate XBP1 in signaling the unfolded protein response. Genes & development **16:**452-466.

233. **Inaba K, Inaba M, Romani N, Aya H, Deguchi M, Ikehara S, Muramatsu S, Steinman RM.** 1992. Generation of large numbers of dendritic cells from mouse bone marrow cultures supplemented with granulocyte/macrophage colony-stimulating factor. J Exp Med **176:**1693-1702.

234. **Iwawaki T, Akai R, Kohno K, Miura M.** 2004. A transgenic mouse model for monitoring endoplasmic reticulum stress. Nat Med **10:**98-102.

235. **LOEWENSTEIN WR, KANNO Y.** 1966. Intercellular Communication and the Control of Tissue Growth: Lack of Communication between Cancer Cells. Nature **209:**1248-1249.

236. **Tabassum DP, Polyak K.** 2015. Tumorigenesis: it takes a village. Nat Rev Cancer **15:**473-483.

237. **Ratajczak J, Wysoczynski M, Hayek F, Janowska-Wieczorek A, Ratajczak MZ.** 2006. Membrane-derived microvesicles: important and underappreciated

mediators of cell-to-cell communication. Leukemia : official journal of the Leukemia Society of America, Leukemia Research Fund, UK **20:**1487-1495.

238. **Rodriguez PC, Hernandez CP, Quiceno D, Dubinett SM, Zabaleta J, Ochoa JB, Gilbert J, Ochoa AC.** 2005. Arginase I in myeloid suppressor cells is induced by COX-2 in lung carcinoma. The Journal of experimental medicine **202:**931-939.

239. **Kurtova AV, Xiao J, Mo Q, Pazhanisamy S, Krasnow R, Lerner SP, Chen F, Roh TT, Lay E, Ho PL, Chan KS.** 2015. Blocking PGE2-induced tumour repopulation abrogates bladder cancer chemoresistance. Nature **517:**209-213.

240. **Diakogiannaki E, Welters HJ, Morgan NG.** 2008. Differential regulation of the endoplasmic reticulum stress response in pancreatic β-cells exposed to long-chain saturated and monounsaturated fatty acids. Journal of Endocrinology **197:**553-563.

241. **Colegio OR, Chu N-Q, Szabo AL, Chu T, Rhebergen AM, Jairam V, Cyrus N, Brokowski CE, Eisenbarth SC, Phillips GM, Cline GW, Phillips AJ, Medzhitov R.** 2014. Functional polarization of tumour-associated macrophages by tumour-derived lactic acid. Nature **513:**559-563.

242. **Wang D, DuBois RN.** 2010. Eicosanoids and cancer. Nature Reviews Cancer **10:**181-193.

243. **Rigas B, Goldman IS, Levine L.** 1993. Altered eicosanoid levels in human colon cancer. The Journal of Laboratory and Clinical Medicine **122:**518-523.

244. **Ristimäki A, Sivula A, Lundin J, Lundin M, Salminen T, Haglund C, Joensuu H, Isola J.** 2002. Prognostic Significance of Elevated Cyclooxygenase-2 Expression in Breast Cancer. Cancer research **62:**632-635.

245. **McLemore TL, Hubbard WC, Litterst CL, Liu MC, Miller S, McMahon NA, Eggleston JC, Boyd MR.** 1988. Profiles of prostaglandin biosynthesis in normal lung and tumor tissue from lung cancer patients. Cancer research **48:**3140-3147.

246. **Kawamori T, Uchiya N, Sugimura T, Wakabayashi K.** 2003. Enhancement of colon carcinogenesis by prostaglandin E 2 administration. Carcinogenesis **24:**985-990.

247. **Nakanishi M, Montrose DC, Clark P, Nambiar PR, Belinsky GS, Claffey KP, Xu D, Rosenberg DW.** 2008. Genetic Deletion of mPGES-1 Suppresses Intestinal Tumorigenesis. Cancer research **68:**3251-3259.

248. **Rodriguez PC, Hernandez CP, Quiceno D, Dubinett SM, Zabaleta J, Ochoa JB, Gilbert J, Ochoa AC.** 2005. Arginase I in myeloid suppressor cells is induced by COX-2 in lung carcinoma. J Exp Med **202:**931-939.

249. **Baratelli F, Lin Y, Zhu L, Yang S-C, Heuzé-Vourc'h N, Zeng G, Reckamp K, Dohadwala M, Sharma S, Dubinett SM.** 2005. Prostaglandin E2 Induces FOXP3

Gene Expression and T Regulatory Cell Function in Human CD4+ T Cells. Journal of immunology (Baltimore, Md : 1950) **175:**1483-1490.

250. **Stolina M, Sharma S, Lin Y, Dohadwala M, Gardner B, Luo J, Zhu L, Kronenberg M, Miller PW, Portanova J, Lee JC, Dubinett SM.** 2000. Specific Inhibition of Cyclooxygenase 2 Restores Antitumor Reactivity by Altering the Balance of IL-10 and IL-12 Synthesis. Journal of immunology (Baltimore, Md : 1950) **164:**361-370.

251. **Wang D, Wang H, Brown J, Daikoku T, Ning W, Shi Q, Richmond A, Strieter R, Dey SK, DuBois RN.** 2006. CXCL1 induced by prostaglandin E2 promotes angiogenesis in colorectal cancer. Journal of Experimental Medicine **203:**941-951.

252. **Chang S-H, Liu CH, Conway R, Han DK, Nithipatikom K, Trifan OC, Lane TF, Hla T.** 2004. Role of prostaglandin E2-dependent angiogenic switch in cyclooxygenase 2-induced breast cancer progression. Proceedings of the National Academy of Sciences of the United States of America **101:**591-596.

253. **Jain S, Chakraborty G, Raja R, Kale S, Kundu GC.** 2008. Prostaglandin E2 Regulates Tumor Angiogenesis in Prostate Cancer. Cancer research **68:**7750-7759.

254. **Hoang B, Zhu L, Shi Y, Frost P, Yan H, Sharma S, Sharma S, Goodglick L, Dubinett S, Lichtenstein A.** 2006. Oncogenic RAS mutations in myeloma cells selectively induce cox-2 expression, which participates in enhanced adhesion to fibronectin and chemoresistance. Blood **107:**4484-4490.

255. **Harris RE.** 2009. Cyclooxygenase-2 (cox-2) blockade in the chemoprevention of cancers of the colon, breast, prostate, and lung. Inflammopharmacology **17:**55-67.

256. **Chan AT, Ogino S, Fuchs CS.** 2009. Aspirin Use and Survival After Diagnosis of Colorectal Cancer. JAMA **302:**649-658.

257. **Salvadó L, Coll T, Gómez-Foix AM, Salmerón E, Barroso E, Palomer X, Vázquez-Carrera M.** 2013. Oleate prevents saturated-fatty-acid-induced ER stress, inflammation and insulin resistance in skeletal muscle cells through an AMPK-dependent mechanism. Diabetologia **56:**1372-1382.

258. **Nielsen MS, Olsen CE, Dich J, Christensen SB, Grunnet N.** 1994. Metabolism of thapsigargin in rat hepatocytes. Drug metabolism and disposition: the biological fate of chemicals **22:**433-437.

259. **Park K, Ikushiro H, Seo HS, Shin K-O, Kim YI, Kim JY, Lee Y-M, Yano T, Holleran WM, Elias P, Uchida Y.** 2016. ER stress stimulates production of the key antimicrobial peptide, cathelicidin, by forming a previously unidentified intracellular S1P signaling complex. PNAS **113:**E1334-1342.

260. **Jung M, Ören B, Mora J, Mertens C, Dziumbla S, Popp R, Weigert A, Grossmann N, Fleming I, Brüne B.** 2016. Lipocalin 2 from macrophages

stimulated by tumor cell-derived sphingosine 1-phosphate promotes lymphangiogenesis and tumor metastasis. Science Signaling **9:**ra64-ra64.

261. **Pecorelli A, Ciccoli L, Signorini C, Leoncini S, Giardini A, D'Esposito M, Filosa S, Hayek J, De Felice C, Valacchi G.** 2011. Increased levels of 4HNE-protein plasma adducts in Rett syndrome. Clinical Biochemistry **44:**368-371.

262. **Lee W-C, Wong H-Y, Chai Y-Y, Shi C-W, Amino N, Kikuchi S, Huang S-H.** 2012. Lipid peroxidation dysregulation in ischemic stroke: Plasma 4-HNE as a potential biomarker? Biochemical and Biophysical Research Communications **425:**842-847.

263. **Dumlao DS, Buczynski MW, Norris PC, Harkewicz R, Dennis EA.** 2011. High-throughput lipidomic analysis of fatty acid derived eicosanoids and N-acylethanolamines. Biochimica et Biophysica Acta (BBA) - Molecular and Cell Biology of Lipids **1811:**724-736.

264. **Mardones P, Dillin A, Hetz C.** 2014. Cell-Nonautonomous Control of the UPR: Mastering Energy Homeostasis. Cell metabolism **20:**385-387.

265. **Zanetti M, Mahadevan NR.** 2012. Cancer. Immune surveillance from chromosomal chaos? Science **337:**1616-1617.

266. **Godinho SA, Picone R, Burute M, Dagher R, Su Y, Leung CT, Polyak K, Brugge JS, Thery M, Pellman D.** 2014. Oncogene-like induction of cellular invasion from centrosome amplification. Nature **510:**167-171.

267. **Zanetti M.** 2017. Chromosomal chaos silences immune surveillance. Science **355:**249-250.